WEATHERSMART NEWS

Scientific meteorological and climatological news from the South African Weather Service

October 2022

April 2022 floods in comparison with other recent flooding events in KwaZulu-Natal

Severe thunderstorms wreak havoc in places over the eastern half of the Eastern Cape on 13 December 2021

New regional weather and climate summary: South-Western Cape

South African Weather Service

WEATHERSMART NEWS

Scientific meteorological and climatological news from the South African Weather Service

Impact-Based Severe Weather Warning System

WHAT IS IMPACT-BASED FORECASTING?

Severe weather is a regular occurrence across South Africa which often negatively affects humans. Due to the vast distribution of vulnerabilities across the country, the same weather hazard can result in different impacts in two areas, depending on the specific vulnerability of the area.

Impact-Based warnings combine the level of impact the hazardous weather conditions expected with the level of likelihood of those impacts taking place

Moving from

What the weather will be:
(Meteorological thresholds)
- 50mm in 24 hours - 35 knot winds

To

What the weather will do:
(Impact Warnings)
- Roads flooded - Communities cut off

Date of issue:
October 2022

Frequency:
6 Monthly

ISSN:
2414-8644

Editorial Team:
Hannelee Doubell (Editor)
Fhatuwani Siluna (Compiler)

Publisher:
South African Weather Service

Address:
Eco Glades Block 1B, Eco Park,
Corner Olievenhoutbosch and
Ribbon Grass Streets,
Centurion, 0157

TABLE OF CONTENTS

Foreword by the Chief Executive Officer

Welcome to the WeatherSMART News edition of October 2022. I am immensely grateful for the astounding work done by the editorial team, and all our loyal contributors, who work assiduously to ensure that the South African Weather Service (SAWS) produces an informative, scientific, and technical publication for all our stakeholders in the weather and climate space.

SAWS continues to be a reputable and authoritative provider of weather and climate services and products, both regionally and internationally, because of our meteorological and climatological expertise.

In this bumper issue, we reflect on the recent floods that occurred in April 2022 in KwaZulu-Natal (KZN), in comparison with other flooding events in the same province. Even though the April floods will probably go down as one of the worst weather disasters in history, it is undoubtedly evident that South Africa has been experiencing an increase in the number of heavy rainfall events in general. To validate this, we have featured an article that covers a study that looks at data from 70 manual rainfall stations across South Africa for the period 1921 to 2020. A second article about the observed trends in the probability of high extreme monthly rainfall in KwaZulu-Natal indicates the likelihood of an increased period of excessive rainfall in KwaZulu-Natal, recommending more frequent updates of rainfall-related statistics for disaster preparedness, design and planning in the province. We further looked at an investigation of extreme short-term rainfall at Bolepi House (our former head office in Erasmusrand, Pretoria, Gauteng), from May 2003 to April 2018, as well as the implications for disaster risk reduction assessments in the country.

In 2017, the City of Cape Town in the Western Cape, was on a countdown to disaster. An unprecedented and unforeseen third consecutive year of drought threatened to cut off water to the City's four million citizens. The City was faced with the prospect of running low on water and being the first global metropole to have dry taps due to drought. Nevertheless, they eventually managed to avert "Day Zero", with water restrictions in place, the Capetonians once again got back to normal life and adapted to being water-wise. In an interesting turn of events, since 2019, the south-western parts of the Western Cape have been blessed with normal to above-normal rainfall, which has been tremendous for the city. You will read more on the study that benchmarks the yearly rainfall accumulation from 2017 to July 2022 for Cape Town. In my opinion, no country is immune to such a water crisis, so let us learn from the Capetonians and intensify our individual efforts towards water conservation.

Climate studies have attributed this, and other extreme weather events covered in this newsletter to anthropogenic climate change. I would like to assure you that SAWS remains committed to the global fight against climate change and will continue to provide credible, research-based solutions to counter this global phenomenon.

We have also included a simplified article of a study that compares daily satellite-based databanks namely SOLCAST, CAMS, CAMSAF and NASA SSE, and the Ångström–Prescott (AP) model, by validating them against BSRN QC and HelioClim model quality-checked observed daily Global Horizontal Irradiance (GHI) from eight ground stations in South Africa.

Through numerous publications that cover different scientific topics, SAWS is committed to maximising its research function to provide sound reliable weather and climate data. I am pleased to announce that the organisation's Climate Service department will be releasing a second publication in the series of Regional Climate and Weather Summaries, which will focus on the South-Western Cape. The publication will provide an overview of the climate and weather in various regions in South Africa. As we wait for this much anticipated read, I encourage all our stakeholders to read the first publication which focused on Gauteng on the SAWS website at https://www.weathersa.co.za/home/regionalweatherclimate. The publication is freely available and going forward, all upcoming editions will be accessible through SABINET.

I hope the readers enjoy this newsletter and find the content valuable and informative, as we intended to enhance people's knowledge of the weather and climate space. With this edition, I hope that everyone is going to be more upbeat and is looking forward to sunnier days.

Ishaam Abader
Chief Executive Officer

THE APRIL 2022 FLOODS IN COMPARISON WITH OTHER RECENT FLOODING EVENTS IN KWAZULU-NATAL

By Nthabiseng Letsatsi and Andries Kruger

Climate studies are confirming that extreme events are becoming more frequent and more intense due to anthropogenic climate change. Analysis of long-term climate observations indicate that the characteristics of extreme weather events is changing over South Africa. This is in agreement with the latest IPCC report (Working Group 1 published in August 2021) which indicates that the evidence of attribution of these changes to human influence has strengthened since the AR5 report. In South Africa, we are observing an increase in the number of heavy rainfall events in general. This creates an urgent need for a good adaptation and mitigation strategy to prevent and reduce weather-related disasters. There are notable severe weather events that were recorded in the past in South Africa, and the most frequent of these are floods as shown below (Figure 1). The most severe flood events experienced in South Africa were mostly caused by cut-off lows, tropical cyclones, and tropical storms.

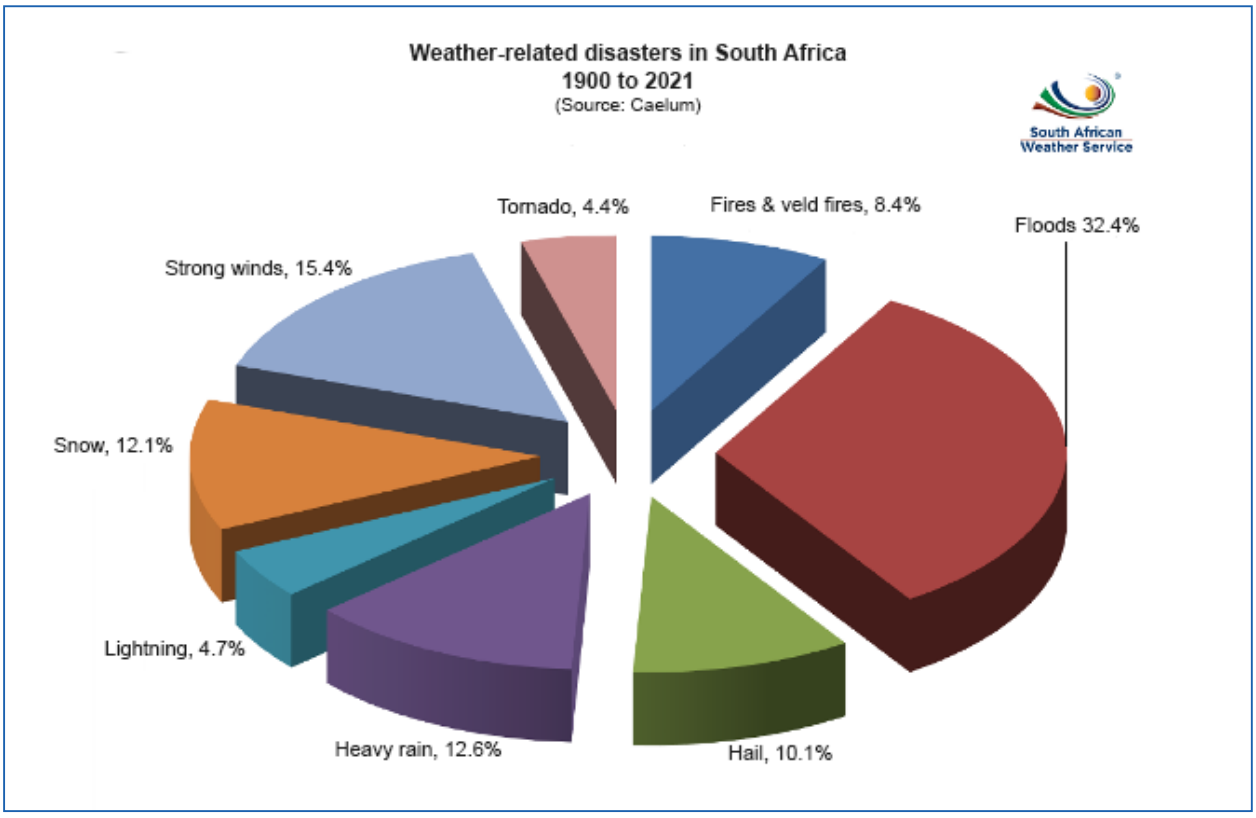

Figure 1: Reported weather-related disasters in South Africa (1900-2021)

Historically, the most extreme large-scale rainfall events over KwaZulu-Natal were caused by different weather systems with different footprints. However, all these events impacted the coastal regions most severely. Below is a concise summary of the extreme rainfall events caused by Cyclone Domoina in January 1984, and the cut-off lows in September 1987, April 2019 and the most recent event in April 2022. Also included are tables presenting the top 20 highest recorded rainfall accumulations measured over the period covering the course of the event.

January 1984: Cyclone Domoina

The Eastern half of KwaZulu-Natal received rainfall above 200 mm, extending to the eastern parts of Mpumalanga, as presented in Figure 2.

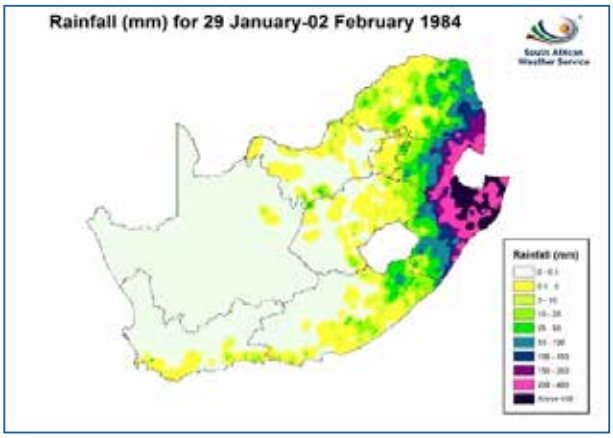

Figure 2: Accumulated rainfall received over period 29 January 1984 to 2 February 1984

The north-eastern parts of KwaZulu-Natal received rainfall above 400 mm, with the highest recording of 1018 mm within 5 days as noted in Table 1 below.

Table 1: Accumulated rainfall for the period 29 January to 2 February 1984

Station	Total rainfall
TOKAZI	1018
CWAKA AGRICULTURE	955
BOSHOEK - NATAL ANTHR COLL	925
RHEBOKFONTEIN	740
SURPRISE STORE	735
CAPE ST LUCIA	727
ST. LUCIA LAKE RESEARCH CENTRE	723
MISSION ROCKS	703
INGWAVUMA – TNK	640
HLABISA MBAZWANA	637
NGOMI – BOS	634
MAHAMBA – POL	631
LANGEPAN – BOS	624
CAPE VIDAL	623
SUNWAYS	622
ST. LUCIA FOREST	619
BLOEMENDAL	616
MPOSA-FAIRVIEW	600
BERGPLAATS	591
ORANJEDAL-NAF	587

The number of casualties were about 60, with more than 500 000 properties and structures damaged or destroyed. This damage was estimated to be more than R100 billion.

Cut-off low: Period: 26-29 September 1987

Nearly the entire KwaZulu-Natal received rainfall more than 200 mm over 4 days, from 26 to29 September 1987.

The eastern parts of KwaZulu-Natal further received rainfall above 400 mm and the highest record was 914 mm in just 4 days at Langepan station.

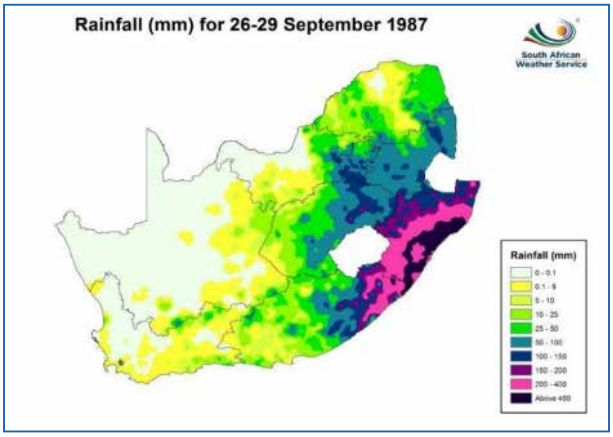

Figure 3: Accumulated rainfall received over period 26 to 29 September 1987

Table 2: Accumulated rainfall for the period 26 to 29 September 1987

Station	Total rainfall
LANGEPAN	914
KWAMBONAMBI-BOS	881
CWAKA AGRICULTURE	874
PADDOCK	757
MARAH	742
ULOA AGRICULTURAL OFFICE	695
NDWEDWE	690
IMPENDLE HILTON	689
STANGER	679
ST FAITHS – POL	678
ONGAYE/MTUNZINI	651
KLOOF PURIFICATION	631
UMBUMBULU	618
MANDINI	618
TANHURST EST.	617
EMPANGENI MAGISTRATE	605
MINNEHAHA FARM	603
MBONA MOUNTAIN ESTATE	596
RIVER VIEW	595
PORT DURNFORD - BOS	594

The number of casualties were about 400, with 50 000 people left homeless and damage estimated at R400 million.

Cut-off low: Period: 22-23 April 2019

The southern parts of KwaZulu-Natal, extending to the north-eastern parts of the Eastern Cape, received more than 50 mm of rain within 48 hours.

The coastal areas received rainfall above 200 mm, with the highest station recording a total of 440 mm within 48 hours.

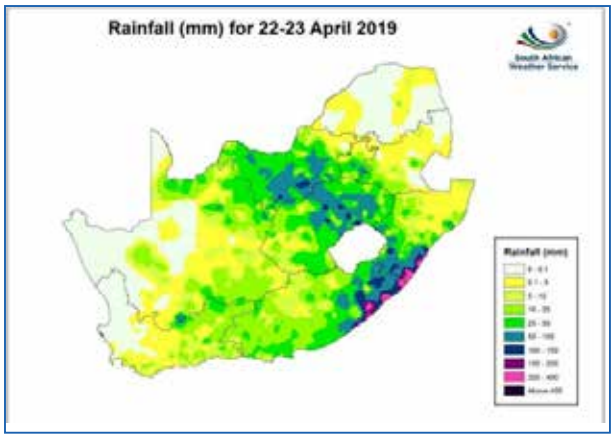

Figure 3: Accumulated rainfall received over period 22 to 23 April 2019

Table 3: Accumulated rainfall for the period 22 to 23 April 2019

Station	Total rainfall
MARGATE AIRPORT	440
DURBAN KENNETH STEINBANK	326
PADDOCK	304
PORT EDWARD	297
SCOTTBURGH - MUN	255
MINNEHAHA FARM	239
UMZINTO - MUN	200
VIRGINIA AIRPORT AAWS	195
HIMEVILLE - MAG	180
GLEN DOONE	176
PENNINGTON SOUTH	165
VIRGINIA	163
MOUNT EDGECOMBE	163
KWAMASHU W/W ARS	146
LANGGEWACHT - BOS	126
LAKE ELAND	116
MIDDELWATER - BOS	106
SUMMERFORD	95
KOKSTAD	82
HIGHMOOR - BOS	82

The casualties were about 85, with 43 more people injured and 235 homes destroyed. The damage was estimated to be over R650 million.

Cut-off low: Period: 9-17 April 2022

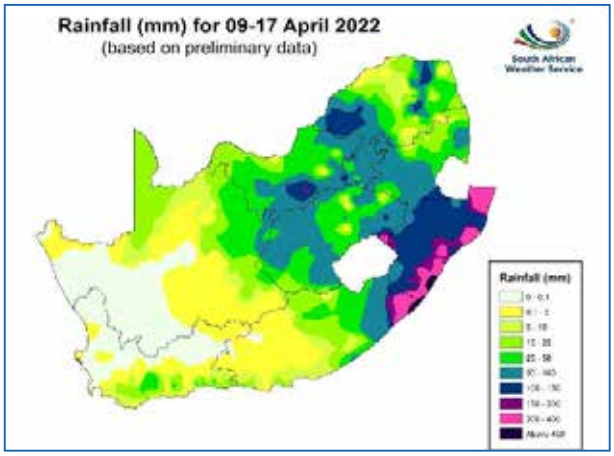

Figure 4: Accumulated rainfall received over period 9 to17 April 2022

Table 4: Accumulated rainfall for the period 9 to 17 April 2022

Station	Total rainfall
MARGATE	575
PENNINGTON SOUTH	530
PORT EDWARD	490
VIRGINIA AIRPORT AAWS	448
MOUNT EDGECOMBE	407
VIRGINIA	376
DURBAN SOUTH WENTWORTH	371
KING SHAKA AWOS	326
MBAZWANA AIRFIELD	322
RICHARDS BAY AIRPORT	295
MANDINI	294
KOSI BAY ARS	267
RICHMOND ARS	266
RIVERVIEW	253
MAPUMULO PRISON	246
ROYAL NATIONAL PARK	219
MTUNZINI	194
ORIBI AIRPORT	167
PIETERMARITZBURG	158
PIETERMARITZBURG - DARVILLE ARS	157

Northern KwaZulu-Natal, stretching along the coast to adjecent areas of the Eastern Cape, received more than 200 mm of rainfall within nine days and the highest total rainfall was 575 mm recorded at Margate.

The casualties were about 440, with 40 000 people left homeless, after 4 000 homes were destroyed. The damage is estimated to be R7 billion thus far.

Some additional statistics

1. The impacts of tropical cyclone Domoina were estimated to be R100 billion over South Africa in 1984, which is higher than the 9 to 17 April 2022 flood impacts estimated at R7 billion thus far. It is not clear if these estimates include both direct and indirect impacts.

2. The highest rainfall accumulation of 1018 mm was recorded during the tropical cyclone Domoina in 1984, over a period of five days.

3. The April 2019 flood had a total rainfall of 440 mm recorded in 48 hours at the Margate Airport weather station.

4. Margate recorded a total of 575 mm in 9 days during the 9 to 17 April 2022 floods. These floods resulted in 440 deaths, which is 40 more people than the 1987 floods, which led to 400 deaths.

Return periods of extreme rainfall totals

A return period is an estimated average time between extreme events to occur. Changes in the probability of occurrence of extreme events can have far greater detrimental impacts on lives, natural systems, and infrastructure than a change in average climate conditions. As a result, the inclusion of extreme weather and climate events in the calculation of return periods is in some cases vertical since they reduce the overall return periods of severe weather events. In turn, this is important for analysing risks so that timely and sensitive decisions about how to manage the present and future risks are made. Table 5 presents the impact of the most recent event on the return periods of extreme daily rainfall totals.

Table 5: Highest daily rainfall totals during the April 2022 storm at the KwaZulu-Natal coast and adjacent interior. (Daily totals in red in indicate the highest ever daily rainfall totals. Return period values in purple indicate for which stations a reduction in return period of the maximum daily total is estimated. The influence of the extreme daily rainfall is also seen in the increase in the amount of rainfall that can be expected after 10 years and 50 years.)

Station	Daily rain	Return period (excl. 2022 daily rain)	Return period (incl. 2022 daily rain)	1:10 year rainfall (excl. 2022 daily rain)	1:10 year rainfall (incl. 2022 daily rain)	1:50 year rainfall (excl. 2022 daily rain)	1:50 year rainfall (incl. 2022 daily rain)
MARGATE AIRPORT	356	486	159	208	228	270	303
MARGATE	311.6	422	124	188	208	241	274
MOUNT EDGECOMBE	307.4	444	265	162	170	224	238
VIRGINIA	304.4	159	71	171	194	249	285
MANDINI	191.8	16	14	172	177	241	248
PORT EDWARD	188	7	7	206	209	287	290
MINNEHAHA FARM	158	5	5	191	192	278	278
MAPUMULO PRISON	144.2	11	11	140	141	193	195
ORIBI AIRPORT	102	94	46	77	82	95	103
PIETERMARITZBURG	98.8	24	19	86	89	109	113
PIETERMARITZBURG - DARVILLE ARS	95.2	30	23	81	83	102	106
GLENORA FARM	66	2	2	109	109	153	153
CEDARA	61.6	2	2	107	106	149	149
WEZA PLANTATION	60	1	1	107	106	140	140
PADDOCK	52.2	1	1	231	228	327	324
MOOI RIVER	43.6	1	1	68	68	87	86
UMZINTO - MUN	41	0	0	187	187	250	251

Conclusion

The KwaZulu-Natal coastal region, including Durban, is prone to occasional flooding as it receives relatively high rainfall and is situated in a hilly region, with numerous gorges. In hilly places, landslides are frequent if the soil is not stabilized. Due to a lack of control over where, how, and what to build in some areas, increased populations of cities like Durban frequently lead to the establishment of residential (most often informal) populations on floodplains (which were formed by previous flooding and will be frequently flooded), or on steep slopes (with frequently unstable soils).

Infrastructure ages over time, and with an influx of people into Durban, it becomes under immense pressure and as a result, there is a need to replace or repair infrastructure to accommodate the growing population.

With expanding suburbs, business and industrial areas, and a higher degree of formal urbanisation than ever before, there is now a higher level of surface runoff with a higher peak discharge. These factors are all linked to more impervious areas. Large new expanses of hard, impermeable surfaces have been developed around Durban as a result of the quick and extensive expansion of human settlement and industrial development, which exacerbates the erosive impact of floodwaters.

Native vegetation has been replaced with shallow-rooted vegetation in some regions, which results in decreased soil-holding ability and a higher likelihood of landslides.

Complex spatial planning is a problem in cities like Durban, where traditional/customary rules are frequently out of step with municipal strategic planning plans.

Whereas larger areas of grasslands, gardens and undisturbed natural vegetation once helped to absorb or disperse floodwaters, the almost wall-to-wall covering of concrete, brick paving or tarred roads in some parts of the city has promoted faster and more intense water channelling and scouring. More information can be found in an insightful article main-authored by Prof. R. Schulze of the University of KwaZulu-Natal (https://www.wrc.org.za/mdocs-posts/what-did-cause-the-april-kzn-floods/)

References

Daily Maverick. 'Human factors', not just the climate crisis, aggravated KZN floods — top hydrology researcher. 'Human factors', not just the climate crisis, aggra... (dailymaverick.co.za)

De Villiers, G.T., and Maharaj, R. 1994. Human perceptions and responses to floods with specific reference to the 1987 flood in the Mdloti River near Durban, South Africa. Water South Africa, 20(1), 9-13.

F. G. BELL; Floods and Landslides in Natal and Notably the Greater Durban Region, September 1987: a Retrospective View. Environmental & Engineering Geoscience 1994;; xxxi (1): 59–74. doi: https://doi.org/10.2113/gseegeosci.xxxi.1.59

Floodlist. 23 April 2019. https://floodlist.com/africa/south-africa-floods-kzn-eastern-cape-april-2019

Grobler, R.R., 2003. A framework for modelling losses arising from natural catastrophes in South Africa. University of Pretoria.

https://www.kzncogta.gov.za/kzn-floods-update/

https://reliefweb.int/report/south-africa/floods-detail-effect-climate-change

https://www.thesouthafrican.com/news/2019-kzn-easter-floods-85-deaths-r650m-in-damage-over-five-days-breaking/

https://www.wrc.org.za/mdocs-posts/what-did-cause-the-april-kzn-floods/

Kovács, Z.P., Du Plessis, D.B., Bracher, P.R., Dunn, P., and Mallory, G.C.L. 1985. Documentation of the 1984 Domoina Floods (Report). SA Department of Water Affairs. https://www.dws.gov.za/iwqs/reports/tr/TR_122_1984_Domoina_floods.pdf

Tooley, G. (2002b) KZN Crises: Engineering Design for the Future. University of KwaZuluNatal Workshop on the April 2022 Floods over KwaZulu-Natal

OBSERVED TRENDS IN THE PROBABILITY OF HIGH EXTREME MONTHLY RAINFALL IN KWAZULU-NATAL

By Andries Kruger

1. Introduction

Recent flooding events in KwaZulu-Natal caused a range of negative impacts, including a large number of human casualties and severe damage to infrastructure. Current research in the Climate Service department points to increased probabilities of rainfall extremes across large parts of South Africa, including KwaZulu-Natal (McBride et al., 2022). While it has been established that the probability of daily extremes has increased in the province over the long term, trends in the probability of extreme rainfall amounts recorded over longer time-periods (e.g. a month or longer) has not been researched in a systematic way. This article explores whether, due to the increased likelihood of daily extremes, there is a likelihood that probabilities of extremely high monthly total precipitation during the wetter months in the province have increased.

2. Analysis approach

Data

South Africa was divided into 94 homogeneous rainfall districts by the South African Weather Service in 1972 (then the South African Weather Bureau, van Rooy (1972)). Monthly average rainfall totals for these districts have been calculated since 1921, by averaging the daily totals of all rainfall stations reporting in a particular district and then calculating the monthly totals. Six of these districts fall within KwaZulu-Natal, namely 25, 26, 30, 31, 44 and 45, as presented in Figure 1.

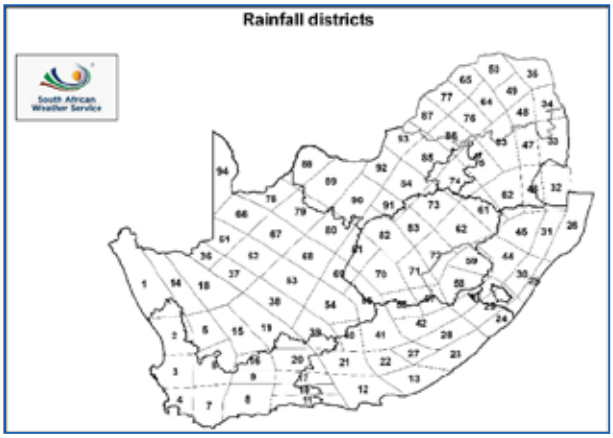

Figure 1: The homogeneous rainfall districts of South Africa (after van Rooy, 1972)

The research focuses on the months of the year when high rainfall amounts are more probable, i.e. September to April, analysed on an individual basis. The results are also discussed on a monthly sequence, from the beginning of spring in September, through summer, to mid-autumn in April.

Methodology

It is established that the gamma and log-normal distributions fit rainfall data at various time scales -including monthly totals - well. The latter distribution was fitted on the time series of the individual months over 30-year shifting window periods, over the period 1921 to 2021/22 (depending on whether the rainfall district data for the current year had already been calculated). A shifting analysis period was selected, as such an approach would exhibit whether the extreme rainfall climate has been non-stationary over the last century. Due to climate change, significant long-term shifts, such as increases or decreases, are highly possible.

The 1:10 and 1:50 year maximum monthly rainfall were then estimated with the fitted distribution over each of the periods, in the sequence 1921 – 1950, 1922 – 1951,..., 1993 – 2022. These return periods were selected as their associated maximum values are most often applied in streamflow estimations, structural engineering etc. albeit most often for shorter time periods.

Simple linear regression was applied to the time series of the return period values and thereafter the significance of the trends was established with the Student's t-test at the 95% level of confidence. A statistically significant positive trend in the return period values will indicate an increase in the maximum monthly total rainfall to be expected over the specific return periods.

3. Results

The results of the analysis are firstly discussed per rainfall district, per month from spring to mid-autumn, which includes a selection of images of the time series of the return period values. Thereafter, the results are summarised by month for the province as a whole.

District 25 (KZN Southern Coastal Region)

The district shows statistically significant increases in return period values in the early spring months. Especially October, presented in Figure 2, shows a very strong trend where the 1:10 year return period value changed from about 140 mm in the 1950s to around 180 mm in the most recent decade. The 1:50 year value increased from around 200 mm to 280 mm over the same period. Late spring and early summer show weaker trends, which turn to significantly negative trends in January. February shows significant increases, due to high monthly totals recorded from the mid-1980s to late 1990s. However, there has been a steady decrease in return period values since then. March shows no trend or declines due to recent low return period values. The same applies to April. However, the high April 2022 rainfall total of 479 mm caused an abrupt increase in the return period value estimations for the 1:10 year from around 130 mm to 160 mm and for the 1:50 year from around 230 mm to 300 mm between 2021 and 2022. This return period value is comparable to what one would typically expect during the months of maximum rainfall in mid-summer.

However, while the April 2022 total is the highest on record for the month in the time series as a whole, more high values in a specific time period are required to have an impact on the trend in the return period value. As an example, this can be seen from the April monthly rainfall totals (presented in Figure 4). From the late 1950s to early 1960s, above-normal rainfall totals were measured over an extended period. The return period values derived from these totals are reflected in Figure 3, where it is shown that the values from the late 1950s and 1960s were consistently above 270 mm. These high values affected the long-term trend to an extent that there is a significantly negative trend over the last century.

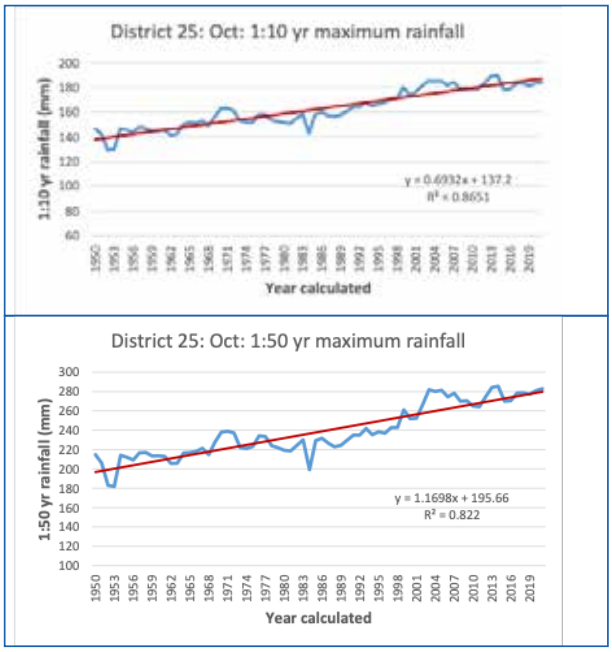

Figure 2: October 1:10 year (left) and 1:50 year (right) maximum rainfall (mm) for District 25, based on the 30-year periods ending in the years as indicated on the x-axis. The red line presents the linear trend.

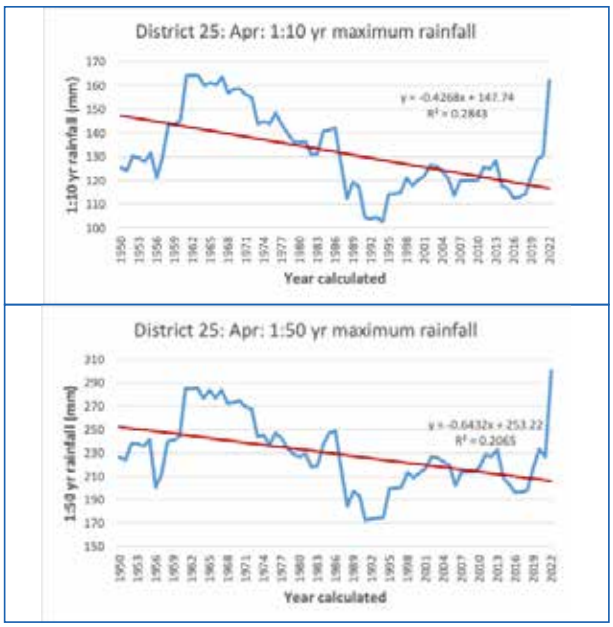

Figure 3: April 1:10 year (left) and 1:50 year (right) maximum rainfall (mm) for District 25, based on the 30-year periods ending in the years as indicated on the x-axis. The red line presents the linear trend.

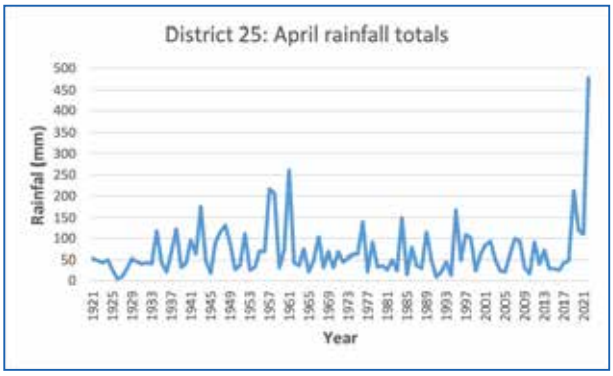

Figure 4: District 25 April monthly rainfall (mm) for the period 1921 - 2022

District 26 (KZN Northern Coastal Region)

The district shows statistically significant increases in return period values in October, presented in Figure 6. As is the case for the Southern Coastal Region, very strong trends are observed, with the 1:10 year return period value changed from about 110 mm in the 1950s to around 170 mm in the most recent decade. The 1:50 year value increased from around 140 mm in the early 1950s to around 260 mm recently. In contrast, November and December show significant decreases. March and April also show significant decreases, presented in Figure 7. However, as is the case for the Southern Coastal Region, an exceptionally high April 2022 rainfall total of 299 mm caused a sudden increase in the return period value estimations for the 1:10 year from around 110 mm to 130 mm and for 1:50 year from around 160 mm to 200 mm between 2021 and 2022.

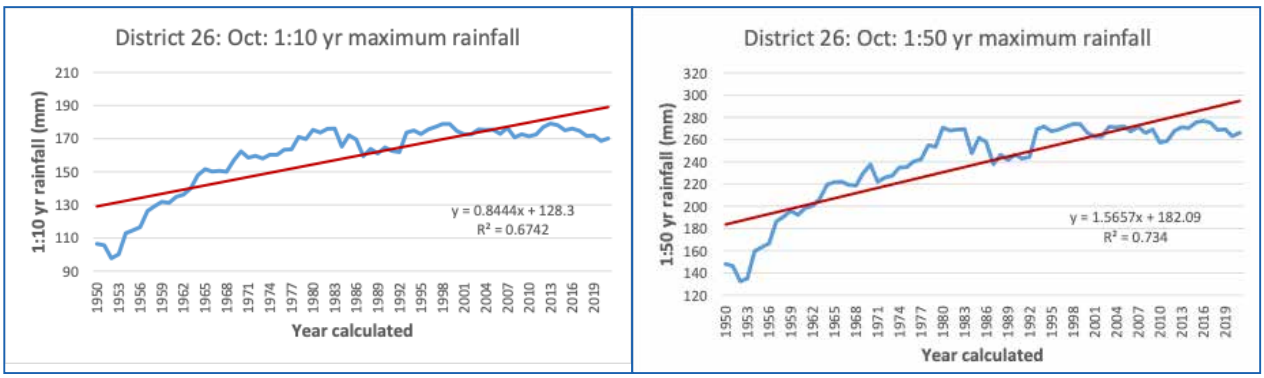

Figure 5: October 1:10 year (left) and 1:50 year (right) maximum rainfall (mm) for District 26, based on the 30-year periods ending in the years as indicated on the x-axis. The red line presents the linear trend.

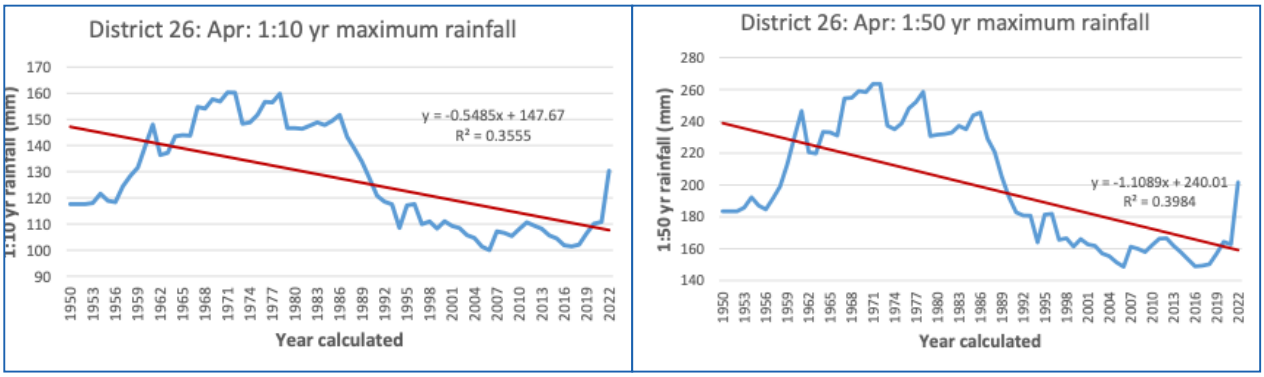

Figure 6: April 1:10 year (left) and 1:50 year (right) maximum rainfall (mm) for District 26, based on the 30-year periods ending in the years as indicated on the x-axis. The red line presents the linear trend.

District 30 (KZN Southern Interior Region)

The district shows statistically significant increases in return period values for September and October. As is the case for the coastal regions, very strong positive trends are observed. In contrast, November to January show significant decreases, February increases, and again decreases for March and April. Exceptionally high April 2020 and April 2022 rainfall totals, of 142 mm and 225 mm respectively, caused a steep increase in the return period value estimations for the 1:10 year value from around 80 mm to 105 mm and for the 1:50 year from around 120 mm to 180 mm over the last four years, presented in Figure 7.

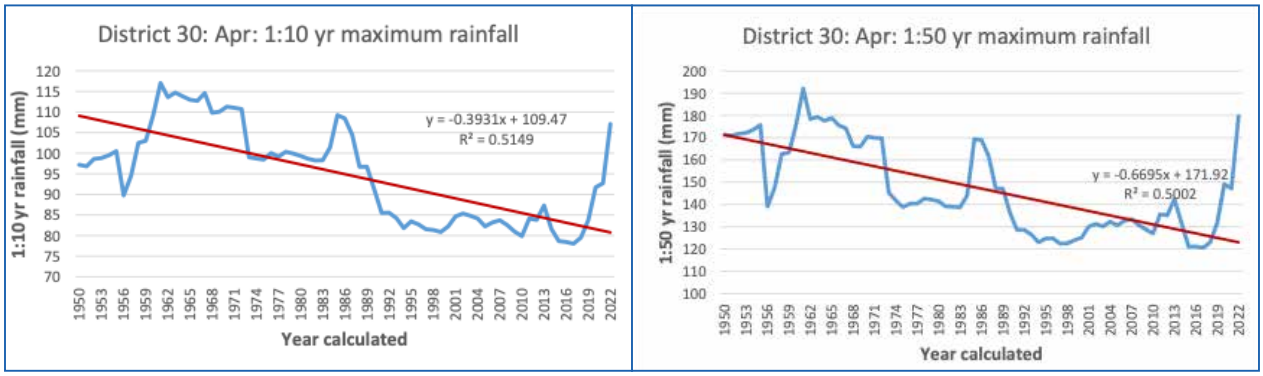

Figure 7: April 1:10 year (left) and 1:50 year (right) maximum rainfall (mm) for District 30, based on the 30-year periods ending in the years as indicated on the x-axis. The red line presents the linear trend.

District 31 (KZN Northern Interior Region)

The district shows statistically significant increases in return period values for October, as well as mid- to late-summer in January (presented in Figure 8) and February. Decreases are evident in March, with an increase in the 1:50 year total for April.

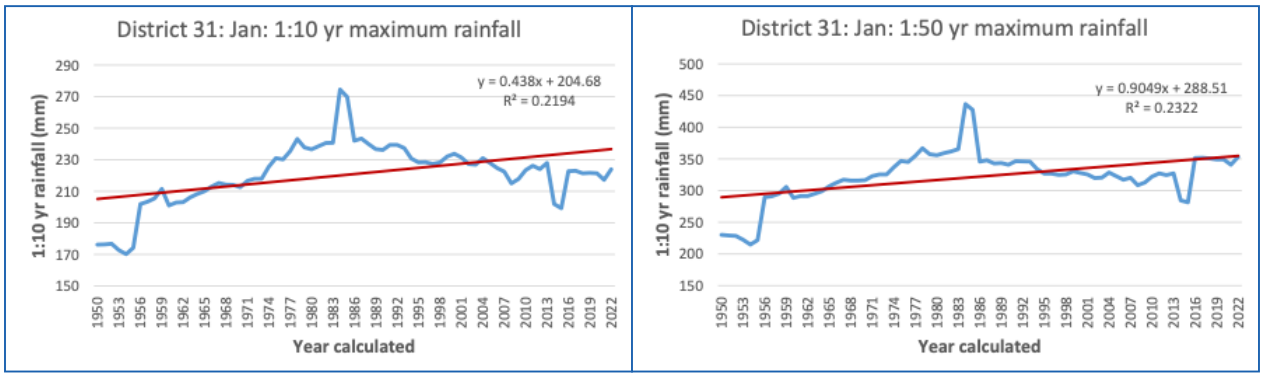

Figure 8: January 1:10 year (left) and 1:50 year (right) maximum rainfall (mm) for District 31, based on the 30-year periods ending in the years as indicated on the x-axis. The red line presents the linear trend.

District 44 (KZN South-Western Interior Region)

The district shows statistically significant increases in return period values for October, as well as summer from December (presented in Figure 9) to February. Decreases are evident in March, but an increase in the 1:50 year total for April is observed.

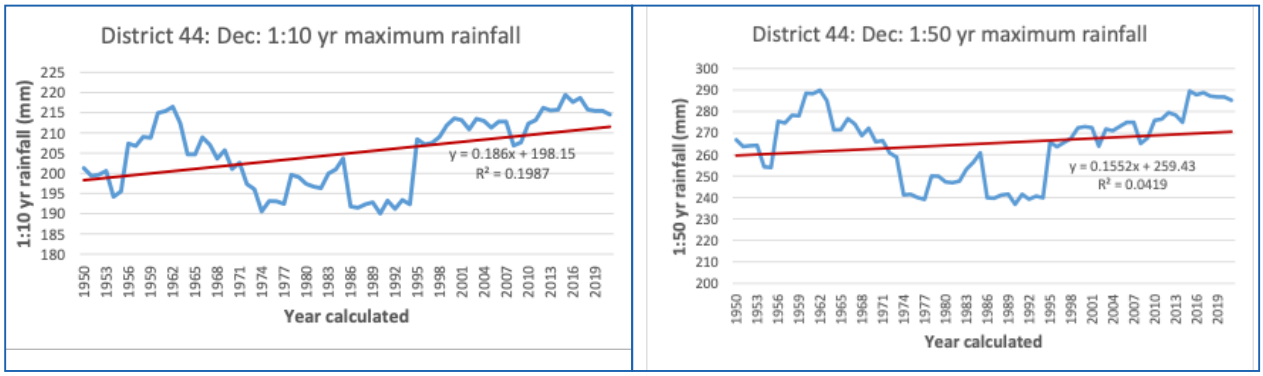

Figure 9: December 1:10 year (left) and 1:50 year (right) maximum rainfall (mm) for District 44, based on the 30-year periods ending in the years as indicated on the x-axis. The red line presents the linear trend.

District 45 (KZN North-Western Interior Region)

The district shows statistically significant increases in return period values for October, but decreases for most of the months and associated return period values from November onwards.

Months with significant increases in return period rainfall

Figure 10 presents the months for which there are rainfall districts with statistically significant trends in both their 1:10 year and 1:50 year monthly rainfall totals. The most noteworthy results are firstly that basically the whole of KwaZulu-Natal experienced an increase in return period values in October. Secondly, and most importantly, is that all of the summer months, from December to February, experienced an increase in return period values in some places in the province.

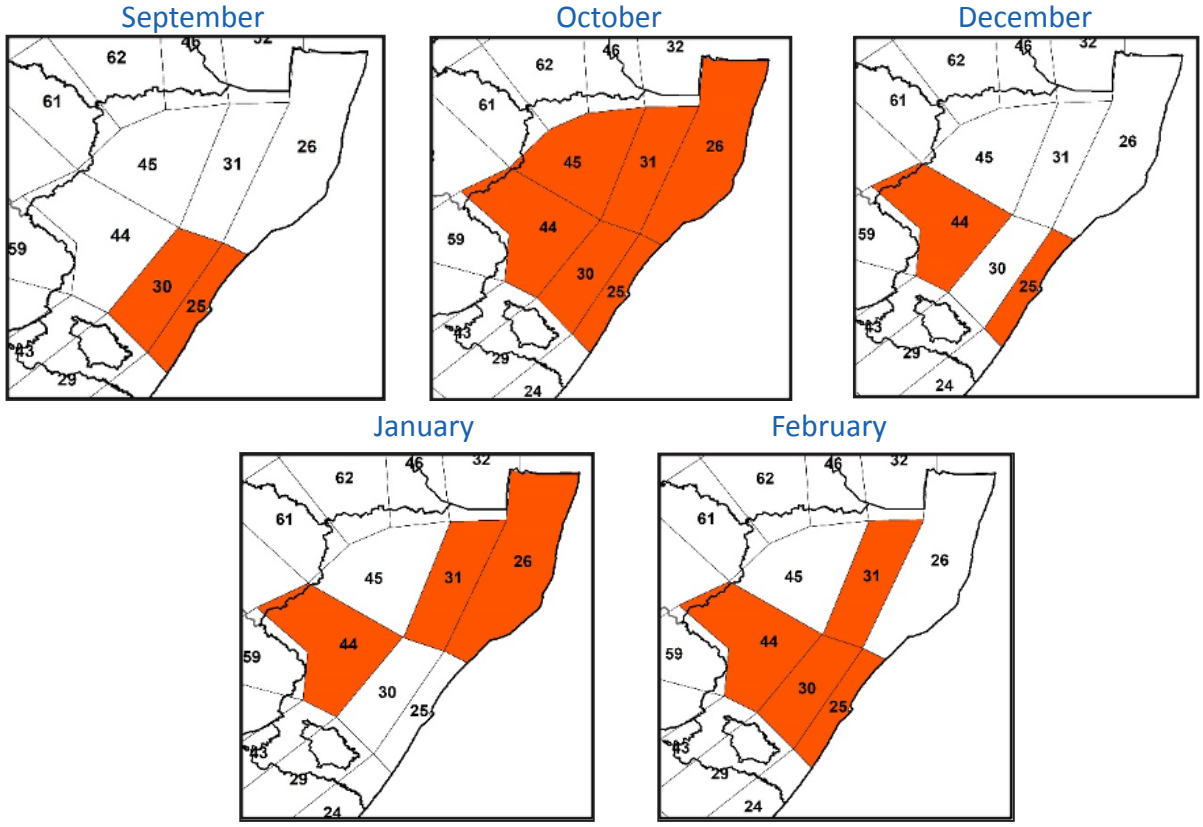

Figure 10: Months which have rainfall districts in KwaZulu-Natal showing significant increases in both the 1:10 and 1:50 year return period maximum monthly rainfall totals

4. Discussion

Previous research has shown that the maximum daily rainfall totals for specific return periods in South Africa have increased significantly over the past century. Situated in the eastern parts of the country, KwaZulu-Natal has experienced increased return period rainfall values reaching levels that are mostly unprecedented in South Africa (McBride et al., 2022).

This exploratory return period analysis, focusing on monthly rainfall, investigated whether there are any signals of increases in the return period levels over sub-annual time periods, specifically months, in the province. The analysis focused on the months with the highest rainfall, when there is usually a stronger likelihood of extended rainfall events or episodes that can be disruptive.

Of concern, and warranting further investigation and research, is that in all the summer months from December to February, when most rainfall is received in the province, increases in monthly return period values have been experienced somewhere in the province over the last century; this finding includes Rainfall District 25, which covers the eThekwini municipality. Taking Rainfall District 25 as an example, the 1:50 year maximum return value for December has increased to more than 300 mm, from a minimum of less than 200 mm in the mid-1980s.

In addition to the above, the increased incidence of shorter-term extreme rainfall incidents will change the maximum expected rainfall amounts over longer time periods for specific return periods significantly, which will have a bearing on preparedness for possible flood-related disasters and their resultant socio-economic impacts. For the KwaZulu-Natal coast and adjacent interior, the return period statistics for April are now comparable to those in the summer months, meaning that the section of the year in which excessive rainfall is deemed likely has probably lengthened. Considering these findings, it has become prudent and even imperative that rainfall-related statistics informing disaster preparedness, design and planning be updated on a more frequent basis, preferable as soon as possible after the occurrence of extreme rainfall events.

References

McBride C, Kruger AC and Dyson L. 2022. Changes in Extreme Daily Rainfall Characteristics in South Africa: 1921 – 2020. Weather and Climate Extremes. In press.

Van Rooy, MP. 1972. District Rainfall for South Africa and the Annual March of Rainfall over Southern Africa. South African Weather Bureau.

ARE DAILY RAINFALL EVENTS IN SOUTH AFRICA BECOMING MORE EXTREME?

By Charlotte McBride and Andries Kruger

Several global studies have found that the annual maximum daily rainfall extremes are increasing over land in intensity and/or frequency (Alexander et al., 2006; Seneviratne, 2012; Westra et al., 2013; Lehmann et al., 2015). Is this the case for South Africa? A recent study looked at data from 70 manual rainfall stations across South Africa for the period 1921 to 2020 to try and answer this question. The stations used in the study are shown in Figure 1.

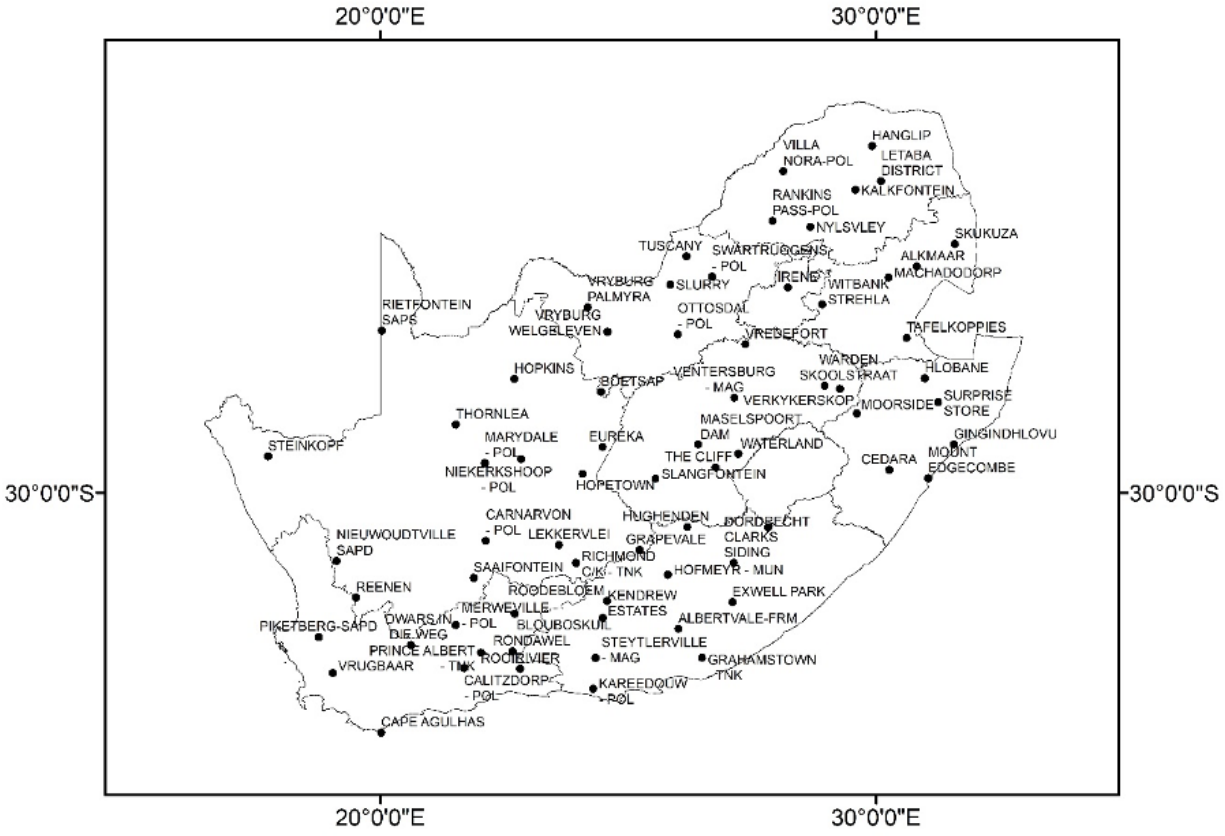

Figure 1: Locations of the 70 rainfall stations which were used to analyse the changes in the occurrence of daily rainfall extremes over the period 1921 to 2020

Data and methodologies

Daily rainfall values for the period 1921 to 2020 from 70 long-term manual rainfall stations were selected for analysis. The data set was split into two successive 50 years periods, i.e., 1921–1970 and 1971–2020 (referred to as period 1 and period 2 hereafter). The number of rain days (≥1mm) per station were counted for both periods.

Research by Dyson (2009) who looked at "heavy rainfall characteristics over the Gauteng Province" to determine thresholds for significant, heavy and very heavy rainfall events was used. This translated into values of 50 mm, 75 mm and 115 mm respectively. In this study, these thresholds were used, and their return period values for 1:10-, 1:50-, and 1:100-year for each station for each period. The student's t-test was used to test for significant differences between periods 1 and 2.

Following from this, the gamma distribution to estimate the probability of a station receiving more than 50 mm on a rainy day in period 1 and 2 was used. The data using the Generalised Extreme Value (GEV) distribution, specifically Type I (Gumbel) was checked, as this distribution is widely used in studies of this nature. However, because in this study the highest daily rainfall per year was used, a researcher could miss values which are considered to be extreme because they were not the highest value in a particular year. To make sure that all extreme values were considered, the peak of threshold method (POT) was also used, where each individual station's daily rainfall totals above the 99th percentile value were considered. By application of this method the return period values for 1:10-, 1:50-, and 1:100-year for each station for each period could then be estimated. For equations and more details on the statistics used in this study please consult Coles et al. (2001).

Results and discussion

There was only a 2% increase in the number of rain days between periods 1 and 2. However, when considering the gamma distribution, most stations experienced an increase in the probability of receiving more than 50 mm per day in the latter half of the analysis period, as presented in Figure 2.

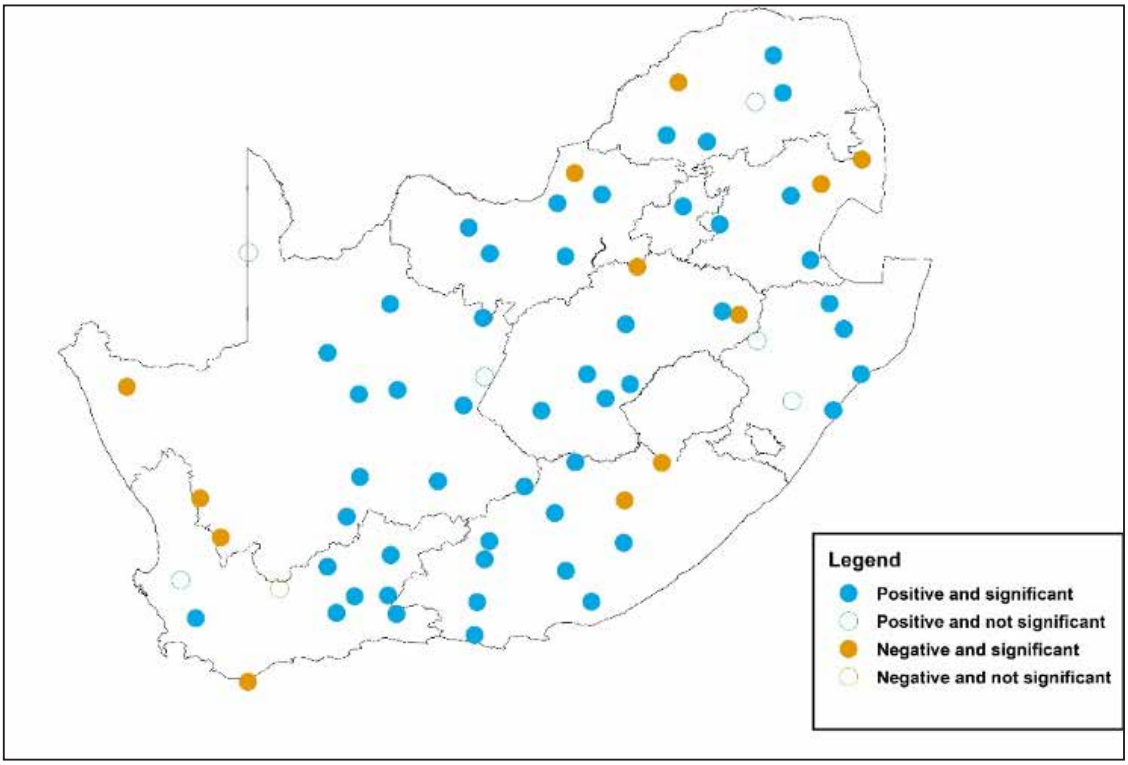

Figure 2: Difference in the probability of receiving 50 mm of rainfall on a rainy day, estimated from the Gamma distribution. (Blue symbols indicate where the probability of receiving above 50 mm is greater in period 2 (1971-2020), while orange symbols indicate where the probability of receiving above 50 mm is greater in period 1 (1921-1970). Shaded symbols indicate statistical significance at the 95% confidence interval (Student's t-test)).

Probabilities of extreme daily rainfall events

A similar spatial pattern is observed in Figure 2, when considering 1:10-, 1:50- and 1:100-year return periods values using the POT method. Most stations showed an increase in return period values for the second period. Areas over

the eastern parts of the country showed that more stations were likely to receive over 200 mm for the 1:10 return period value, while stations over the western parts of the country had a higher probability of above 100 mm for their 1:10 return period value in period 2 (Figure 3b). These values increased to over 400 mm and 200 mm, respectively, for the 1:50 return period value (Figure 3d). When considering the 1:100-year return period value, the expected values increased to over 500 mm for stations in the east, e.g. the Letaba district, Surprise Store, Gingindhlovu and Mount Edgecombe (Figure 3f). Also, more stations have more than 200 mm for their 1:100-year return period values over the western parts of the country in period 2 (Figure 3f).

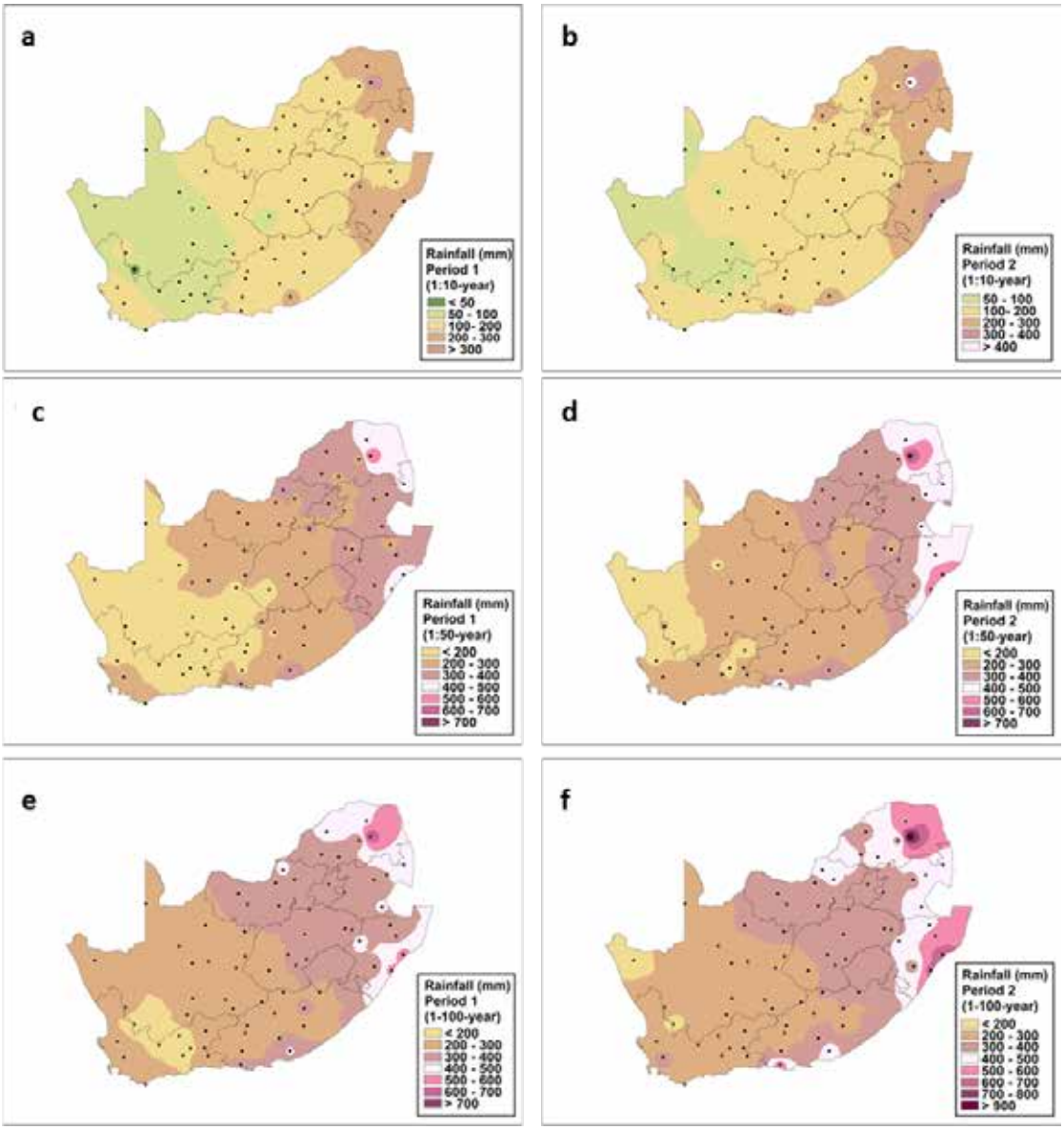

Figure 3: Spatial distribution in 1:10- (a Period 1; b Period 2), 1:50- (c Period 1; d Period 2), and 1:100-year (e Period 1; f Period 2) return period values using the POT method. Inverse distance weighting was used as the interpolation method.

Return periods for specific thresholds of daily rainfall

The specific thresholds of daily rainfall values for significant (>50mm), heavy (>75mm) and very heavy (>115mm) rainfall events were then investigated. Results are depicted in Figure 4. Of particular interest is the increase from only one station in period 1 to five stations in period 2 for a return period of less than a year for receiving more than 50 mm a day.

Most of the country showed a return period of less than five years for 75 mm for both periods 1 and 2. Most stations also showed a decrease in return periods of 115 mm per day in period 2 (Figure 4f).

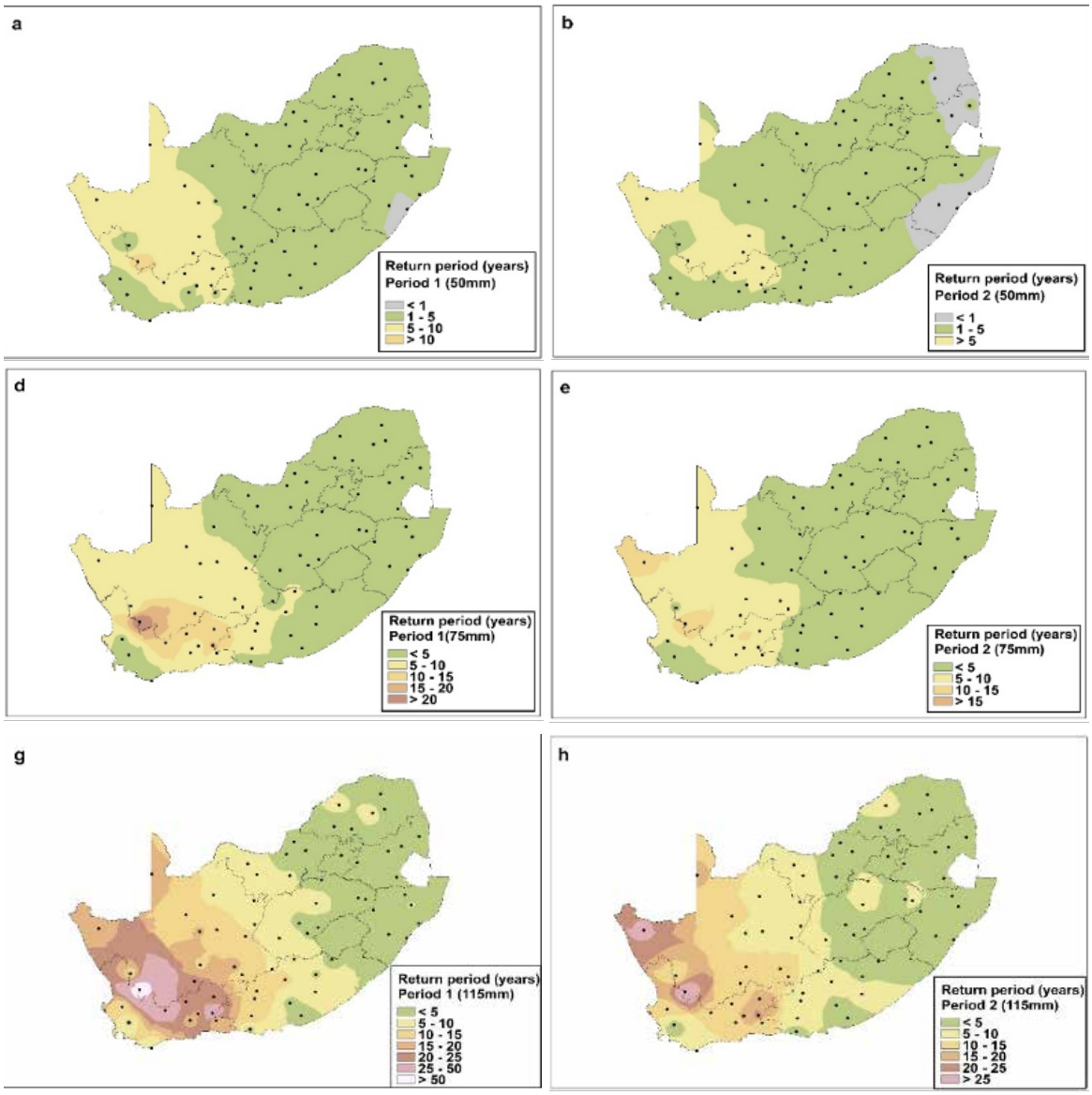

Figure 4: Return periods for 50 mm, 75 mm and 115 mm for both periods using the POT distribution. 50 mm for period 1 (a), 50 mm for period 2 (b); 75 mm for period 1 (c), 75 mm for period 2 (d) and 115 mm for period 1 (e), 115 mm for period 2 (f). Grey areas in figures (a and b) represent areas where return periods are less than a year.

Conclusion

The results from this study indicate that the magnitude and probabilities of extreme rainfall events are changing over South Africa. With most of the country showing an increase in the probability of receiving above 50 mm a day and the increase in return period values for 1:10, 1:50 and 1:100-year return periods, there should be a concern for the increased likelihood of potential flooding. We have seen examples of what flooding is capable of doing with the recent KwaZulu-Natal floods in April 2022. The highest daily rainfall measured during this event was at Virginia airport (351.2 mm). This study highlighted the increase in the probability of return period values for the 1:50 and 1:100 years of over 400 mm over the eastern parts of the country. Thus the rainfall which caused the KwaZulu-Natal floods is looking to become more frequent over this part of the country.

In addition, the western interior also shows a decrease in return periods for receiving significant rainfall, raising the concern that more focus should be given to the threat of flooding in a changing climate and that proactive planning will be needed to ensure the safety of people, robust infrastructure and adaptive agricultural practices.

References:

Alexander, L. V., Zhang, X., Peterson, T. C., Caesar, J., Gleason, B., Klein Tank, A. M. G., Haylock, M., Collins, D., Trewin, B., Rahimzadeh, F., Tagipour, A., Rupa Kumar, K., Revadekar, J., Griffiths, G., Vincent, L., Stephenson, D. B., Burn, J., Aguilar, E., Brunet, M., Taylor, M., New, M., Zhai, P., Rusticucci, M. and Vazquez-Aguirre, J. L. (2006) Global observed changes in daily climate extremes of temperature and precipitation. Journal of Geophysical Research, 111(D5). https://doi.org/10.1029/2005jd006290

Coles, S., Bawa, J., Trenner, L. and Dorazio, P. (2001) An introduction to statistical modeling of extreme values. London: Springer.

Dyson, L. (2009) Heavy daily-rainfall characteristics over the Gauteng Province. Water SA, 35(5). https://doi.org/10.4314/wsa.v35i5.49188

Lehmann, J., Coumou, D. and Frieler, K. (2015) Increased record-breaking precipitation events under global warming. Climatic Change, 132, 501-515. https://doi.org/10.1007/s10584-015-1434-y

Seneviratne, S. I., N. Nicholls, D. Easterling, C.M. Goodess, S. Kanae, J. Kossin, Y. Luo, J. Marengo, K. McInnes, M. Rahimi,M. Reichstein, A. Sorteberg, C. Vera, and X. Zhang (2012) 'Changes in Climate Extremes and their Impacts on the Natural Physical Environment', in Barros, C.B., Stocker,T.F., Qin,D., Dokken, D.J., Ebi, K.L., Mastrandrea, M.D., Mach,K.J., Plattner, G.-K,., Allen, S.K., Tignor, M., and Midgley, P.M. (ed.) Managing the Risks of Extreme Events and Disasters to Advance Climate Change Adaptation. Cambridge, UK, and New York, NY, USA: Cambridge, pp. 109-230.

Westra, S., Alexander, L. V. and Zwiers, F. W. (2013) Global Increasing Trends in Annual Maximum Daily Precipitation. Journal of Climate, 26(11), 3904-3918. https://doi.org/10.1175/jcli-d-12-00502.1

AN INVESTIGATION OF EXTREME VERY SHORT-TERM RAINFALL AT BOLEPI HOUSE IN ERASMUSRAND, TSHWANE FROM MAY 2003 TO APRIL 2018: IMPLICATIONS FOR DISASTER RISK REDUCTION ASSESSMENTS IN SOUTH AFRICA

By Jan H. Vermeulen

Introduction

Extreme short-term rainfall events mostly cause damage to infrastructure, property, the loss of livestock and even the loss of lives resulting from flash floods. Such extreme, very short-term or hourly rainfall events (Wu and Lin, 2017) are also referred to as downpours, cloudbursts or torrential rains across the world. For example, Nielsen and Schumacher (2018) describe a storm associated with a tornado on 30 October 2015 over south-central Texas, USA that produced up to 177 mm of rainfall per hour that led to flash flooding.

A South African example of a cloudburst happened at Linksfield, Johannesburg on 9 November 2016, where there was extensive damage to roads and hundreds of vehicles, with the tragic loss of seven lives from a severe or supercell thunderstorm (Caelum, 2017). The City of Johannesburg reported that this event also severely impacted 862 persons from 373 households in the Setswetla informal settlement, next to the Jukskei River in Alexandra, downstream from Linksfield (Mvulane, 2020). Measured at the O.R. Tambo International Airport (ORTIA), this downpour produced 83 mm of rainfall in the preceding hour ending at 18:10, with 17.2 mm as the highest 5-minute rainfall amount recorded at 17:35.

To forecast extreme weather events, the South African Weather Service (SAWS) has set up the National Forecasting Centre for Disaster Risk Reduction at its head office. The SAWS head office is located in the Eco Park, Centurion in the City of Tshwane Municipality, and prior to this, was located at Bolepi House (BH) building in Erasmusrand, City of Tshwane Municipality between May 2003 and April 2018. SAWS moved to Erasmusrand from the Forum Building in the city centre of Pretoria in early May 2003. Weather observation stations were located at both BH and the Forum Building, but not at the site of the current head office because the Irene Weather Office, which has an observation station, is only a couple of kilometres away to the east.

The World Meteorological Organization (WMO) requires a 30-year period for calculating the climate of an observation station (Wêreldspektrum, 1982). The current 30-year period prescribed by the WMO is from 1991 to 2020 (Arguez and Vose, 2011). Although the 15-year period available for BH measurements is only half a 30-year climate record, it gives extremes of 5-, 10-, 15-, 30-, 45-, 60- and 120-minute rainfalls - specifically, very short-term, or hourly rainfall events considered with the higher resolution 5-minute rainfalls providing finest detail. These extreme events need to be forecast accurately to reduce the risks of flash flooding disasters.

This article introduces the concepts of percentage cloudburst, percentage downpour and percentage shower and then applies them to the BH's 5-minute, hourly and daily rainfall observations from May 2003 to April 2018. Secondly, to determine various percentiles and highest of 5-minute, hourly and daily rainfalls at BH or Erasmusrand. The results compared to the highest values and expected maximums in the return period of 25 years for the City of Tshwane Municipality, formerly known as Pretoria, based on annual maximums (WB36, 1983). Results of downpours that have a rain rate (<= 25.0 mm/5-min) will be evaluated as possible extreme, very short-term or hourly rainfall forecast thresholds for Disaster Risk Reduction (DRR).

Data and methods

Daily, hourly, and 5-minute rainfall data for Erasmusrand was supplied by the SAWS. Daily rainfall data had 69 records missing, amongst them for December 2010, and consequently the data was 98.7% complete for the period from 20 May 2003 to 12 April 2018. In addition, between 1 January and 15 April 2005, daily rainfall amounts of 0.0 mm per day were archived in the database, except for 1.1 mm on 28 February 2005. As this period covers mid-summer to autumn in a summer rainfall region, data from this period is faulty. Therefore, this period is regarded as incorrect or faulty because there are always rainfall events January, February and March – and the correctness of the data set is 98.1%. The hourly and 5-minute data sets were 99.5 and 100% complete, respectively. Nearly 26 days' hourly rainfall data was missing from 22 May to 18 July 2003. The hourly and 5-minute data sets that both had no faulty data were 100% correct. As an example, although the hourly and 5-minute rainfalls for the 50.6 mm hourly rainfall at 13:00 on 30 December 2010 were correct and

available, the daily rainfall was missing, possibly because of communication challenges. The 50.8 mm daily rainfall for 30 December 2010 was calculated from hourly values.

Factors (percentage contribution in brackets) leading to gaps or missing data are tipping bucket blockages (41), network or communication problems (28), damaged parts (22) and others (9) (Lu and Zhang, 2020). The numbers in brackets, adding up to 100, give the percentage of each challenge or problem to missing 5-minute data. These may have been factors or reasons that contributed to hourly and daily rainfall sets of data at Erasmusrand not being 100 % complete. Faulty or incorrect data removed during Quality Control process of SAWS resulted in data being 99.9 % correct.

The daily, hourly, and 5-minute rainfall data sets were received from Climate Services in Excel spreadsheets. Each set was checked for missing and faulty data and all the sets were sorted from the largest to the smallest rainfall amounts, with zero's being discarded. This then highlighted the highest rainfalls for each set and enabled the calculation of various percentiles for each set.

An inspection of 17 5-minute rainfalls bigger than 8.3 mm revealed 14 storm events. The American Meteorological Society's Glossary of Meteorology (2015) uses a threshold of 100 mm/h rainfall intensity to identify a cloudburst. In other words, rainfall of cloudburst intensity must equal or exceed 100 mm/h or 8.33 mm in five minutes. The start, duration, rainfall and highest 5-minute rainfall of the 14 storms were determined, and then the highest 5-minute accumulated 10-minute, 15-minute and hourly rainfalls were determined for each event. If the highest 5-minute rainfall is bigger than 25.0 mm it is a cloudburst, and the associated highest hourly rainfall is the percentage cloudburst. If highest 5-minute rainfall is bigger than 8.3 mm and smaller than or equal to 25.0 mm it is a downpour, and the associated highest hourly rainfall is the percentage downpour. When highest 5-minute rainfall is smaller than or equal to 8.3 mm it is a shower, and the associated highest hourly rainfall is the percentage shower.

It is instructive to distinguish between 5-minute-, 10-minute-, 15-minute-, etc. downpours as follows: if highest 10-minute rainfall is bigger than 16.7 mm it is a 10-minute-downpour, if highest 15-minute rainfall is bigger than or equal to 25 mm it is a 15-minute-downpour, etc. Multiples of 8.33 mm/5-minutes are considered, meaning that a 5- or 10-minute- downpour has cloudburst intense rain for 5 or 10 minutes, respectively etc. Twelve is the number of 5-minute periods in an hour. The daily rainfall for each event found in the daily rainfall set.

Results and discussions

The 5-minute, hourly and daily rainfall data from the weather station at BH, Erasmusrand revealed there were zero cloudburst (> 25 mm/5-min) events but fourteen downpour (> 8.3 mm/5-min) storms. For Erasmusrand there was zero 15-minute-downpours, four 10-minute-downpours, ten 5-minute-downpours and a multitude of showers of which eight are presented in Table 1.

Table 1: Percentage 10-minute, percentage 5-minute downpours and percentage showers with date, start time, duration, rainfall, storm rate and highest of 5-minute, 10-minute and 15-minute as well as daily rainfall for the Bolepi House, Erasmusrand building from May 2003 to April 2018.

% Downpours	Date	Start time	Duration (min)	mm	Rate (mm/h)	5-Minute	10-Minute	15-Minute	Daily R
50,6	30/12/2010	12:10	50	50,6	61	9,6	18,4	23,8	50,8
37,4	13/1/2005	23:15	55	37,4	41	9,8	18,2	24,4	37,6
28,8	19/12/2014	19:00	45	28,6	38	10,4	17,0	22,8	28,8
23,2	22/11/2011	20:20	35	22,8	39	9,8	17,8	19,4	30,2
Averages: 35,0			**46**	**34,9**	**45**	**9,9**	**17,9**	**22,6**	**36,9**
% Downpours									
43,6	2/12/2013	15:55	60	43,6	44	9,6	15,0	17,6	48,6
32,4	15/12/2014	17:45	60	32,4	32	10,0	15,4	20,2	36,4
32,2	17/2/2007	20:05	55	32,2	35	8,6	13,8	21,2	36,3
30,4	23/11/2012	23:45	40	30,4	46	8,6	14,0	19,2	36,8
25,6	20/03/2011	16:25	60	25,6	26	9,4	16,6	18,0	33,0
24,2	10/11/2016	17:55	60	24,2	24	9,6	16,0	17,4	49,0
22,6	29/03/2008	13:50	55	22,6	25	8,6	14,4	18,6	24,6
20,2	4/11/2005	17:15	35	19,8	34	9,8	15,8	17,4	20,5
18,4	4/12/2007	20:15	35	18,4	32	9,0	14,8	16,6	22,8
12,4	22/10/2016	2:50	20	12,4	37	11,0	11,8	12,2	12,6
Averages: 26,2			**48**	**26,2**	**33**	**9,4**	**14,8**	**17,8**	**32,1**
% Showers									
38,8	29/01/2010	20:50	60	38,8	39	5,6	10,4	14,8	41,2
36,8	18/01/2008	14:40	60	36,8	37	5,8	10,6	16,4	42,2
34,6	17/02/2015	1:55	45	34,4	46	6,8	12,8	17,6	35,2
27,8	23/04/2010	16:30	60	27,8	28	5,8	11,6	14,8	43,6
27,8	21/03/2018	18:40	60	27,8	28	5,2	9,8	14,2	42,6
25,2	15/12/2010	20:30	60	25,2	25	7,8	14,4	18,0	77,0
24,2	4/04/2010	13:05	60	24,2	24	6,4	10,2	10,2	41,4
22,0	30/09/2017	21:55	60	22,0	22	3,6	7,2	10,2	32,2

The 30 December 2010 50.6 % downpour is the highest hourly rainfall (mm) for Erasmusrand. This thunderstorm also has the highest storm rainfall rate of 61 mm/h for its 50 minutes duration. Heavy downpours were forecast for the day with a passing upper trough. Figure 1 indicates a high pressure system ridging to the south of the country, with a low pressure over the Northern Cape. A ridging high to the south of South Africa is indicative of an-upper air trough affecting the country (Van Heerden and Hurry, 1992). The 30 December 2010 and 13 January 2005 downpours had three and two 5-minute rainfalls bigger than 8.3 mm, respectively in their downpours and the remaining twelve downpour events had one each.

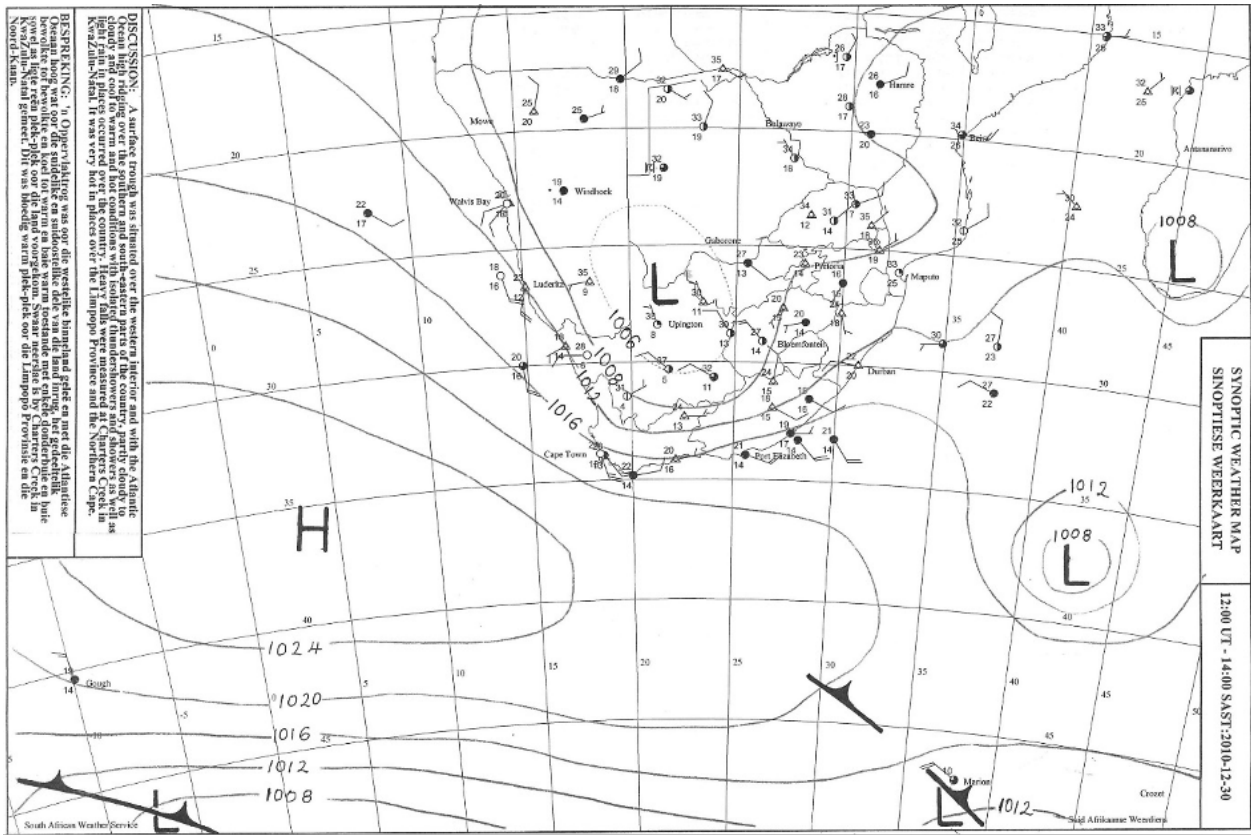

Figure 1: Synoptic weather map for 30 December 2010

The average storm rainfall rates of the downpours-10 and downpours-5 are 45 and 33 mm/h, respectively. Table 1 indicates three 5-minute values bigger than or equal to 10.0 mm which is also called a frequency. Kruger and Mbatha (2021) reports for 5-minute rainfalls bigger than or equal to10.0 mm frequencies of 14 and 5 for Irene and OR Tambo International Airport (ORTIA), respectively for the 1991 to 2020 period. The 15-year climate frequency of three for Erasmusrand extrapolate to a frequency of six for thirty years. The frequency of 6 of the Erasmusrand events compares well with the frequencies of 5 and 14 for ORTIA and Irene, respectively. The Irene and ORTIA weather stations are fairly close to one another in the Gauteng Province.

Start time means the beginning of the Percentage-downpour (D) storm. The Duration of storms that were 60 minutes were usually longer. This means that there was sometimes more rainfall after D or the hour of maximum rainfall. The Rainfall of storms with a Duration of less than 60 minutes are smaller or equal to D. When the Rainfall of the Duration is less than D, it means that some rain fell in remainder of the hour of D.

The highest recorded 5-minute rainfall is 11.0 mm, which occurred during 20 minutes from a 5-minute-downpour of 12.4 mm on 22 October 2016. The second highest recorded 5-minute rainfall of 10.4 mm occurred during a 45 minutes duration 10-minute-downpour of 28.8 mm on 19 December 2014 (see Table 1).

The highest 15-minute rainfall, 24.4 mm, occurred during the 55 minutes duration of the 10-minute-downpour, 37.4 mm, on 13 January 2005. The highest hourly rainfall, 50.6 mm, occurred during a fifty minute duration 10-minute-downpour and the second highest hourly rainfall, 43.6 mm, occurred during a sixty minute duration of a 5-minute-downpour. The average hourly rainfall, 35.0 mm of the 10-minute-downpours is 8.8 mm more than average of the 5-minute-downpours. In addition, the average 15-minute rainfall, 22.6 mm of the downpours-10 is 4.8 mm more than the average of the downpours-5. In summary, the 10-minute-downpours, although less frequent, produced on average higher hourly rainfalls and storm rainfall rates than the 5-minute-downpours.

The 14 downpours all occurred from October to March, during the rainfall season. December's five events are the highest frequency followed by the four for November. Zero downpours occurred in the dry season from April to September. The highest 5-minute rainfall, 7.6 mm, was

at 13:40 on 7 May 2011 with an hourly rain of 9.6 mm and 10.0 mm daily rainfall. The 7 May 2011 storm was a 9.6 % shower. The highest percentage shower, 38.8 mm, was at 21:50 on 29 January 2010 with a 41.2 mm daily rainfall. The highest percentage shower of the dry season, 27.8 mm, was at 17:30 on 23 April 2010 with a 43.6 mm daily rainfall.

The 99.99, 99.9, 99, 90 and 50 percentiles and highest of rainfalls are presented in Table 2 along with the date and time of the highest event. Lastly the highest 15-minute, 30-minute, 45-minute, hourly and daily rainfalls of BH in Erasmusrand compared with highest for month and year of Pretoria - Lynwood Road climate station from WB36 (1983).

Table 2: Percentiles, highest and Date&Time of highest for BH, Erasmusrand rainfalls (mm) from May 2003 to April 2018 compared with the highest measurements of the Pretoria weather station (0513405A2) for 1938 to 1972 from WB36.

	Percentiles					Highest	DateTime	WB36 Highest	
	99.99%	99.9%	99%	90%	50%			Month	Year
Daily		121,1	46,6	22,2	4,0	121,1	22-Mar-2018	91,7	135,1
Two-hourly						50,8	30-Dec-2010 2:00 PM		
Hourly	50,6	32,2	18,2	5,2	0,8	50,6	30-Dec-2010 1:00 PM	44,2	75,1
%-Downpour						50,6	30-Dec-2010 1:00 PM		
45-Minute						50,2	30-Dec-2010 12:55 PM	43,3	61,0
30-Minute						39,6	30-Dec-2010 12:40 PM	40,0	48,0
15-Minute						24,4	13-Jan-2005 11:30 PM	23,4	33,5
10-Minute						18,4	30-Dec-2010 12:25 PM		
5-Minute	10,4	8,0	4,2	1,0	0,2	11,0	22-Oct-2016 3:00 AM		

The daily percentile 99.9% of 121 mm indicates a monthly extreme rainfall event whereas 99% of 47 mm indicates a possible heavy rainfall event, and 99.9 % is the same as highest rainfall (121 mm). The 22 March 2018 flooding in Pretoria was caused by a cut-off-low system bringing 229 mm daily rainfall to the Mountain View area.

The hourly percentile 99.99% of 50.6 mm indicates a monthly extreme rainfall event, 99.9 % of 32.2 mm indicates a possible heavy rainfall event, 99% of 18 mm significant rainfall and 99.99% is the same as highest rainfall (50.6) mm. The 30 December 2010 event discussed in Table 1 also gave the highest two-hourly rainfall of 50.8 mm that was also equal to the daily rainfall. The highest two-hourly rainfall was determined by inspection of sorted hourly rainfalls. The 30 December 2010 downpour also gave the highest 45-minute, 30-minute and 10-minute rainfalls of 50.2, 39.6 and 18.4 mm respectively, for Erasmusrand.

The 5-minute percentile 99.99% of 10.4 mm indicates possibly an extreme rainfall event, 99.9% of 8.0 mm indicates nearly cloudburst intense rainfall of 96 mm/h and 99% of 4.2 mm indicates a significant rain shower. The 99.99%, 10.4 mm, is smaller than the highest 5-minute rainfall of 11.0 mm during a downpour that produced 12.4 mm in 20 minutes (see Table 1).

The highest 15-minute rainfall of 24.4 mm on 13 January 2005 is included for comparison with Pretoria- Lynwood Road in WB36 (1983). The 37.4 percentage downpour on 13 January 2005 caused by an upper-air trough system. Erasmusrand's highest rainfall for 15-minute, 45-minute, hourly and daily rainfalls are all greater than the corresponding month's highest measurements for Pretoria for a 35-year period of recording, but smaller than the highest for the year. These highest rainfalls for the year were all in November for Pretoria - from 1938 to 1972. The smaller highest of Erasmusrand, when compared to highest for the year expected because of a 15-year observation period compared with a 35-year period of observation. Erasmusrand's 30-minute rainfall of 39.6 mm is smaller than the 40.0 mm for December for Pretoria from 1938 to 1972.

The Percentage-downpour (D) or maximum accumulated hourly rainfall of 50.6 mm indicated because it is often higher than the hourly rainfall. For example, Pretoria Mountain View reported 43.8 mm 17:00 on 20 November 2020 while the D was 63.6 mm 17:35 for storm caused by upper air trough system. The D or maximum hourly rain rate is the highest 5-minute accumulated hourly rainfall of a storm.

The three highest measurements of 15-minute, 30-minute, 45-minute, hourly and daily rainfalls of Erasmusrand are compared in Table 3 with monthly and annually based estimated maximum rainfalls in return period of 25 years (EMiRP25) of Pretoria for 1938 to 1972

from WB36 (1983). This extremity test indicates seven events are monthly extreme while only two annually.

Table 3: Three highest and Date&Time for BH in Erasmusrand rainfalls (mm) from May 2003 to April 2018 compared with Estimated Maximum rainfalls in Return Period of 25-years (EMiRP25) of Pretoria

			WB36	
	Bolepi House		Monthly	Annually
	Highest	DateTime	EMiRP25	EMiRP25
Daily	121,1	22-Mar-2018	80,6	107,2
	97,0	09-Mar-2016	80,6	107,2
	79,4	03-Mar-2014	80,6	107,2
Hourly	50,6	30-Dec-2010 1:00 PM	39,4	51,0
	43,6	02-Dec-2013 4:55 PM	39,4	51,0
	38,8	29-Jan-2010 9:50 PM	43,0	51,0
45-Minute	50,2	30-Dec-2010 12:55 PM	35,8	47,6
	38,2	02-Dec-2013 4:45 PM	35,8	47,6
	36,8	14-Jan-2005 12:00 AM	39,2	47,6
30-Minute	39,6	30-Dec-2010 12:40 PM	30,0	40,9
	31,8	13-Jan-2005 11:45 PM	32,8	40,9
	30,4	17-Feb-2015 2:30 AM	26,7	40,9
15-Minute	24,4	13-Jan-2005 11:30 PM	22,5	27,7
	23,8	30-Dec-2010 12:30 PM	19,6	27,7
	22,8	19-Dec-2014 7:20 PM	19,6	27,7

The maximum highest measurements of Erasmusrand for 15-minute to daily rainfalls are all larger than the monthly based EMiRP25 making them monthly extreme events. The 50.2 mm in 45-minutes 30 December 2010 and 121.1 mm daily 22 March 2018 are only two cases that are extreme, based on annually estimated maximums. Annually-based tests that are stricter are probably the best to decide the extremity of an event or storm, but they disregard seasonality. In summary, monthly and annual tests have pros and cons.

Impacts

Widespread flooding in the City of Tshwane Municipality resulted from the extreme daily rainfall of 121.2 mm on 22 March 2018 at Erasmusrand (Table 3), preceded by a 27.8 mm Percentage-shower (Table 1) the previous day. Erasmusrand received 163.7 mm of rain on 21 to 22 March 2018 from a cut-off low system. Mountain View reported 343.6 mm for the two days and had a 76.4 mm Percentage-downpour on 21 March 2018. This downpour produced 60.2 mm in 35 minutes and had a daily rainfall of 114.6 mm. The 76.4 mm > 51.0 mm annually based hourly 25-year return period for Pretoria (Table 3) makes the Mountain View storm an extreme event.

Streams in the area burst their banks from the 50.6 mm in 50-minutes lunchtime downpour on 30 December 2010. This 10-minute-downpour's intensity was remarkably memorable. The 22 November 2011 10-minute-downpour with D of 23.2 % initiated local flooding while impacts for the remaining two 10-minute-downpours are possibly negligible. Impacts of the identified 5-minute-downpours were however not investigated. The 4 April 2010 dry season storm with a 41.4 mm daily rainfall was a 24.2 % shower which caused flash flooding of the Moreleta spruit (see Figure 2); a tributary of the Tshwane River (formerly known as Apies River).

Figure 2: Kimiad stream overflowing in Moreleta Park on the afternoon of 4 April 2010

Conclusions

The study indicated there were four 10-minute-downpours (10-minute rainfall > 16.7 mm) over the 15-year period at Erasmusrand. This means that one 10-minute-downpour could be expected every 3.5 to 4 years. The 51 % downpour of 30 December 2010 was the highest 10-minute- downpour. There were ten 5-minute-downpours (10-minute rainfall < 16.7 and 5-minute > 8.3 mm) over the 15-year period. One 5-minute-downpour per year can be expected for every two out of three years. The 44% downpour of 2 December 2013 was the highest 5-minute-downpour. All downpours grouped together give a total of fourteen for the 15-year period of observation. It means that roughly one downpour per year could be expected at Erasmusrand or Pretoria.

The hourly data set of Erasmusrand is 99.5% available and 100% correct, the 5-minute data set of Erasmusrand is 100% available and 100% correct. Both hourly and 5-minute data sets were better quality than the daily data set that was 99% available and 98% correct. The 100% availability of the five-minute data set meant that daily rainfalls were calculated where necessary. Five-minute data was the best of the three sets, followed by hourly.

References

American Meteorological Society. 2015. AMS Glossary of Meteorology:

http://glossary.ametsoc.org/wiki/Main_Page

Arguez A. and Vose R.S., 2011: The definition of the standard WMO Climate Normal: the key to deriving alternative climate normals. Bulletin of the American Meteorological Society, 92(6), 699-704.

Caelum, 2017: Caelum – 1991 to 2016, unpublished Newsletter, South African Weather Service, Pretoria, South Africa.

Kruger, A.C. and Mbatha, S., 2021: Regional weather and climate of South Africa: Gauteng, Weather Smart, October, 45-46.

Lu, J. and Zhang, X., 2020: Auto station precipitation data making up using an improved neuro net. Meteorological Applications, 27(6), e1960.

Mvulane P., 2020: Settling on water pathways: A case study of Setswetla vulnerability to flash floods. MSc Dissertation, University of Witwatersrand, Johannesburg.

Nielsen, E.R and Schumacher, R.S, 2018: Dynamical insights into extreme short-term precipitation associated with supercells and mesovortices, Journal of Atmospheric Sciences, 75, 2983-3009.

Van Heerden, J. and Hurry, L., 1992: Suider-Afrikaanse Weerpatrone, Via Afrika Beperk, p31.

WB36, 1983: Climate of South Africa, Weather Bureau (WB) 36: Part II, Third Edition.

Wêreldspektrum, 1982: Klimaat, Ensiklopedie Afrikana, 15, p. 42.

Wu, M. and Lin, G., 2017: The very short-term rainfall forecast for a mountainous watershed by means of an ensemble weather prediction system in Taiwan. Journal of Hydrology, 546, 60-70.

DRIER AND WARMER START FOR THE 2022 WINTER OVER THE WESTERN CAPE

By Elani Heyneke

South Africa, especially the Cape Town Metropole, was in the limelight during 2017 when Day Zero was slowly approaching. Should this have materialised, the City of Cape Town would have been the first global metropole to have dry taps due to a multi-year drought. This multi-year drought occurred between 2015 until 2017, when below normal rainfall had been observed. Fortunately, a few weeks before Day Zero, sufficient rain fell in the catchment area and Day Zero was then postponed. Finally, when the dam levels recovered, Day Zero and the strict water restrictions were lifted and Capetonians could once again go back to normal life. Coincidentally, they have been very water-wise since the dreadful ordeal that they encountered.

The south-western parts of the Western Cape have been blessed with normal to above-normal rainfall since 2019, with the veldt and dam levels recovering to pre-drought conditions. For this study, the 2021 yearly rainfall accumulation over the Western Cape will be compared to that of 2022 as well as with the Long Time Average (LTA - 20-year period). The lowest yearly accumulated rainfall was observed during 2017, at the end of the multi-year drought, and by 2018, the accumulated rainfall amounts started to increase on a yearly basis as seen in Figure 1. The 2021 yearly accumulated rainfall amount was higher compared to the LTA. By comparing the first half of 2021 with 2022, it can be seen that April, May, and July were much drier than the previous year, although there was a spike in rainfall during June 2022.

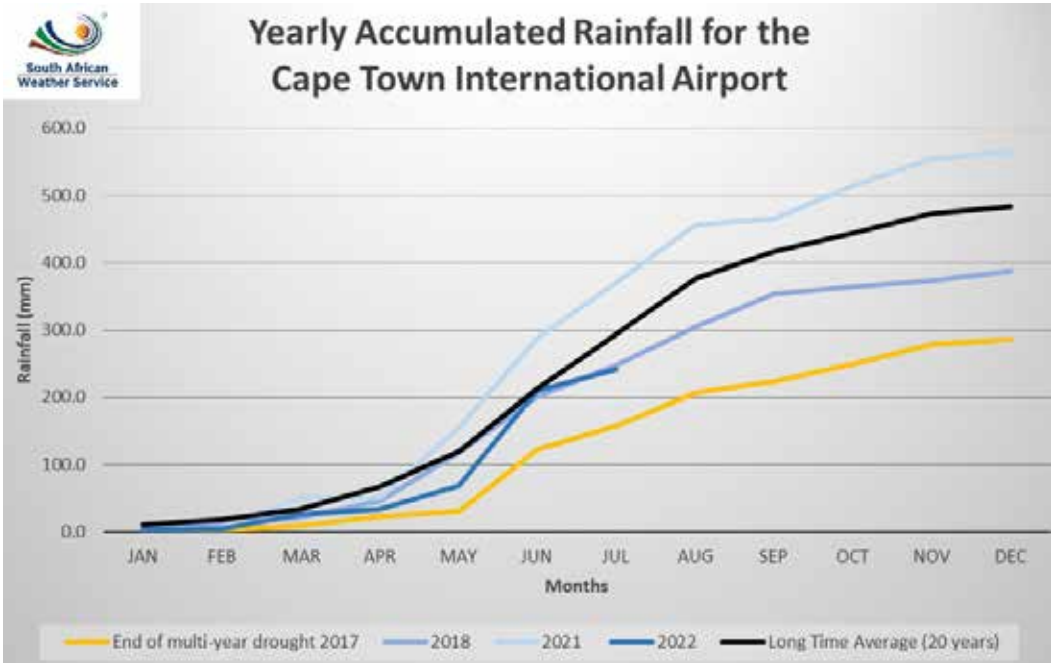

Figure 1: Yearly accumulated rainfall for the Cape Town International Airport (Source: SAWS)

At the start of 2022, the seasonal outlook was looking bleak for the south-western parts of the Western Cape, with normal to above-normal temperatures and normal to below-normal precipitation expected for the winter rainfall region. This outlook implied a possible warmer and drier season and has sparked some interest from the public, since the multi-year drought was still fresh in Capetonians' minds.

The accumulated rainfall for the Cape Town International Airport for the start of 2022 was still close to the LTA as seen in Figure 1, although this trend dipped below the average during April and May. The spike seen during June 2022 is a very interesting case, since 82% of the total rainfall measured during this month occurred over a three-day period as seen in Figure 2. During June 2022, two records were broken. Firstly, the highest day

(maximum) temperature for the month of June at the Cape Town International Airport (30.9°C) on 7 June 2022. Secondly, a week after this event, the highest 24-hour rainfall measured since 1960 was reported at the Cape Town International Airport (80.4 mm).

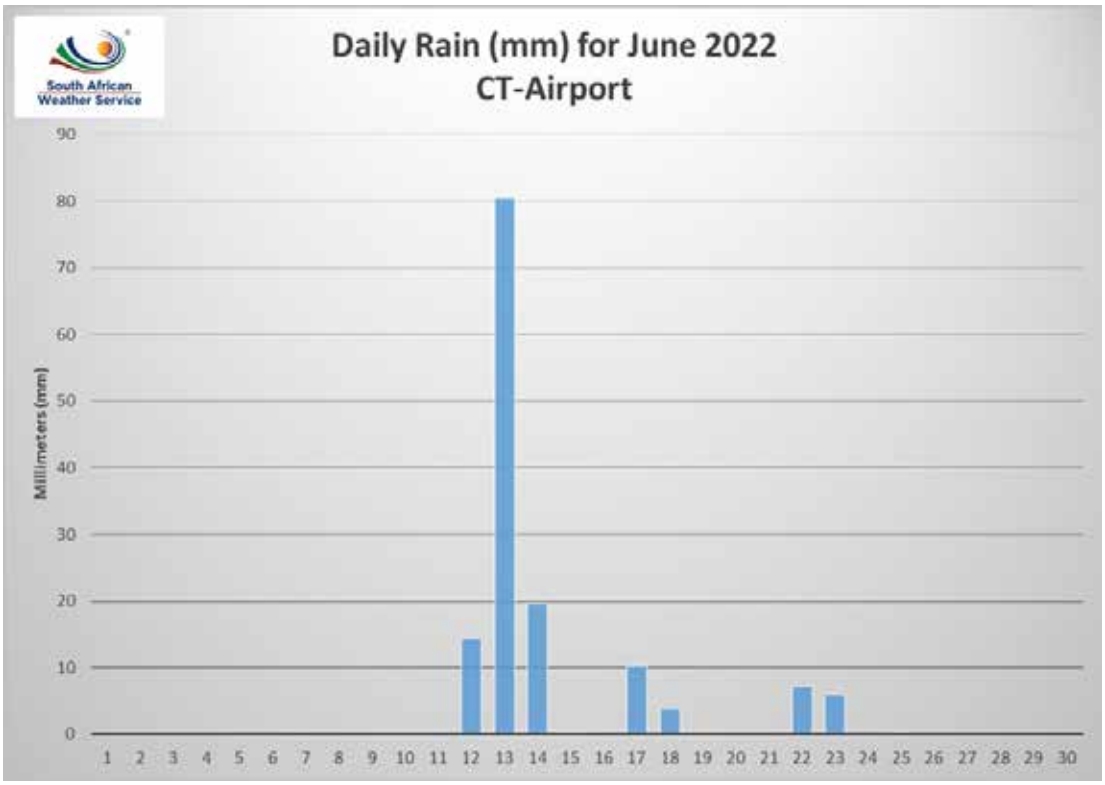

Figure 2: Daily Rainfall (mm) for June 2022 measured at the Cape Town International Airport (source: SAWS)

This is evidence that, should one or two significant weather systems affect the south-western parts of the Western Cape during the remainder of August and September, the yearly-accumulated rainfall trend can normalise (be closer to the LTA). Unfortunately, in an event where this should not occur, the winter of 2022 will indeed be a below-normal year in terms of rainfall amounts. However, the winter rainfall region can still receive rainfall during summer, especially since the seasonal outlook is indicating a possibility of a normal to above-normal summer rainfall season.

A few thoughts and comments that can be taken from this study is the following:

1. Droughts and flood events will always be part of nature. The way humans handle and plan for such events is crucial in order to ensure the safety of humans and animals as well as to protect property and livelihoods.

2. Even though a drier rainfall season is predicted, it does not exclude a couple of flooding events as seen during June 2022 over the Cape Metropole. A below-normal rainfall season/period is considered a hit when the measured accumulated rainfall for that period is below the average, even if it is with 1 mm.

3. The Capetonians learned hard lessons during the multi-year drought (2015-2017) and adapted to being water-wise. Therefore, it is each and everyone's responsibility to look after our natural resources to ensure that the future generation can enjoy nature and clean drinking water.

NEW REGIONAL WEATHER AND CLIMATE SUMMARY: SOUTH-WESTERN CAPE

By Andries Kruger, Sifiso Mbatha and Sandile Ngwenya

Introduction

The Department: Climate Service will soon release the second publication in the series of Regional Climate and Weather Summaries (https://www.weathersa.co.za/home/regionalweatherclimate) which focuses on the South-Western Cape. The series intends to provide a broad overview of the climate and weather of different regions in South Africa, especially those regions that are of relative greater economic and/or demographic significance in the country. The South-Western Cape publication is comprehensive and consists of 79 figures and graphs, 15 tables and comprises almost 60 pages.

It is the view that these publications should present baseline information on the weather and climate of a particular region. This article presents a summary of the contents of the publication and those aspects of the weather and climate which, in general, can be expected to be included in forthcoming publications for other regions.

The first publication, on Gauteng, is freely available from the SAWS website. This publication and new annual editions will be available through SABINET.

Topics covered

The eventual topics which were decided on for inclusion in the publications broadly follow those included in the series of SAWS publications that provide overviews of the South African climate and are mainly divided into a range of common weather parameters. The first of these publications on surface winds and which covered the whole country, was completed in 2002. The publications that followed were developed according to the same principle, with the last one, published in 2008, on surface temperature. The above publication series covered their individual topics in detail, and it was envisaged in the planning phase that the regional climate publications will at least cover most of the relevant aspects of the climate included in this series. In addition to the above publications, a range of additional content that could potentially be included in the new publication was identified from a desktop analysis of international publications. Thereafter the proposed content was arranged into a coherent structure.

Contents

The content of the summary follows a logical structure, with an introduction explaining the factors that control the region's climate and therefore the general climate in relation to other climate regimes in South Africa. Following this introduction, the main climate parameters in which the envisaged audience will mostly be interested in are discussed in detail in separate chapters. A conclusion chapter discusses the impact of climate change on the region through evidence of observed climate change and its impacts.

Introduction

The factors influencing the weather and climate are presented, how the province is situated in relation to the diverse climate regions of South Africa and the differences in weather experienced on a seasonal basis. The region covered is presented in Figure 1 and is situated in the extreme south-west of South Africa, experiencing relative moderate weather and climate conditions. The Csa (winter rain with hot summers) and Csb (winter rain with cool summers) dominate the region and coincide with the climate region named the South-Western Cape climate region, according to a more detailed classification system developed by SAWS, as presented in Figure 2.

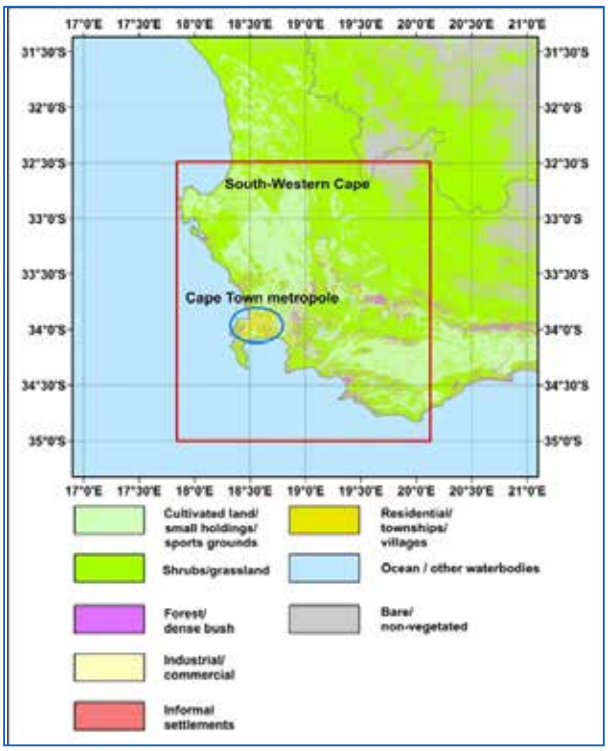

Figure 1: The South-Western Cape region (presented as the red rectangle) with the Cape Town Metropole in the blue encircled area (covered mostly by industrial and commercial activities and residential areas).

Wind

The climate controls described in the previous section have a direct influence on the general wind field over the region. The high-resolution wind resource map developed by the Wind Atlas for South Africa project (WASA: www.wasaproject.info) is included and sheds more light on the spatial variation of the average wind speed in the region. The wind speed tends to follow the topography, with the mountainous and higher-lying areas experiencing higher wind speeds. However, the coastal areas around the Cape Peninsula and further to the east also exhibit high wind speeds in general, as presented in Figure 3.

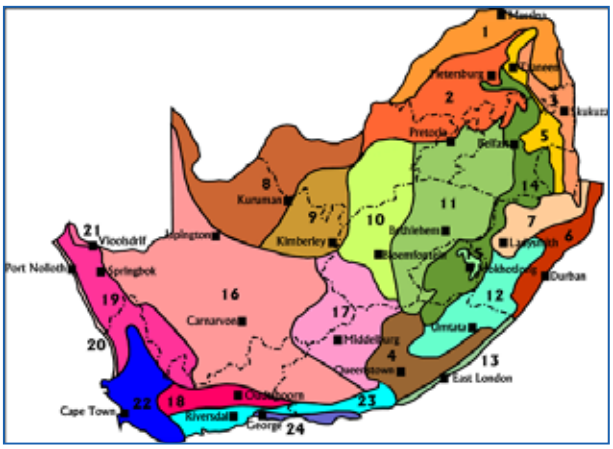

Figure 2: The Climatic Regions of South Africa: 1. Northern Arid Bushveld 2. Central Bushveld 3. Lowveld Bushveld 4. South-Eastern Thornveld 5. Lowveld Mountain Bushveld 6. Eastern Coastal Bushveld 7. KwaZulu-Natal Central Bushveld 8. Kalahari Bushveld 9. Kalahari Hardveld Bushveld 10. Dry Highveld Grassland 11. Moist Highveld Grassland 12. Eastern Grassland 13. South-Eastern Coast Grassland 14. Eastern Mountain Grassland 15. Alpine Heathland 16. Great and Upper Karoo 17. Eastern Karoo 18. Little Karoo 19. Western Karoo 20. West Coast 21. North-Western Desert 22. Southern Cape Forest 23. South-Western Cape 24. Southern Cape.

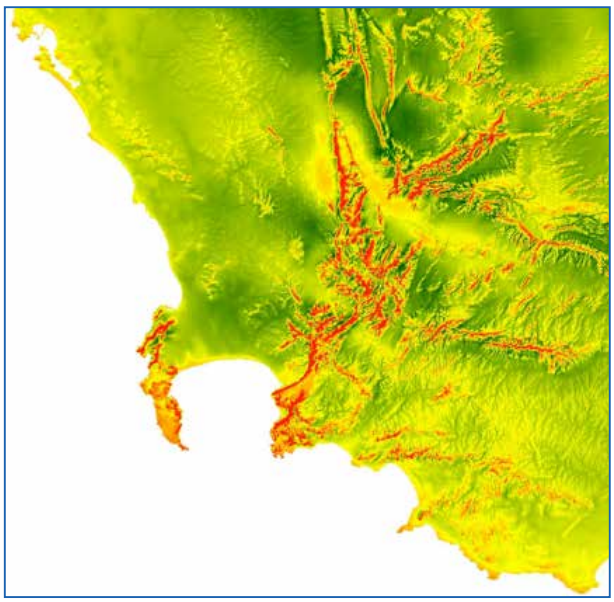

Figure 3: WASA High Resolution Wind Resource Map for the South-Western Cape. Mean wind speed (m/s) at 50 m above ground with lower wind speeds in green (< 3 m/s) and higher wind speeds in red (> 7 m/s) (www.wasaproject.info).

Also discussed are the annual and diurnal variation of wind speed and strong winds of short duration and the causes thereof. For example, Figure 4 presents the 5-minute measurements of wind gust (m/s), wind direction (degrees), surface temperature (°C), rainfall (mm) and surface pressure (hPa) at the Cape Town International Weather Office on 24 June 1997, when one of the strongest wind gusts was recorded at the station. This strong wind gust occurred during the passage of a cold front.

Figure 4: 5-Minute measurements of wind gust (m/s), wind direction (degrees), rainfall (mm) and surface pressure (hPa) at Cape Town International on 24 June 1997.

Surface temperature

The average surface temperature is governed by the general circulation patterns and topography, amongst others. Thismeans that seasonal temperatures, as well as minimum and maximum temperature, are presented in map format, from which it can for example be deduced that the northern parts of the region generally experience higher temperatures than the south (this feature of surface temperature is related to the topography, where lower (higher) elevations experience higher (lower) temperatures). In addition, it is evident that the ocean has a moderating effect on the surface temperature, especially in winter. As an example, Figure 5 presents the mean winter (JJA) minimum temperature (°C) over the South-Western Cape, based on topography and measured data over the period 1991 – 2020.

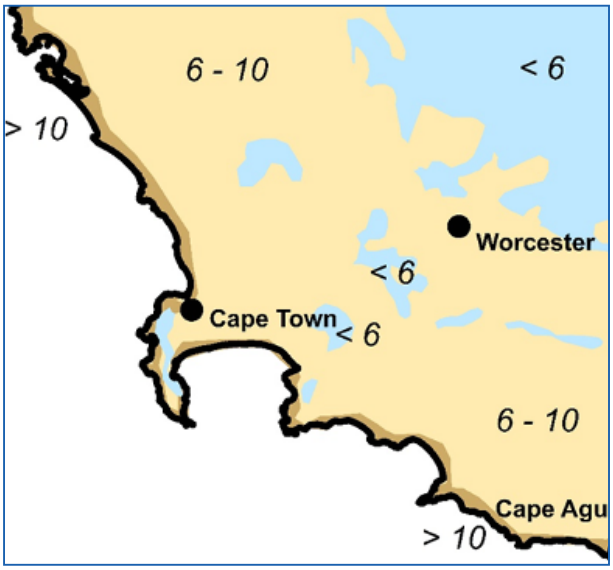

Figure 5: Mean winter (JJA) minimum temperature (°C) over the South-Western Cape, based on topography and data over the period 1991 – 2020.

Extreme temperatures and the synoptic conditions that occurred during the recording of all-time maximums and minimums are discussed in detail. Figure 6 presents the highest ever temperature recorded in the region, i.e. 46,1°C at the Paarl automatic weather station.

Figure 6: 5-Minute graph of surface temperature measured on 7 March 2010 at Paarl automatic weather station.

In addition, frequency tables of temperature in specified ranges of 5°C at specified times for some automatic weather stations in the province are included. The topics of apparent temperature and the likelihood of frost are discussed.

Sunshine and Cloudiness

The South-Western Cape receives a relative high amount of sunshine, compared to the rest of the world, but not particularly so for South Africa. The province receives mostly between 60% and 70% of the maximum possible sunshine. In comparison the western interior receives more than 80% and the east coast mostly below 55%. This spatial variation of mean sunshine received over the country is presented in map format, with additional monthly maps. An analysis of daily sunshine shows that, on an annual basis, Cape Town International Airport experiences less than 10 overcast days, in the region of 20 cloudy days, about 280 sunny days and about 150 fine days, with the last mentioned mostly occurring in the summer. The monthly variation of the days is presented graphically in Figure 7.

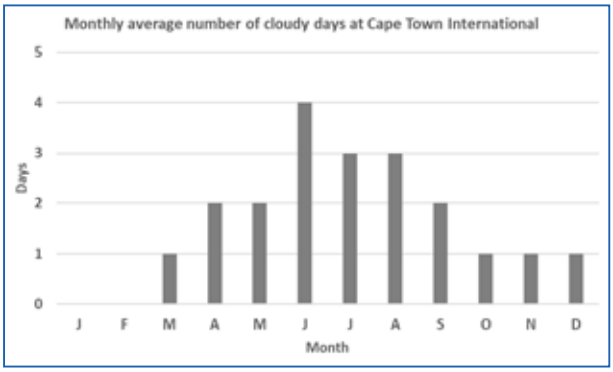

Figure 7: Average number of cloudy days at Cape Town International Airport (1991 – 2020).

With the drive to change from fossil fuels to renewable energy sources, it is primarily wind and solar energy that have both become increasingly important for our future energy needs. While the South-Western Cape's position in the south of South Africa makes the local exploitation of wind for energy generation very viable, the use of solar energy is also an option as a source of energy in the province. Solar energy resource information is widely available, particularly in atlas format. Developers and users of solar energy are mostly interested in the direct normal irradiation, global horizontal irradiation, and resultant power potential. Atlases with this information are readily available from the Global Solar Atlas web portal (https://globalsolaratlas.info/), endorsed by the World Bank, and presented in the publication.

Precipitation

As an introduction, the annual and seasonal distribution of rainfall is presented in map format, in Figure 8.

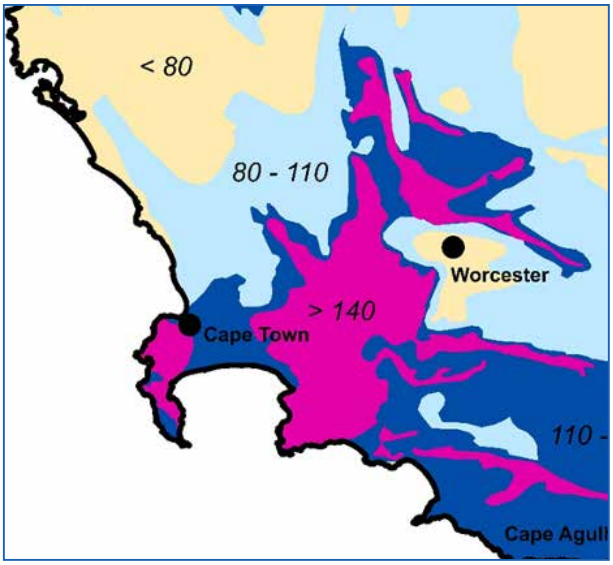

Figure 8: Mean autumn (MAM) rainfall (mm) based on topography and data over the period 1991 – 2020 (yellow < 80, light blue 80 - 110, dark blue 110 - 140, purple > 140 mm).

The frequencies of wet and dry years, the Standardised Precipitation Index (SPI) and the Standardised Precipitation Evaporation Index (SPEI) and trends thereof over the long-term is discussed (see Figure 9).

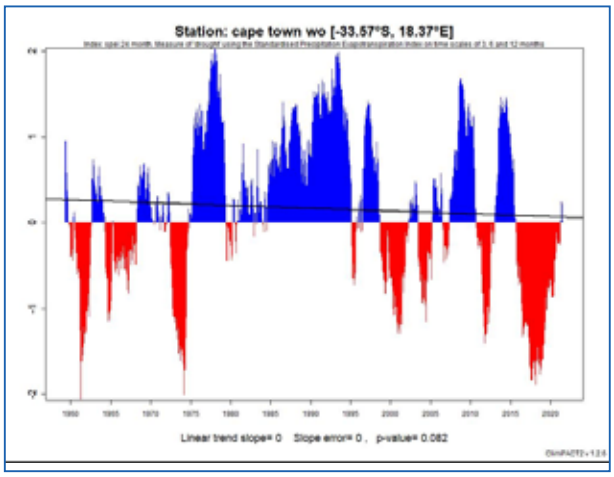

Figure 9: 24-month SPEI for Cape Town International Airport (1957 – Sep 2021).

Following on the above the average number of rainy days per month, above specific thresholds are presented, as well as the likelihood of rainfall during specific hours of the day in the different seasons.

Floods are usually caused by persistent rainfall of various intensity over a prolonged period or a lot of rainfall over a short period of time. In the South-Western Cape, most flooding is caused by the former, but high rainfall amounts over shorter periods of time also occur from time to time. The automatic weather station technology that SAWS utilises provides the rainfall amounts to a frequency of five minutes. The frequencies with which the rainfall exceeded 5 mm, 10 mm, and 15 mm within a five-minute period over the 1991 – 2020 period were analysed and are presented in tabular format. In addition, the mean monthly frequencies of reported heavy precipitation events are presented.

Climate change

Due to the increase in greenhouse gases since the Industrial Revolution, of which carbon dioxide is the most important, the atmosphere has been gradually warming over a long period of time. The increase in atmospheric warming can be traced back for centuries and has increased over the last 100 years by about 1°C. The long-term changes in the climate and extreme weather occurrences are discussed. For example, Figure 10 presents the annual average surface temperature deviation at OR Tambo International Airport for the period 1951 to 2020, which clearly indicates a warming trend close to 0,25°C/decade over the analysis period. The hottest year was 1999, with the 19 hottest years on record since then.

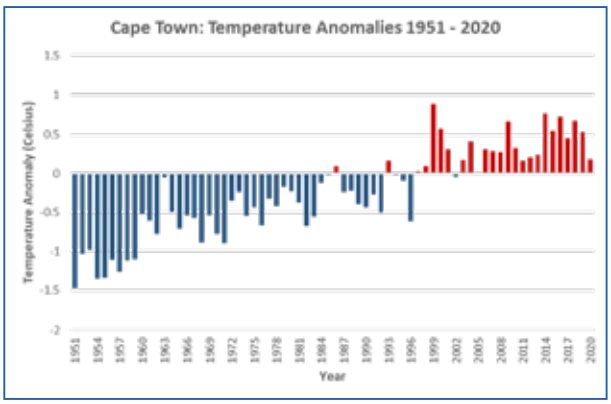

Figure 10: Annual average surface temperature deviation at Cape Town International Airport for the period 1951 to 2020 (base period: 1981 – 2010).

As mentioned, climate change is mostly experienced through increased occurrences of anomalous weather events, e.g. very hot days. The trends in the frequencies of extreme events in the province, in comparison to the rest of the country, are discussed.

An assessment of the frequencies of specific weather events (e.g. floods) over a long period of time can only be done through an analysis of media reports. SAWS produces the CAELUM publication which provides a geocoded list of significant weather events which were reported in South Africa from 1647. It should be noted that such reports are highly dependent on demographics and population density, where a relatively high population density and the presence of the print media and other documenters makes the documentation of a significant weather events more probable. Also, the amount of damage and/or loss of life that a significant weather event causes also influences its coverage in the media. Nonetheless, it is of importance to analyse these reports and to assess the most prevalent events and determine whether a trend in these events can be discerned. It is shown that in the South-Western Cape most significant weather reports are on floods and strong winds and their related impacts. The annual number of reports on floods, hail and strong wind were analysed over the period 1961 – 2020 and presented graphically. For all these types of events increasing trends are noticeable, as shown for heavy rain and flooding in Figure 11. These trends can be ascribed to an increase in population density (and therefore more people are affected and they also report events), as well as a probable increase in severe weather events, which warrants further analysis.

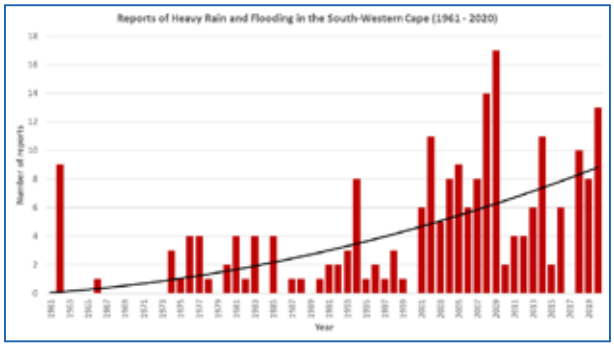

Figure 11: Annual number of reports on heavy rain and flooding in the South-Western Cape over the period 1961 – 2020.

Way forward

The series of regional weather and climate publications continues in the 2022/23 financial year, with the next publication focusing on the KwaZulu-Natal Province. The publication will be available in March 2023.

SEVERE THUNDERSTORMS WREAK HAVOC IN PLACES OVER THE EASTERN HALF OF THE EASTERN CAPE ON 13 DECEMBER 2021

By Ayabonga Tshungwana, Nompumelelo Kleinbooi and Mandisa Manentsa-Titisi

Widespread damage occurred in places over the Eastern Cape, due to severe thunderstorms that developed around the Local Municipality (LM) of Raymond Mhlaba and moved eastwards towards the Wild Coast on 13 December 2021, leaving a trail of destruction behind it.

Introduction

Heavy rainfall and flooding often occur over the eastern half of the Eastern Cape. A high percentage of heavy rainfall events occur generally during summer, when the influence of tropical weather systems becomes dominant over South Africa.

The Eastern Cape has its highest escarpment in the east, where it reaches about 12000 ft above mean sea level. Thunderstorms would usually develop over the mountains and move south of the escarpment, where most rural areas are situated.

On 13 December 2021, severe thunderstorms with heavy downpours resulted in widespread damage over Fort Beaufort, King William's Town, and surrounding areas. The weather systems that were dominant were a surface trough over the western interior of the country, accompanied by upper-air perturbations ahead of an upper-air trough. Moreover, high temperatures aided in the rapid development of thunderstorms.

Synoptics

A cold front was expected to pass through the south of the country, while a surface trough was situated over the western interior of the country as seen on Figure1. This, together with upper-air perturbations ahead of the steep upper-air trough (Figure 2), resulted in widespread showers and thundershowers across the province. Some of these thunderstorms were severe and resulted in heavy downpours, strong, damaging winds, excessive lightning and hail in places over Raymond Mhlaba LM, Buffalo City Metro, Amahlathi LM and Matatiele LM.

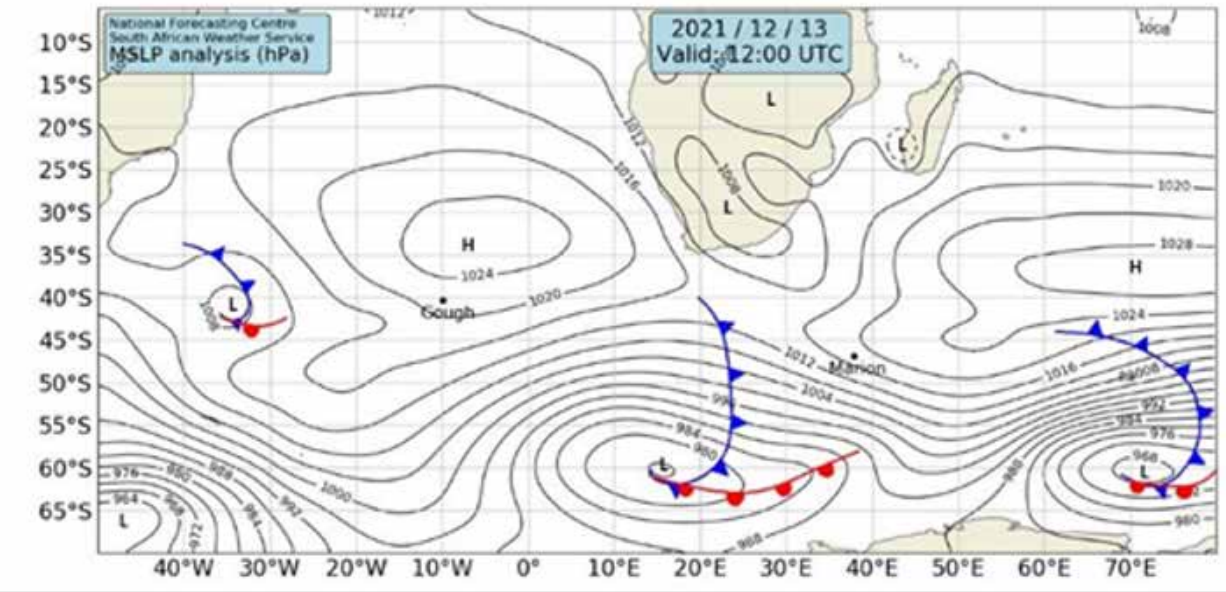

Figure 1: A chart showing the dominant surface systems on 13 December 2021

The surface and upper-air troughs and perturbations resulted in the availability of moisture and atmospheric instability, which are the main ingredients for thunderstorm development. In the case of severe thunderstorms, the availability of mid-level moisture, excessive instabilities and wind shear are necessary for their development.

The section below shows the different model output indicating the various ingredients that were favorable for severe thunderstorm development.

UM4km model data

Upper-Air Data

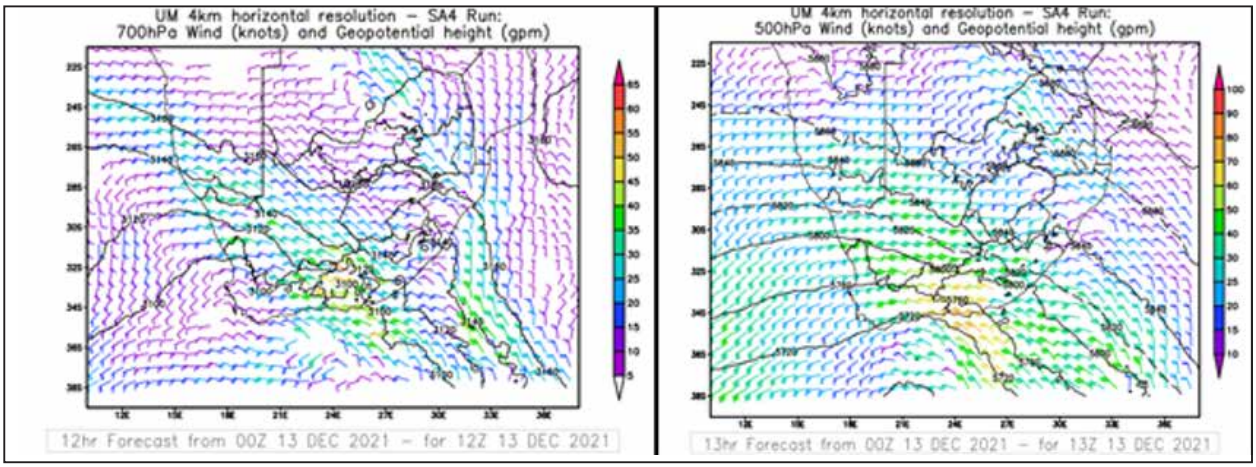

Figure 2: Geopotential heights, indicating a steep upper-air trough along the West Coast at 700 and 500 hPa on 13 December 2021 at 12h00Z and winds indicating strong divergence over the central parts of the country

Moisture and humidity

High relative humidity of around 80 to 90% was expected at 700 hPa over most parts of the province, as can be seen in Figure 3, and over the southern central parts of the province at 600 hPa.

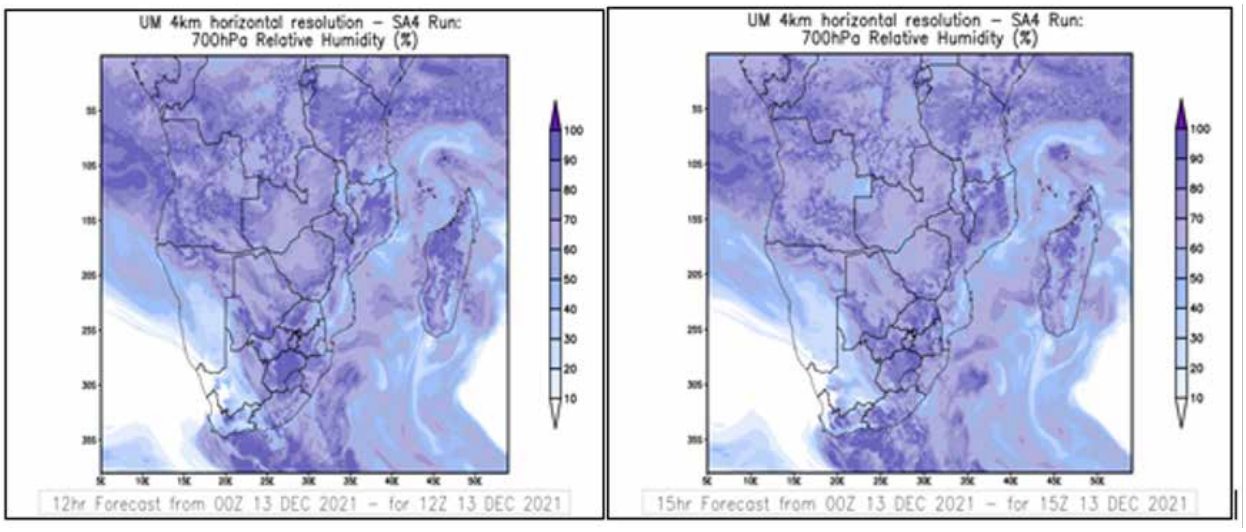

Figure 3: Relative humidity showing moisture over most parts of the Eastern Cape at 700 hPa, and mostly over the southern central parts of the Eastern Cape at 600 hPa

Instability indices

Accompanying the high relative humidity, were high instabilities as indicated in figures 4 - 7, namely, TTI's reaching 56 at 12Z and 59 at 15Z over most parts of the province. The LI was between -5 to -8, with the surface CAPE values between 1600 to 2200 J/kg mainly south of the escarpment, from Raymond Mhlaba LM going eastwards.

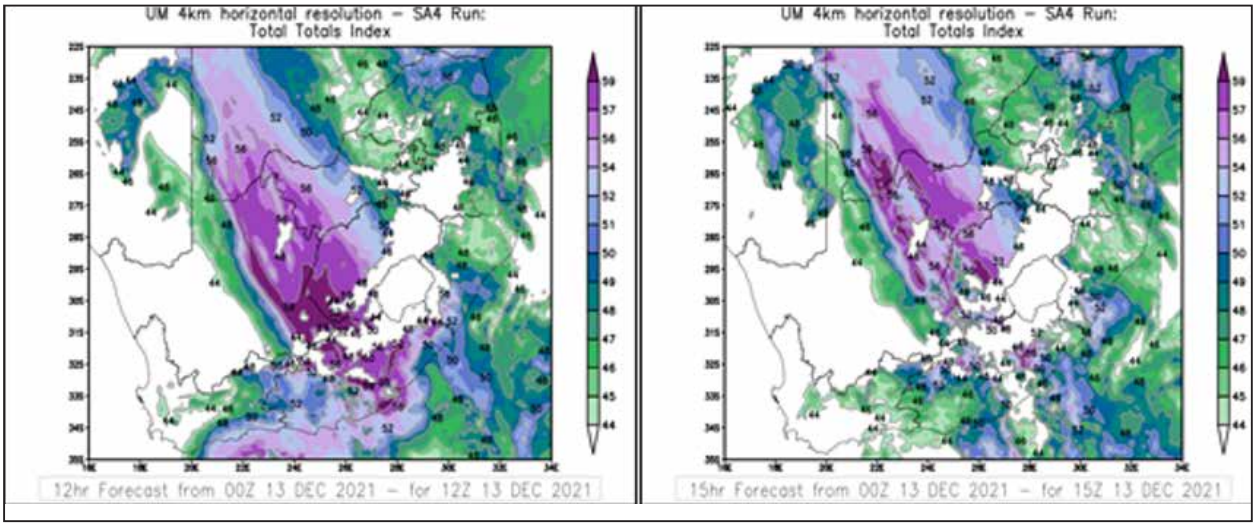

Figure 4a: TTI values indicating high instability over the northern and eastern parts of the Eastern Cape

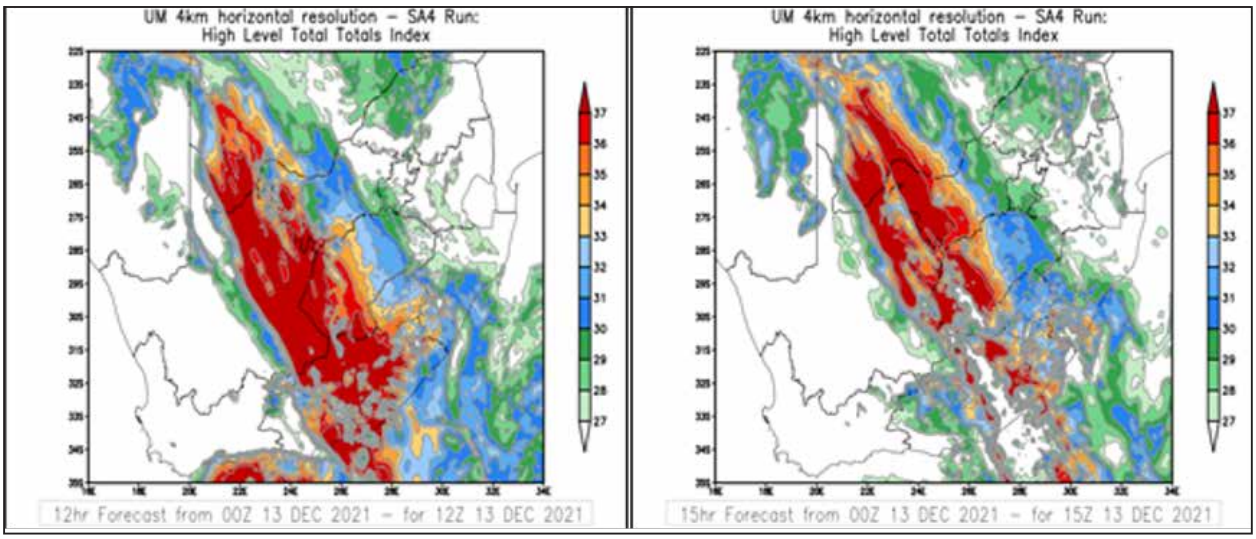

Figure 4b: High-level TTI values indicating high instability over the central and eastern parts of the Eastern Cape

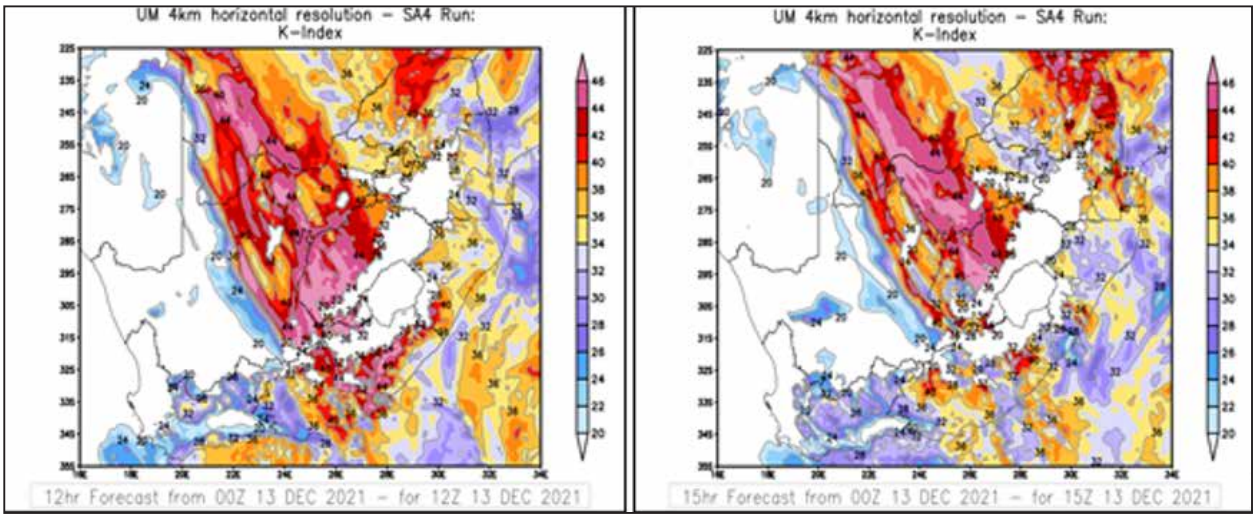

Figure 5: Images indicating K-indices, with high values over the central parts of the province

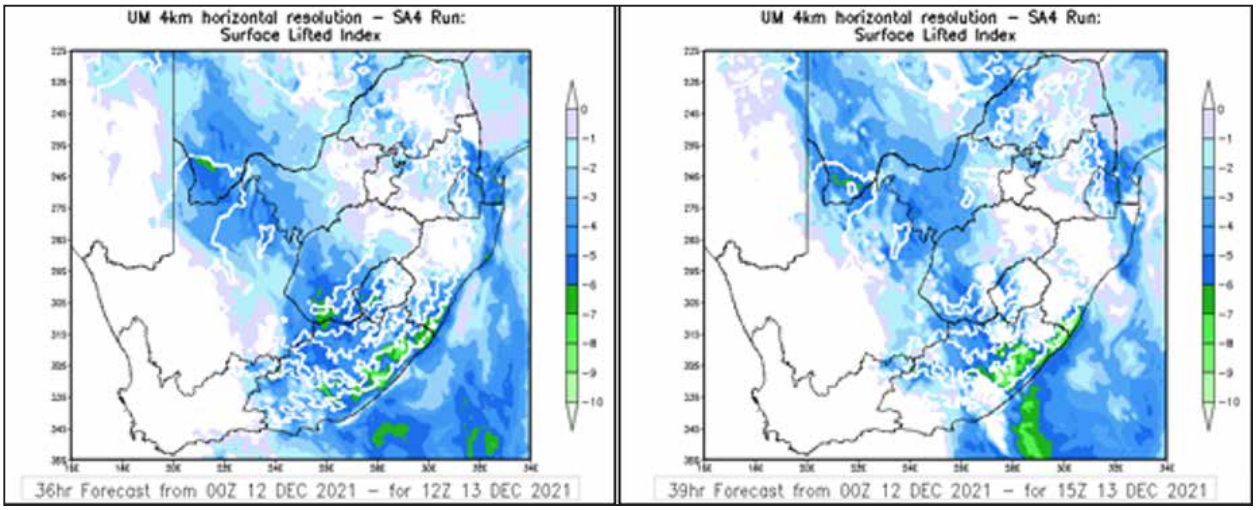

Figure 6: Images indicating surface lifted index, with high instabilities in areas between Adelaide and Mbizana

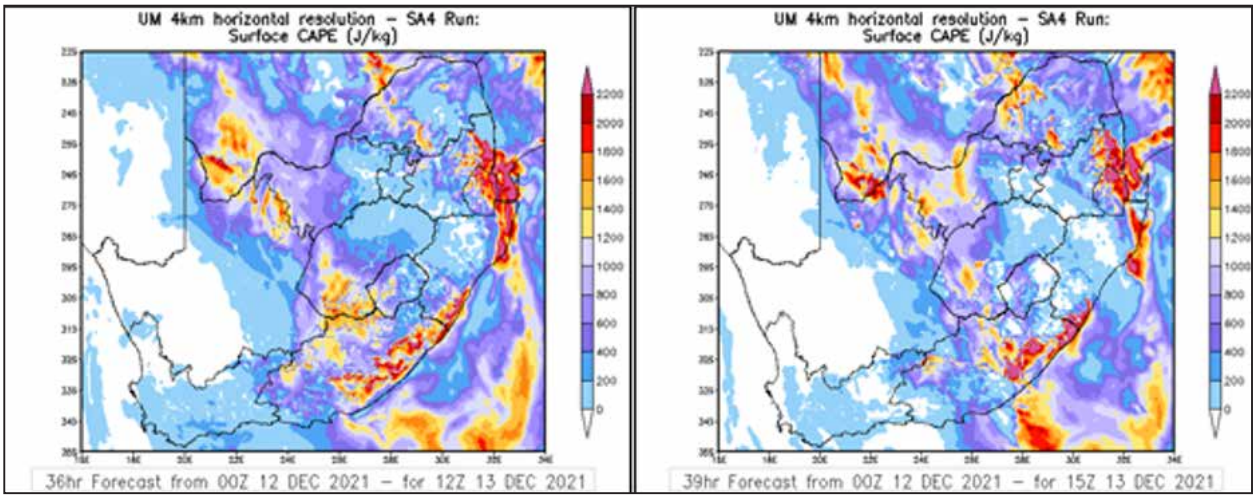

Figure 7: Images indicating surface CAPE, with high values between Adelaide and Mbizana on 13 December 2021

Wind shear

High values of 20 to 30 knots are indicated over most parts of the province at 15Z, with a very bright spot of strong wind-shear of 30 to 40 kt indicated over the central parts of the province at 15Z (Figure 8), while high values are indicated over the western parts at high levels. This coincides with the position of the surface trough and upper-trough.

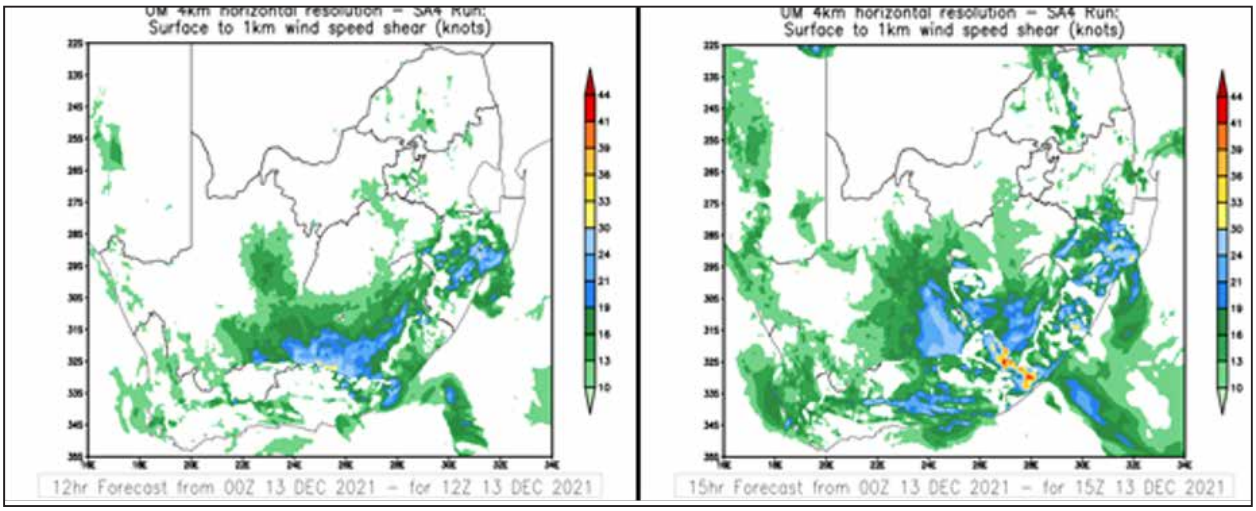

Figure 8: Images indicating low-level wind-shear over the province, with high values over the central parts of the province at 12z and 15z on 13/12/2021

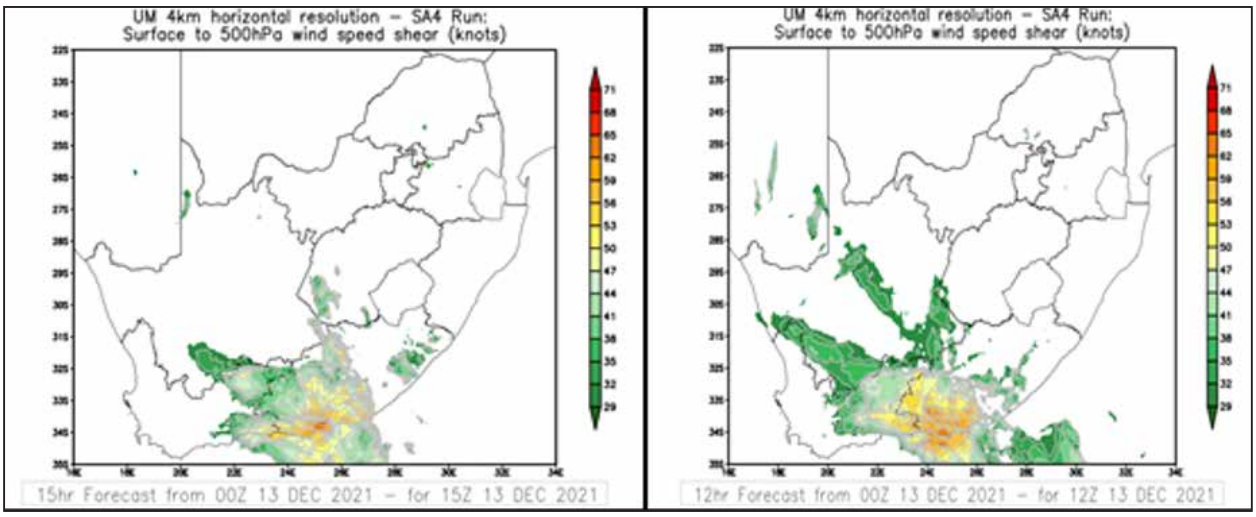

Figure 9: Images indicating high-level wind-shear over the province, with high values over the western parts of the province at 12z and 15z on 13 December 2021

Low level winds

A convergence area can be seen over the central parts of the province in Fig 10 and 11. This area coincides well with the areas of Instability, wind shear and area of significant amounts of rainfall that were expected (seen on fig.12). The patchy strong low-level winds were an indication that the expected severe thunderstorms could produce strong and gusty winds.

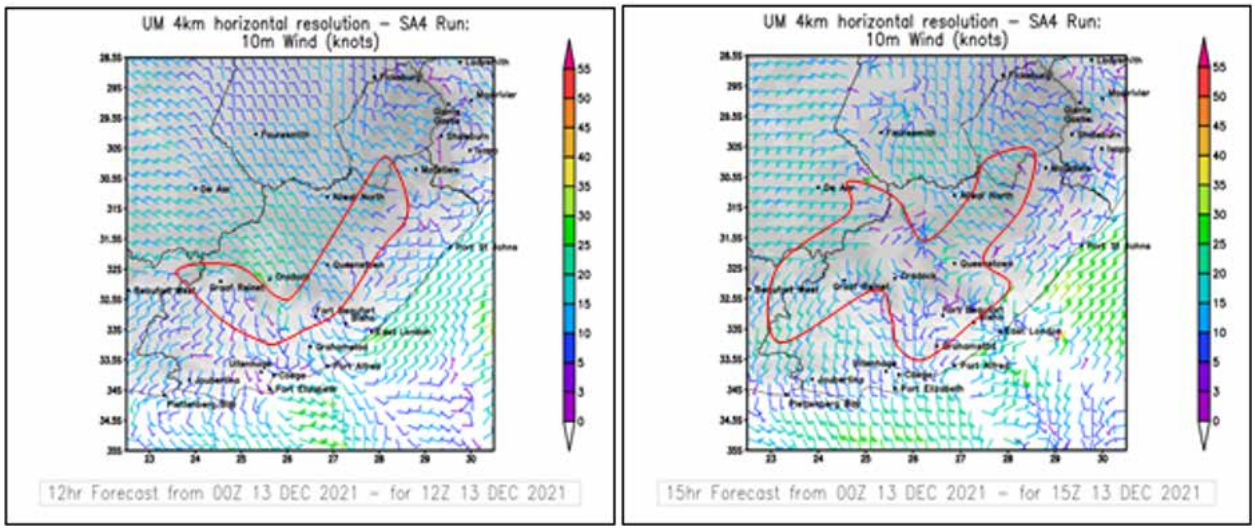

Figure 10: Images showing 10 m winds at 12Z and 15Z, with the convergence zone (red polygon) over the western and central parts of the province

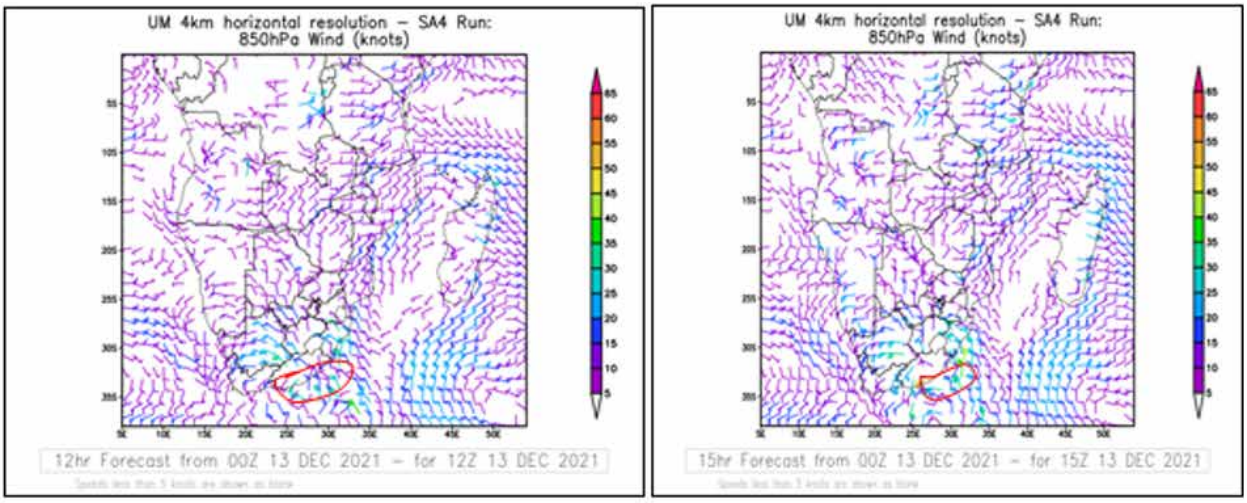

Figure 11: Images showing 850hPa winds at 12Z and 15Z, with the convergence over the western parts of the province at 12Z, moving the eastern parts at 15Z

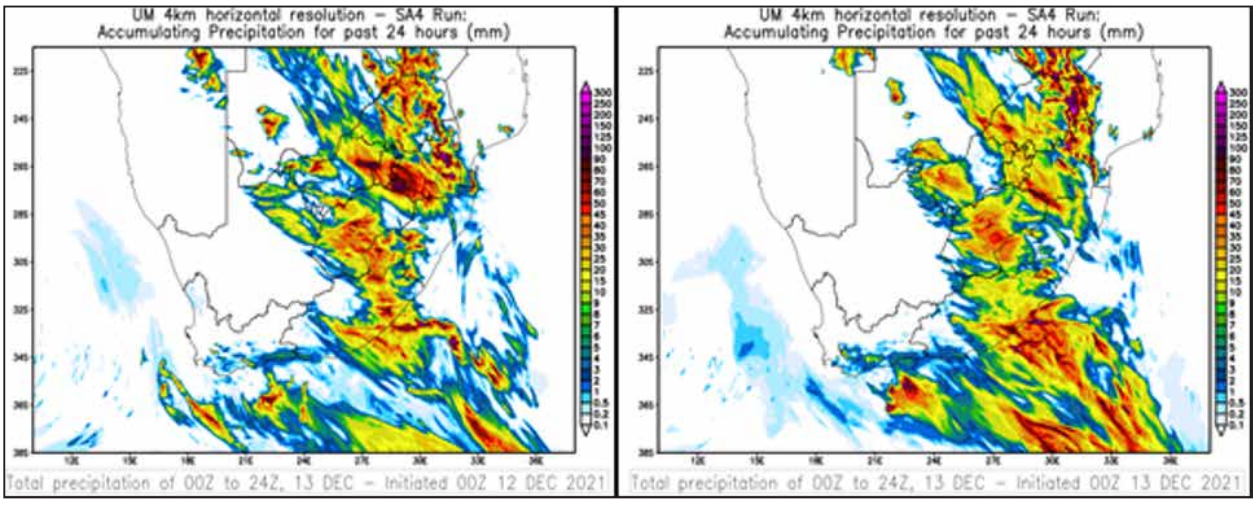

Figure 12: Image indicating total expected precipitation for 13 December 2021 using the UM4km 00Z for 12 and 13 December, with high values indicated between Fort Beaufort and Coffee Bay

Additionally, the significant rainfall accumulations, seen in Figure12 indicated the potential of the expected severe thunderstorms producing heavy downpours leading to flash flooding over the central and eastern parts of the province.

GFS model data

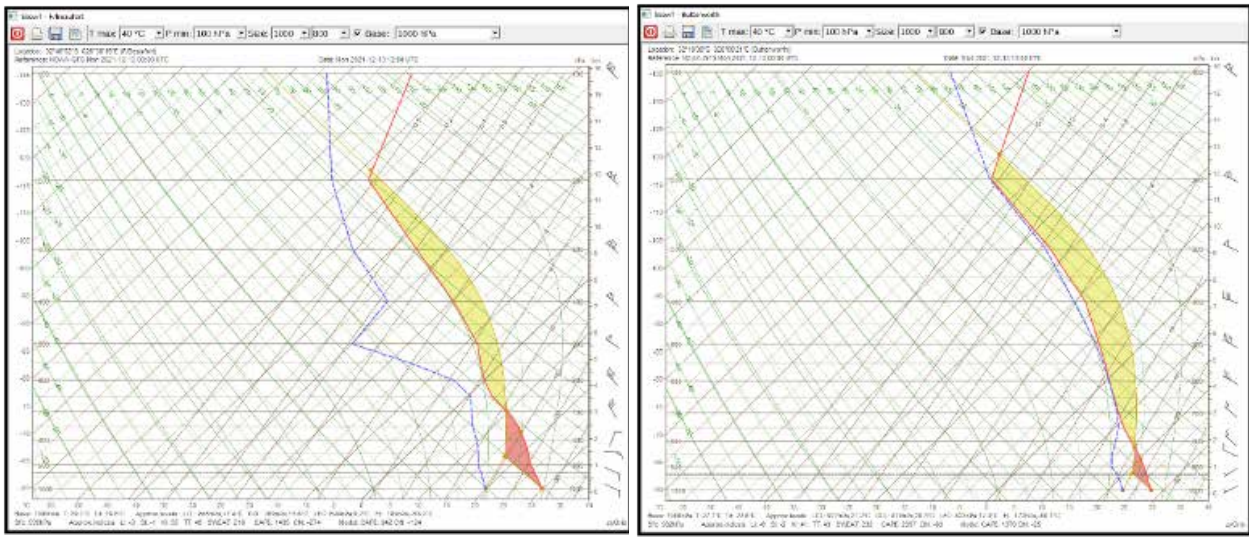

Figure 13: Image showing SkewT's for Fort Beaufort and Butterworth areas at 12Z and 15Z respectively on 13 December 2021

On 13 December 2021, the model output from Figure 2-13 showed availability of moisture, excessive instability and wind shear, which favored the development of severe thunderstorms over a wide area of the Eastern Cape. Fig.13a showed dry-air intrusion over Raymond Mhlaba LM, which indicated the possibility of large hail, while Figure 13b indicated the possibility of downpours and large amounts of small hail. This resulted in the forecasters issuing a warning for severe thunderstorms.

1. Issued warning

IBF Warning Issued

A low likelihood for significant impacts (yellow level 4) warning was issued for Amathole, Chris Hani, Joe Gqabi, Alfred Nzo and OR Tambo DMs on 12 December 2021. The expected impacts are listed on Figure 14.

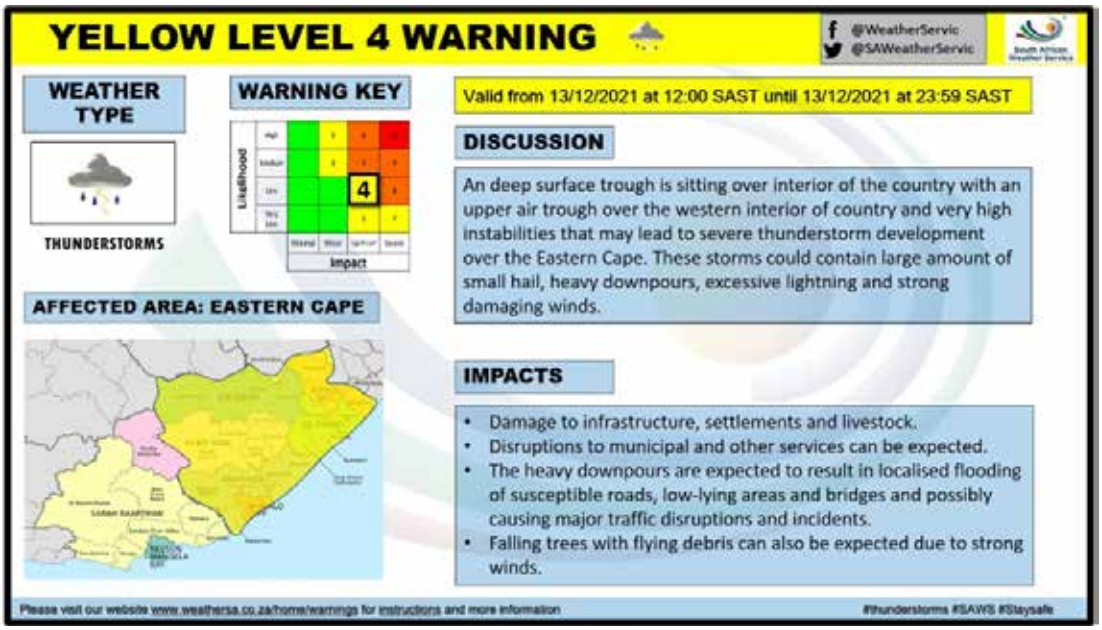

Figure 14: IBF warning issued for the eastern half of the Eastern Cape on 13 December 2021

2. Observations

Satellite Imagery

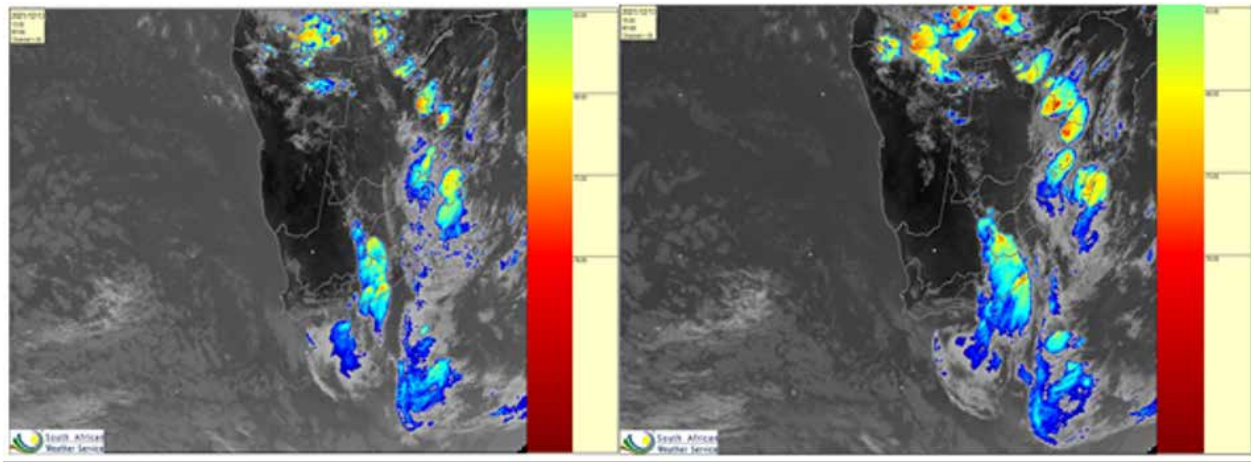

Figure 15(a): IR Satellite image on 13 December 2021 at 13 and 15Z, showing high reflectivity of the cloud top temperatures over Eastern Cape

Radar Imagery

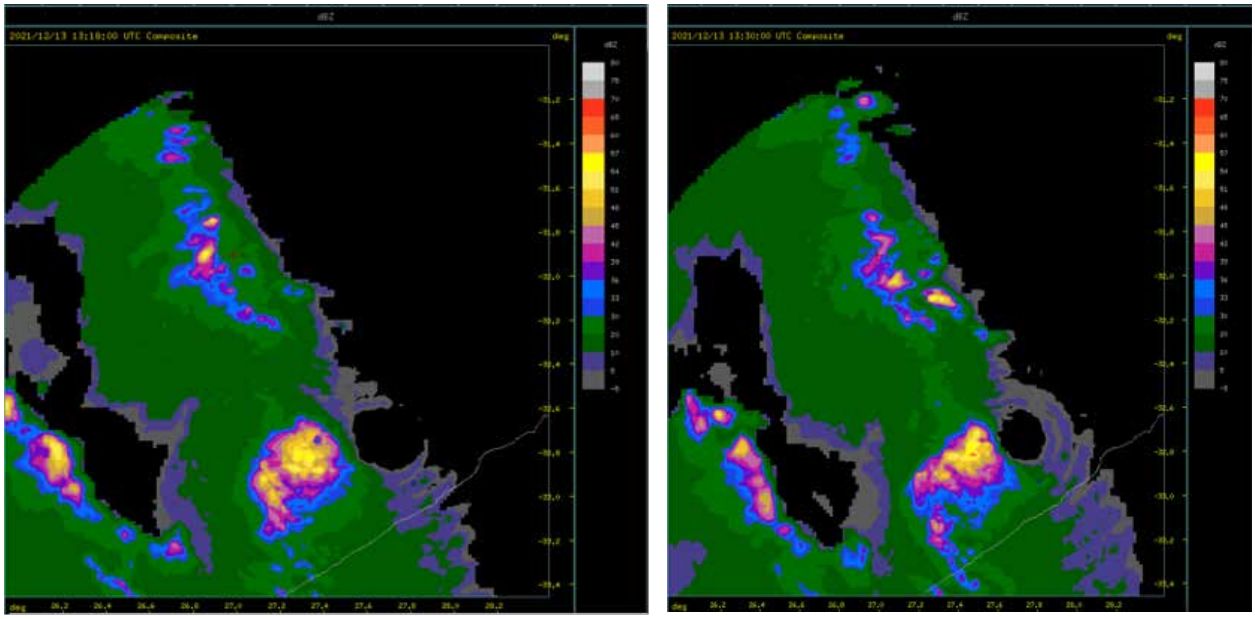

Figure 15(b): Radar images on 13 December 2021 at 13Z

Radar and Satellite are observational tools that are useful in detecting storm properties, such as the severity and movement. On 13 December 2021, both Satellite and Radar images in Figure 15, were showing high reflectivity over the interior of the province, between 13:00Z up to 15:00Z, and that coincided with areas where severe damage occurred.

3. Observed Impacts

Wind impacts

Figure 16: A collage showing wind impacts over Fort Beaufort, Adelaide and Matatiele on 13 December 2021

The images in Figure16 show the impacts that occurred because of the strong winds, where the roof of a school in Fort Beaufort was blown away. Additionally, there were reports of power and communication interruptions, trees blown over and damage to property in places across the Eastern Cape, due to strong winds.

Hail Impacts

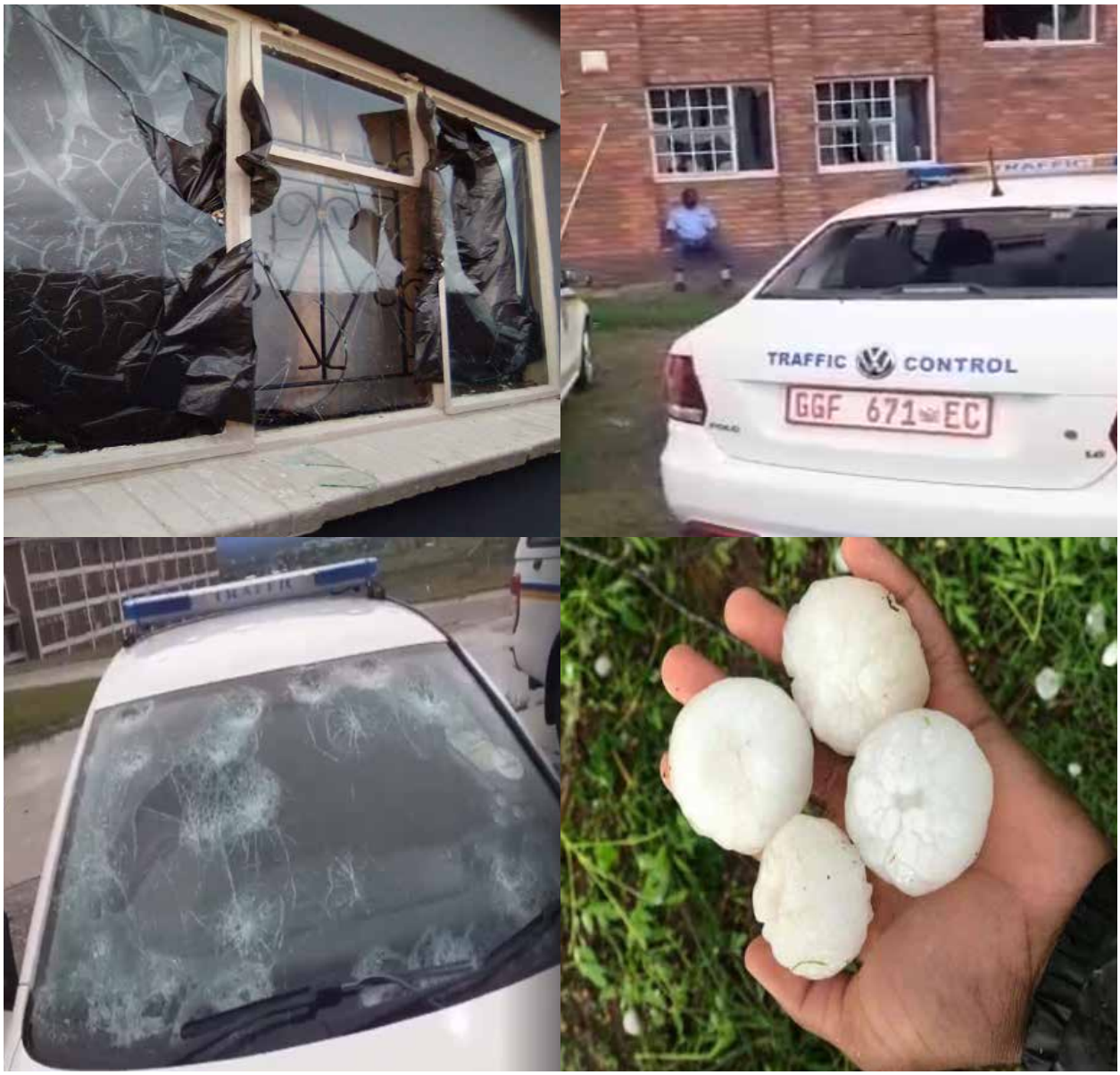

Figure 17: Hail impacts over Adelaide on 13 December 2021

Further, most of the hail impacts were observed over Raymond Mhlaba LM, where golf-ball size hail resulted in a number of cars and houses being damaged or having broken windows and windscreens.

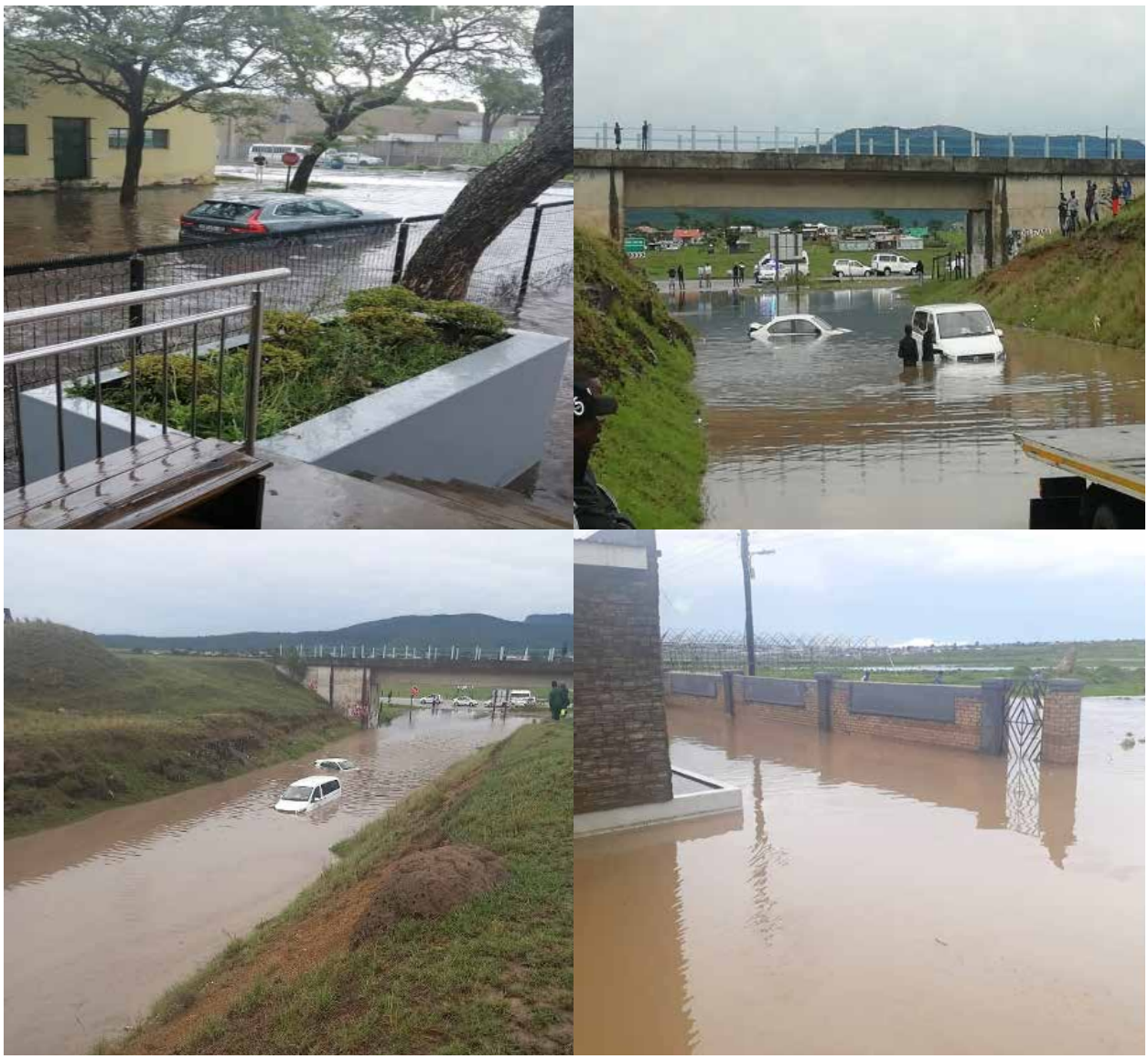

Figure 18: Flooding over King Williams's Town and Dimbaza location on 13 December 2021

The significant amounts of rainfall resulted in flash flooding, as seen in Fig.18. Motorists around King Williams Town and Dimbaza location were heavily affected as the severe thunderstorm dumped 24mm of rain in about 15 minutes, with a total of 41mm recorded in less than 24 hours. Heavy downpours also affected OR Tambo DM, where 142 people were left homeless and about 41 chickens in a small chicken business situated in Mthatha were killed due to the flooding (News24, 2021).

Observed rainfall amounts for 13 December 2021

Form: Eastern Cape Synoptic List for 06 SAST 14 December 2021

South African Weather Service

Station Synop Nr	Tx T Tn Td	Rel. Hum. App Temp	QNH P.T. P.C.	TotC LCA MCA	LCB LCT HCT	Weather	Wind Dir WS WG KT KPH	Tot. Rain	Vis.
Plettenberg Bay 68931	21.7 17.1 16.4 16.4	95.66 23.64	1017 ✓ 1				6 8 KT 11 15 KPH	6.2mm	
Joubertina 68833	26.3 18.3 11.6 15.5	64.99 22.5	1016 ✓ 0.3				3 7 KT 6 13 KPH		
Patensie 68835	26.9 17.5 16 16.7	90.93 23.84	1016 ✓ 0.5				2 4 KT 4 7 KPH	6mm	
Uitenhage 68839	26.7 19.1 15.8 16.5	81.21 25.4	1015 ✓ 0.5				4 8 KT 7 15 KPH	22.2mm	
Port Elizabeth 68842	26.6 17.7 16.7 17.1	93.88 24.45	1015 ✓ 1.2	8 8	2		3 KT 6 KPH	3.4mm	20km
Coega 68837	26 18.6 16.2 16.9	85.95 25.1	1015 ✓ 0.5				7 11 KT 13 20 KPH	7.2mm	
Port Alfred 68843	26.9 20.2 15.7 16.9	75.38 26.46	1015 ✓ 0.6				10 16 KT 19 30 KPH	4mm	
East London 68858	29.5 20.9 16.4 17.7	75.49 27.54	1015 2.2	6 5	5 7		15 KT 28 KPH	7.6mm	34km
Port St. Johns 68674	34.6 25.3 22	23.53	1015 ✓ 2.8				7 15 KT 13 28 KPH	13mm	
Graaff-Reinet 68737	34.2 17.3 10.9 11.6	66.07 21.13	1016 ✓ 0.1				4 8 KT 7 15 KPH		
Fort Beaufort 68747	30.9 20.4 14.6 14.3	69.37 26.08	1016 ✓ 1.1				1 KT 2 KPH	28.6mm	
Grahamstown 68849	28.6 15.4 13.7 13.3	89.61 20.33	1016 ✓ 0.6				8 13 KT 15 24 KPH	4.8mm	
Bisho/KWT 68752	30.4 16.5 13.6 14.3	83 21.5	1017 ✓ 1.2				12 16 KT 22 30 KPH	41mm	
Queenstown 68647	30.2 16.2 11.6 12.5	74.2 20.23	1018 1.3				KT KPH	20.4mm	

Figure 19: Rainfall measured in places over the Eastern Cape for 13 December 2021.

4. Conclusion

Widespread rainfall occurred over the Eastern Cape as forecasted, with significant falls resulting in flash flooding over King Williams' Town, Fort Beaufort, Mthatha and Queenstown as seen in Fig.17 & 19. Additionally, strong damaging winds resulted in damages to property and settlements over Raymond Mhlaba LM with localised incidents of damages to vehicles, due to fallen trees over Matatiele LM. Moreover, large hail over Dimbaza location and Raymond Mhlaba LM caused damages to vehicles and broken windows. In summary, most of the expected impacts occurred.

COMPARISON OF SATELLITE-BASED AND ÅNGSTRÖM–PRESCOTT ESTIMATED GLOBAL HORIZONTAL IRRADIANCE (GHI) UNDER DIFFERENT CLOUD COVER CONDITIONS IN SOUTH AFRICAN LOCATIONS

By Mr. Brighton Mabasa , Dr. Meena D. Lysko and Prof. Sabata J. Moloi

1. Introduction and Background

The Sun is the source of energy that influences atmospheric motions and the climate of the Earth. Solar radiation is the term that was coined for the energy emanating from the Sun. The amount and distribution of incoming solar energy affects the weather and climate on Earth. The quantity and intensity of solar radiation reaching the Earth varies over time and space. The amount of solar radiation that reaches the Earth's surface is affected by the distance between the Sun and the Earth, as well as the existence of clouds and other atmospheric constituents.

The transmittance of the atmosphere attenuates the incoming solar radiation before it reaches the ground surface throughout its passage through the atmosphere. The amount of solar radiation at the ground surface is about 50% of what it is at the top of the Earth before it interacts with the atmosphere. The interaction of the solar radiation from the top of the atmosphere, the atmosphere and the ground surface are summarized in Figure 1. The sum of direct solar irradiance (DNI) and diffuse horizontal irradiance (DIF) is the global horizontal irradiance (GHI).

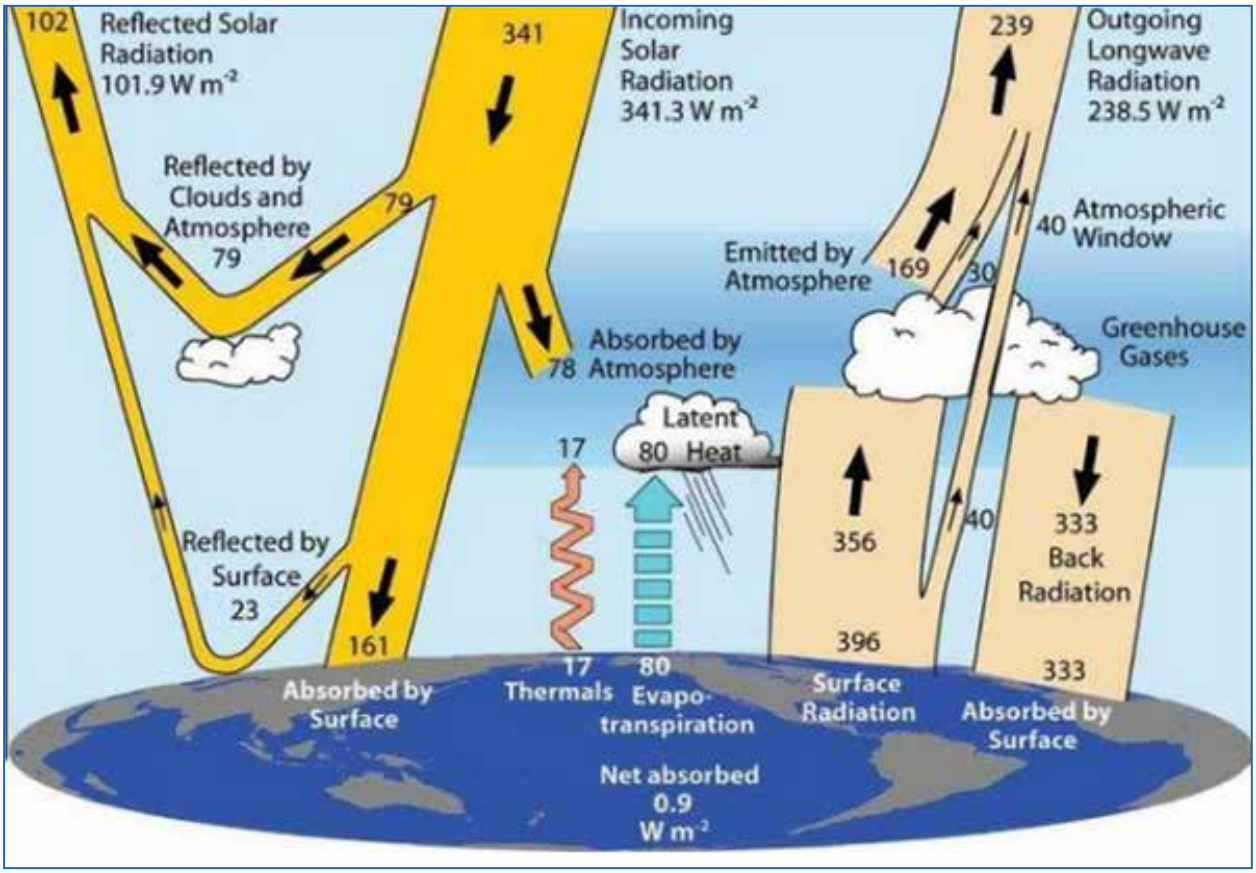

Figure 1: Global Mean radiative balance between Earth (ground surface) and Atmosphere, short wave radiation on the left. (Adapted from Trenberth et al. 2009)

A pyranometer is used to measure the GHI arriving from the whole hemisphere. Accurate GHI data are highly valuable for the economic and technical evaluation of solar technologies, engineering designs, and the development, calibration, and validation of pragmatic models. Environmental studies, climate change studies, agricultural sciences, ecology, and meteorology all benefit from GHI. As a result, obtaining reliable GHI at a site is important.

GHI measurements taken with a pyranometer from in-situ solar radiation stations are the most precise way to gather GHI data. Nevertheless, GHI recording sites are few and far between, as well as expensive to establish, maintain, and calibrate. As a result, GHI in situ measured data are sparse. To compensate, reliable data is collected at a sparsely distributed network to create, calibrate, and validate models that can be reliably applied to approximate and predict exploitable solar irradiance at other sites.

Estimates of GHI can also be generated by interpolating against observed GHI. Uncertainty in the generated data is a disadvantage of this technique. Satellite-derived GHI datasets can provide dependable alternate GHI datasets and compensate for the lack of in situ radiometric sites by increasing the quantity of GHI data. The Ångström–Prescott (AP) model and satellite-based datasets (CAMS, CMSAF, and SOLCAST) showed that it is capable of accurately estimating the GHI data in South Africa.

The objective of this work is to determine the sensitivity of the satellite-based databases (NASA SSE, CAMS, CMSAF, and SOLCAST) and the Ångström–Prescott (AP) model to cloud presence, i.e. to quantify the datasets' capabilities in estimating GHI under clear, all-sky, and overcast cloud conditions. The traditional statistical benchmark relative root mean square error (rRMSE) was implemented to quantify the capabilities of the datasets in varied sky conditions.

2. Study Area and Methodology

2.1 Study Area and Data

The study area was eight radiometric stations namely: Upington, DeAar, Irene, Polokwane, Thohoyandou, Mthatha, Durban and George in the network of the South African Weather Service (SAWS). All eight locations are radiometric stations that record 1-min GHI data. The eight stations use a Kipp & Zonen CMP11 secondary-standard pyranometer to measure GHI. GHI measurements are taken using a Campbell Scientific CR1000 data logger at 0.2 hertz (5s) sampling frequency and integrated to 1 min. Sunshine duration data were collected using Campbell–Stokes sunshine recorders

2.2 Clear-Sky and Cloud-Sky Determination

There are several techniques for determining the total amount of clouds covering the sky over a period and classifying that period as clear-sky, cloud-sky, or overcast-sky. Ground-based observations (trained meteorological observers using a naked eye), ceilometer devices, total sky imagers, sunshine index (n/N) threshold, clearness index (GHI/GHI_TOA) threshold, reanalysis, and satellite-based datasets are examples. To determine clear-sky and overcast-sky days, the mean daily (cfc day, i.e., average percent of cloud amount during daylight) fractional cloud cover (CFC): cloud property dataset using SEVIRI, Edition 2 (CLAAS-2) was used. The CLAAS-2 satellite set is generated using the geostationary Meteosat Spinning Enhanced Visible and Infrared Imager (SEVIRI). It has a 0.05° × 0.05° (~5.5 km × 5.5 km) spatial resolution. A clear-sky day was classified as one in which the daily mean fraction of the sky that was covered by clouds was less than or equal to 5%, i.e., CFC≤ 5%. An overcast day was classified as one in which the daily mean fraction of the sky that was covered by clouds was greater than or equal to 95% i.e., CFC≥95%.

3. Results

Figure 2(a) depicts an hourly curve for a clear-sky day (Irene station on 24 May 2019), whereas Figure 2(b) depicts a daily curve for an overcast-sky day (Irene station on 15 November 2019) for observed GHI, CAMS, CMSAF, and SOLCAST. As NASA SSE and AP datasets are not available on an hourly timescale, they are not represented in the line graphs. CAMS, CMSAF, and SOLCAST successfully estimated the GHI under clear-sky conditions based on Figure 2a. According to Figure 2(b), under overcast-sky conditions, CAMS, CMSAF, and SOLCAST all demonstrated poor rendition, i.e., they diverged from the observed GHI dataset line. It is also clear from Figure 2(b) that the CAMS, CMSAF, and SOLCAST datasets differ in how they estimate GHI in the presence of clouds (i.e., they diverge), implying that different algorithms that are implemented to parameterize clouds by different data providers perform differently.

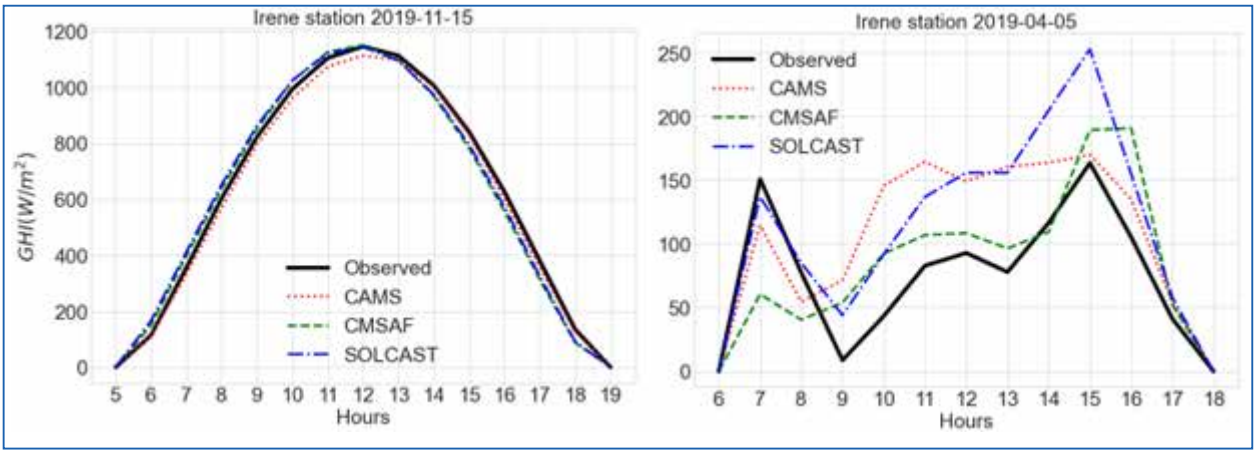

Figure 2: (a, left) Hourly clear-sky day and (b, right) overcast-sky day {Cloud cover information was detected by using CLAAS-2 satellite-based dataset}

This demonstrates that datasets that are used to estimate GHI do not precisely parameterize the actual fraction of the sky that is covered by cloud fluctuation. When the estimated data are compared to the observed GHI data, this inadequacy is one of the primary bias sources.

From Figure 3 which shows the daily rRMSE results under clear skies. Overall, the datasets datasets (AP, SOLCAST, CAMS, CMSAF, and NASA SSE) performed quite well under clear-sky conditions, with a rRMSE of less than 6.5 % across all the stations.

From Figure 4 which depicts daily rRMSE under all-sky conditions : daily rRMSE for CAMS was between within 5%≤rRMSE≤12% for all the stations; for CMSAF it ranged between 5%≤rRMSE≤12% for all the stations; for SOLCAST it ranged between 4%≤daily rRMSE≤10% for all the stations; for AP it ranged between 5%≤daily rRMSE≤11% for all the stations and for NASA SSE the daily rRMSE was less than 10% in Upington (8%) and De Aar (10%), it was in a range 10%<rRMSE<15% in three stations, and greater than 15% in Thohoyandou (16%), Durban (16%), and George (22%).

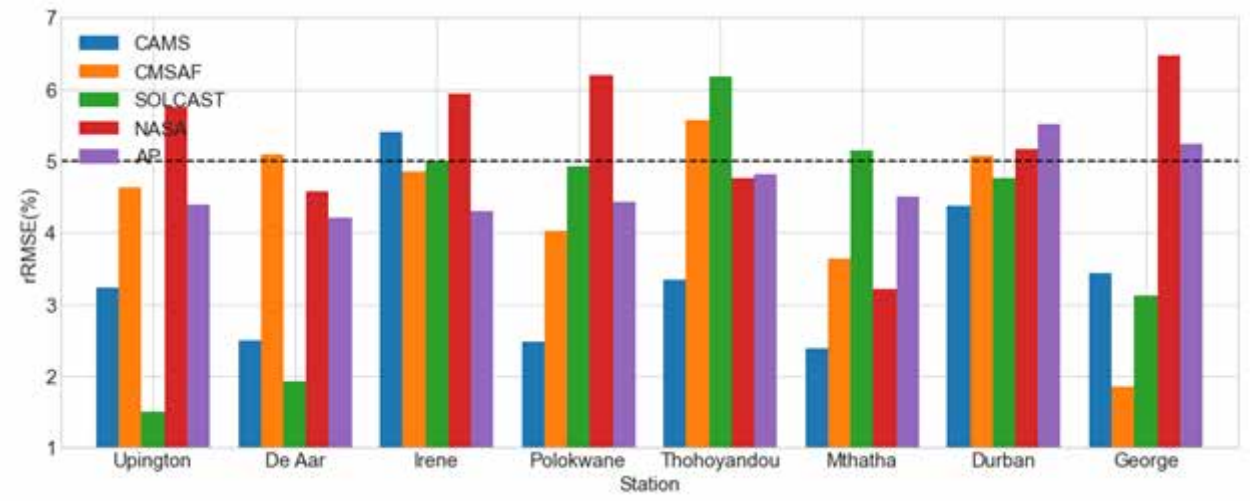

Figure 3: The daily rRMSE of the derived GHI datasets under clear-sky conditions

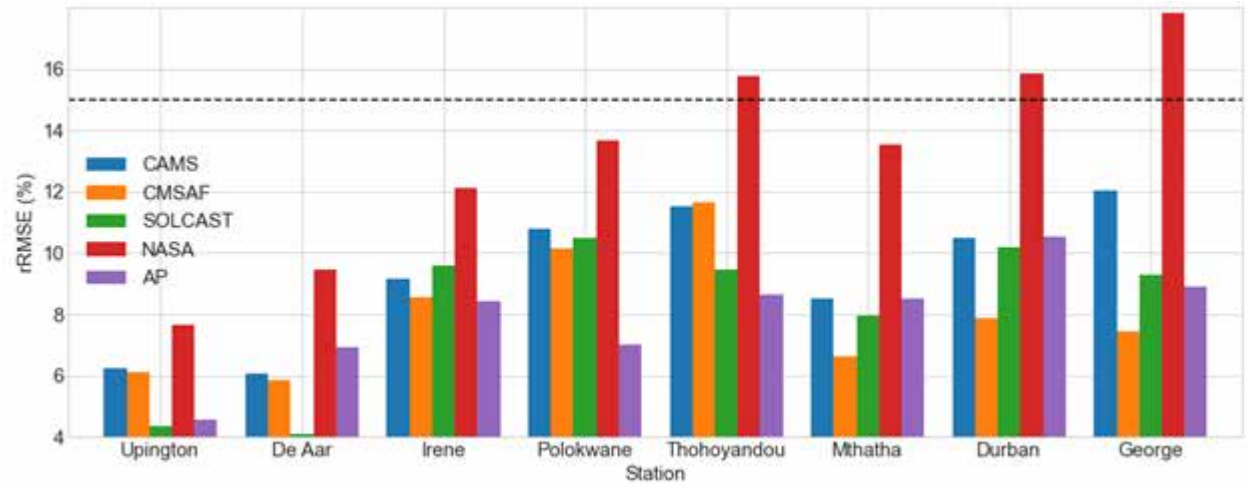

Figure 4: The daily rRMSE of the derived GHI datasets under all-sky conditions

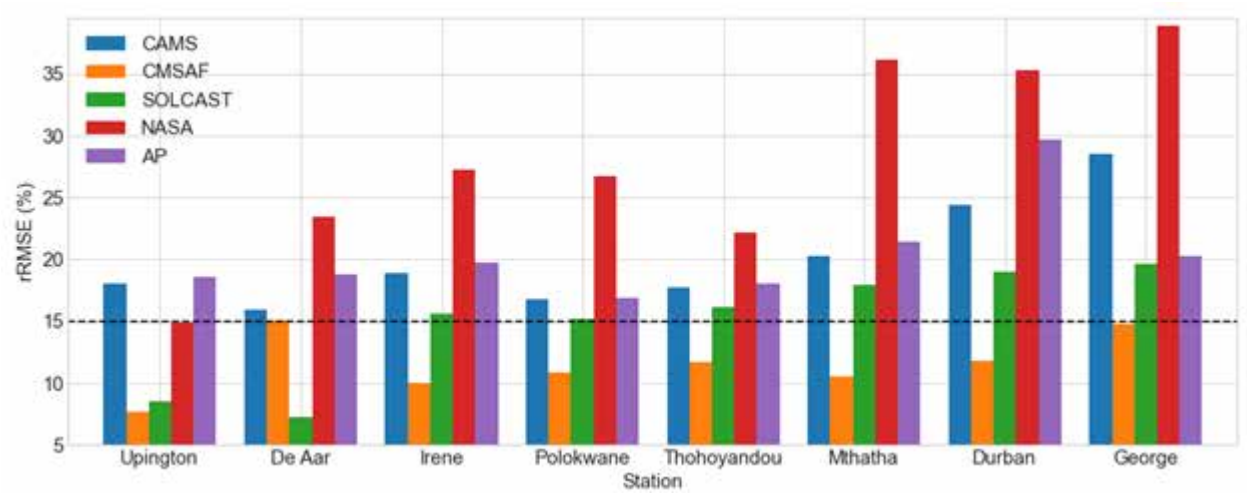

Figure 5: The daily rRMSE of the derived GHI datasets under overcast conditions

From Figure 5, which shows daily rRMSE under overcast conditions: For the CAMS dataset, no station performed well (rRMSE >15%); the rRMSE ranged from 16% (at De Aar) to 29% (at George). The AP model performed poorly, with rRMSE ranging from 17% (at Polokwane) to 30% (at Durban). SOLCAST performed well (rRMSE 15%) in Upington (9%) and De Aar (7%), but poorly at the other stations, with rRMSE ranging from 15% (at Polokwane) to 20% (at George).

4. Discussion

CMSAF satellite-based dataset exhibited a smaller differential in rRMSE under different cloud conditions in practically all the stations. CMSAF's high performance in the presence of clouds is related to an improvement in the look-up tables (LUTs) based eigenvector hybrid approach by adding variables that are introduced by cloudy skies to treat cloudy skies. The SOLCAST dataset performed well in estimating GHI under cloud conditions. This could be due to the usage of dependable and accurate Meteosat satellites with high spatial resolution (1–2km) cloud information data from the European Organization for the Exploitation of Meteorological Satellites (EUMETSAT) across Africa. The REST2v5 clear-sky model with water vapor data from ERA5 and aerosols data from MERRA2 is utilized as a consistent cloud detection algorithm. CAMS performed relatively poorly in estimating GHI under overcast conditions. The low performance could be ascribed to the McClear model failing to identify actual cloud-free conditions in some places due to errors in aerosols that are used as inputs to the McClear model.

AP had a low difference in all the stations while NASA SSE had a large difference in almost all the stations except in Upington. It is also observed that the differences are high in Mthatha, Durban and George, these are coastal stations this might be due to low number of clear sky days (annual average of less than 6%), according to Mabasa et al. (2021). Merchand et al. (2019) also found a poor spatial consistency performance in coastal stations compared to inland stations, which was postulated to be because of underestimation of clear-sky conditions. NASA SSE's quite substantial rRMSE disparities (good performance) in Upington might be because of the homogenous terrain compared to the other stations, and the grid is practically similar to the point of standardization. Increases in rRMSE with increasing total fractional cloud coverage were also reported in the works of [Jed et al. (2022), Ameen et al (2018), Li et al (2021), Zhang et al. (2016), Xia et al (2017) and Eissa et al (2015)].

5. Conclusion

The study compared daily GHI extracted from four satellite-based databanks (namely SOLCAST, CAMS, CMSAF and NASA SSE) and the Ångström–Prescott (AP) model, by validating them against BSRN QC and HelioClim model quality-checked observed daily GHI from at 8 ground stations in South Africa. The study investigated the performance of the datasets under clear-sky and overcast-sky conditions. The research indicated that the presence of clouds affects the performance of the estimated datasets: clear-sky conditions (excellent performance), all-sky conditions (intermediate performance) and overcast-sky conditions (poor performance). SOLCAST was the best performing overall in estimating daily GHI under clear-sky and all-sky conditions; CMSAF was overall best under overcast-sky conditions while NASA SSE was the overall worst performing dataset in different cloud cover conditions. The relatively poor performance of the NASA SSE datasets in the study area could be attributed to their low spatial resolution of 0.5° × 0.5° (~55 km × 55 km). The feasibility of the datasets decreased significantly as the proportion of sky that was covered by clouds increased. Cloud parameterization schemes and spatial resolution should be enhanced to improve datasets performance.

CUMULUS PARAMETERIZATION WITHIN THE CCAM

By Patience T. Mulovhedzi, Robert Maisha, Mary-Jane Bopape and Thando Ndarana

The Conformal Cubic Atmospheric Model (CCAM) is a variable-scale global atmospheric model, which applies a semi-implicit semi-Lagrangian method to solve its hydrostatic equations and can be run in a stretch-grid to provide high resolution over a limited area of interest and quasi-uniform mode over the whole globe (Engelbrecht et al. 2009; Engelbrecht et al., 2011). The model was developed by the Commonwealth Scientific and Industrial Research Organisation (CSIRO; McGregor, 1996; Engelbrecht et al., 2011). The CCAM is a seamless model, i.e. it can be applied for a wide range of timescales, and can run both as a global and regional model. The CCAM has a cube structure, which means there are no challenges with the convergence of meridians along the polar regions. The model employs several parameterization schemes to improve the representation of physical processes in NWP models and to simplify "processes that are too small-scale/ complex to be physically represented in the model by a simplified process" Stensrud (2007). These include cumulus parameterization schemes – which are essential for accurately representing the characteristics and processes of convective processes and precipitation in NWP models (Huang and Gao, 2017).

Cumulus convection parameterization, also referred to as convection schemes, is a technique to address limitations of numerical weather and climate models in representing the physical processes and transports within convective clouds by predicting the time evolution of the collective influence of individual convective clouds on the large-scale system/environment (Arakawa and Schubert, 1974; Baba, 2020). This helps increase the skill and accuracy of NWP models in predicting convective precipitation and feedback of individual convective clouds to the large-scale weather system. Furthermore, convection schemes determine the sub-grid processes within an NWP model, such as the vertical distribution of total vertical mass flux, the total detrainment of mass and the thermodynamical properties of the detraining air (Arakawa and Schubert, 1974). These cumulus convection schemes are generally applied at gray zone horizontal scales: resolutions between 100 m (where convection is explicitly resolved) and 10 km (where convection is implicitly parameterized; Prein et al., 2015). Within the gray zone, convection/updrafts cannot be explicitly resolved, hence require parameterization (Huang et al., 2014; Sullivan et al., 2016).

There are mainly two types of convection parameterizations, namely, shallow convection - for fair weather cumulus and stratocumulus and deep convection - for congestus and cumulonimbus convection (Pickering, 2015). Cumulus convection scheme comprise (a) the trigger function, which describes the triggering mechanism/activation for convection, (b) the cloud model, for vertical distribution, and (c) the closure assumptions, which define convective intensity/regulation of convection by large-scale/grid-scale variables (Hong and Pan,1998; Yano et al., 2013). Moreover, there are different categories of cumulus convection schemes, namely, scale-aware, mass flux and convective adjustment schemes (Miller,1985; Huang et al., 2014; Yoshimura et al., 2015; Freitas et al., 2021). Scale-aware scheme automatically adapt to variations in grid size and offer a smooth transition from unresolved to resolved cloud scales (Huang et al., 2014; Freitas et al., 2021). Mass-flux schemes are most used because of their ability to explicitly compute mass flux for sub-grid scale convective updraft and downdraft and are suitable for computing convective transport of material (Yoshimura et al., 2015). Convective adjustment schemes ensure a realistic representation of the vertical temperature and moisture profiles by simultaneously adjusting them to quasi-equilibrium states for both shallow and deep convection (Miller,1985). Each one of these methods are used to describe physical processes within convective cells and produce different results for precipitation at different locations around the globe.

The CCAM comprises one cumulus scheme, namely, the CSIRO9. The CSIRO9 cumulus scheme is an Arakawa-based mass-flux that assumes that in each convecting grid square, there is an upward mass flux within a saturated aggregated plume along with compensating subsidence of environmental air, which may also be in the form of a downdraft (McGregor et al., 1993). The CSIR09 cumulus scheme is also scale aware, producing

mainly resolved precipitation at higher resolutions (Thatcher, 2021). The CSIRO9 has three different versions/updates, namely, 2015a version, 2015b version with gravity wave drag function, and the 2017 version. This article highlights the differences between these different versions of the CCAM in order to identify the benefits in model development for the CCAM.

Model simulations

The CCAM simulations were run with its three different cumulus settings for the case of 25th January 2021, when ex-tropical cyclone Eloise was located over the eastern parts of Botswana, causing cloudiness and heavy rainfall over the Limpopo, KwaZulu-Natal and the North-West provinces (SAWS, 2021). The model was run at different horizontal resolutions, but only the 4.4 km resolution is discussed in this article. The model was compared against ground observations, also known as synops, which were regridded at 0.5 x 0.5 ° resolution and 0.1 x0.1 ° multi-satellite Global Precipitation Measurement Mission (GPM) data.

The diurnal cycle for areal average precipitation over the country shows that the model runs have a dry bias throughout the day except at 12Z and 14Z when the 2015a version of the cumulus scheme matches the observations. The model runs were not able to capture the main observed peak, which was observed at 04Z, which is within the model 6-hour spin-off period. The 2015a version generally depicts more accuracy that the other versions, and all the model versions simulate light rainfall better.

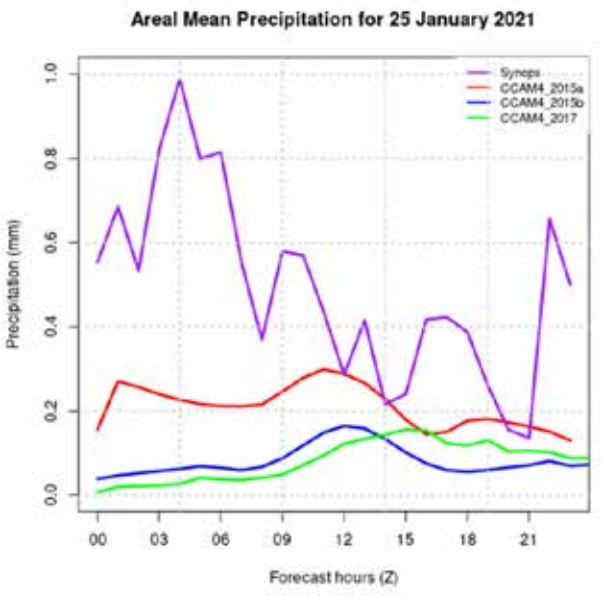

Figure 1: Diurnal cycle for areal average precipitation (in mm) for CCAM model simulations with the three different versions of the cumulus scheme and the ground observations

There are slight differences between the model forecasts in the spatial distribution for total precipitation, e.g. the 2017 cumulus scheme produces less rainfall over Botswana (Fig. 2c), while the 2015 versions produce more clear patches over the parts of the eastern interior (Fig. 2a-b). The ground observations depict more intense precipitation, over the Botswana boarder and the northern parts of the country, than the model was able to capture (Fig. 2d). The GPM shows intense precipitation over parts of Namibia and Botswana that the models were not able to represent well. The model was able to capture the intense precipitation that was observed over the eastern parts of the country.

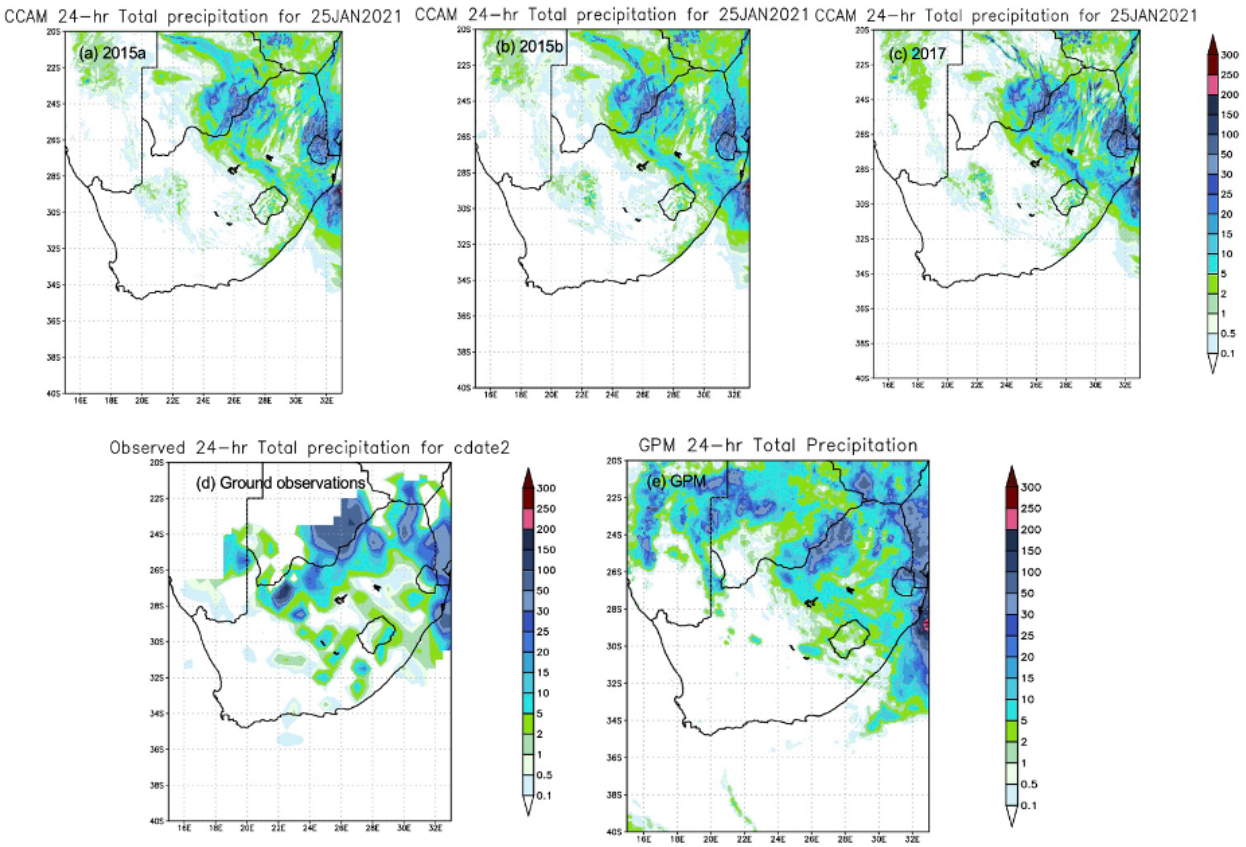

Figure 2: Spatial distribution for 24-hour accumulated precipitation for the three different versions of the CCAM cumulus scheme (a-c), the synop observations (d) and the GPM (e)

Discussions and conclusions

The areal averaged precipitation as well as the spatial distribution for observations is higher than the model simulations. The model simulations are not able to capture the fluctuating observed rainfall amounts, especially for heavy rainfall. However, the model simulations show performance in simulating light rainfall amounts. There are minor differences in the way the different versions of the CCAM cumulus schemes simulate precipitation. This study was based on a single case study of a high-impact weather event. Also, the high-resolution model was compared against sparse/course-resolution observations. For this reason, no concussions can be drawn regarding the model performance or even the benefits/shortcomings of model development.

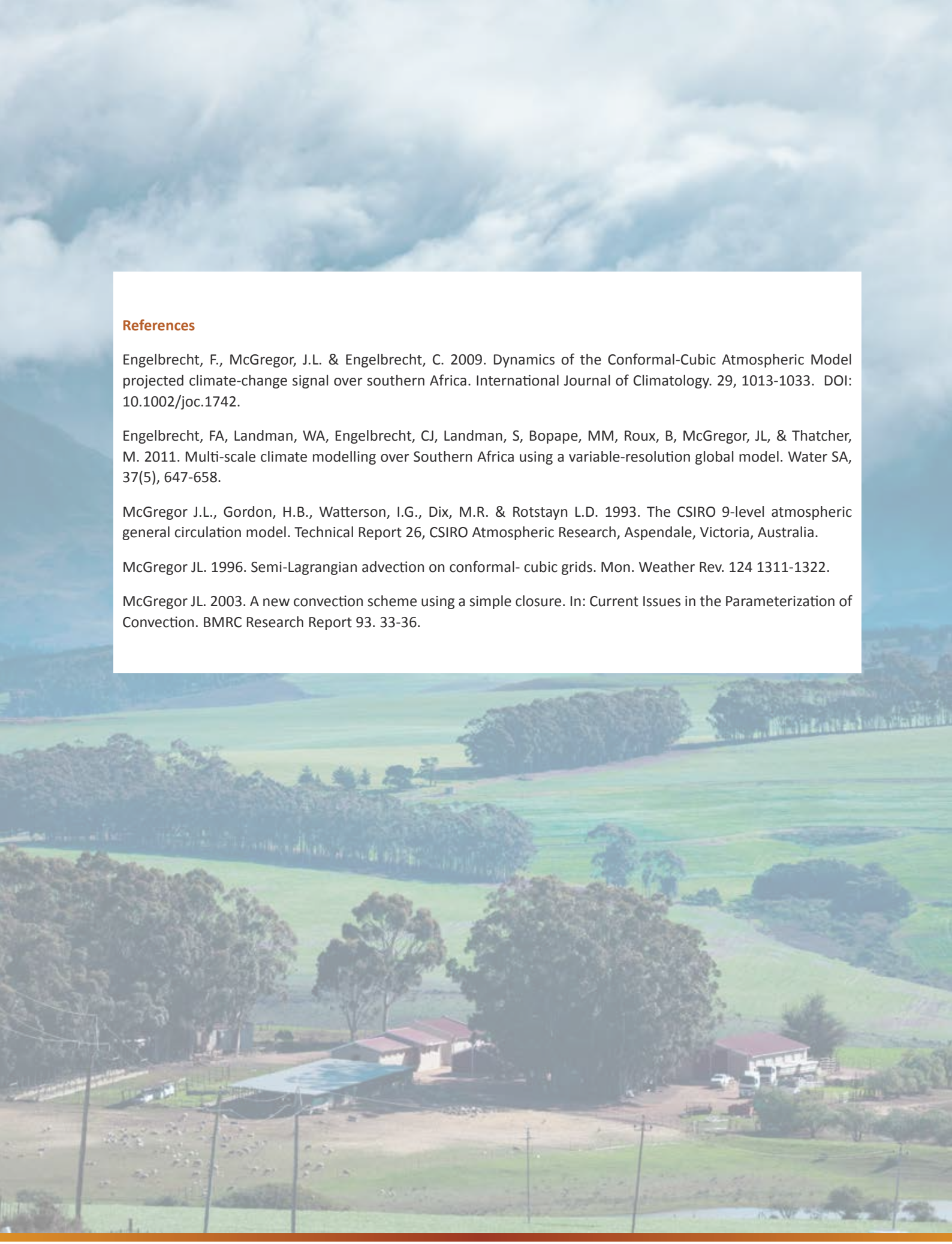

References

Engelbrecht, F., McGregor, J.L. & Engelbrecht, C. 2009. Dynamics of the Conformal-Cubic Atmospheric Model projected climate-change signal over southern Africa. International Journal of Climatology. 29, 1013-1033. DOI: 10.1002/joc.1742.

Engelbrecht, FA, Landman, WA, Engelbrecht, CJ, Landman, S, Bopape, MM, Roux, B, McGregor, JL, & Thatcher, M. 2011. Multi-scale climate modelling over Southern Africa using a variable-resolution global model. Water SA, 37(5), 647-658.

McGregor J.L., Gordon, H.B., Watterson, I.G., Dix, M.R. & Rotstayn L.D. 1993. The CSIRO 9-level atmospheric general circulation model. Technical Report 26, CSIRO Atmospheric Research, Aspendale, Victoria, Australia.

McGregor JL. 1996. Semi-Lagrangian advection on conformal- cubic grids. Mon. Weather Rev. 124 1311-1322.

McGregor JL. 2003. A new convection scheme using a simple closure. In: Current Issues in the Parameterization of Convection. BMRC Research Report 93. 33-36.

MEET THE AUTHORS

Ms Elani Heyneke

Elani Heyneke started her forecasting career at the South African Weather Service's Bloemfontein Regional office in 2017 after completing her BSc and BSc (Hons) in Meteorology, with the University of Pretoria and thereafter her post graduate certificate in Weather Forecasting. She has a passion for severe weather forecasting, especially severe thunderstorms and is currently pursuing her MSc focusing on South African squall lines. She relocated to the Cape Town Regional office at the end of 2021 and is enjoying the challenge and beautiful scenery that the Cape has to offer.

Ms Nompumelelo Kleinbooi

Nompumelelo Kleinbooi is a forecaster currently based at the Gqeberha Weather Office. She completed her BSc (undergraduate) and honours degree in Meteorology at the University of Pretoria in 2015 and 2016 respectively. In 2017, she completed the SAWS forecasting internship programme offered by the Regional Training Centre (RTC). Apart from forecasting, she enjoys engaging different stakeholders and has an interest in the climate variability of South Africa.

Dr Andries Kruger

Dr Andries Kruger is a Chief Scientist: Climate Data Analysis and Research in the Climate Service department of the South African Weather Service. His present and previous duties include the creation and writing of general climate publications, climate change and variability research with historical data as input, ad hoc scientific projects of which the numbers have increased substantially in recent years, climate data and information requests, where advanced statistical analyses are required, drought monitoring, and assisting in the quality control of climate data. In 2011, Dr Kruger obtained a PhD (Civil Engineering) degree at the University of Stellenbosch on the research topic "Wind Climatology and Statistics of South Africa relevant to the Design of the Built Environment".

Before that, he obtained an MSc (Environmental and Geographical Science) degree at the University of Cape Town. He has published papers both locally and internationally and authored a SAWS series of publications on the general climate of South Africa. He is widely recognised, both nationally and internationally, for his research, which involves advanced statistical analyses and interpretation of historical climate data.

Ms Nthabiseng Letsatsi

Ms Letsatsi recently became permanent as a Climate Information and Publication Scientist working in the Climate Information unit after joining the organisation as a Geographic Information System intern in 2019 under the mentorship of Mr Musa Mkhwanazi. She is passionate about how meteorological data can be used to make informed decisions and describes herself as a focused person with a great aptitude for learning.

Mr Brighton Mabasa

Mr Brighton Mabasa is a Research Scientist in Applications (Renewable Energy Applications and Scientific consulting) at the South African Weather Service (SAWS). His responsibilities in the group include SAWS Solar Radiometric Network monitoring and maintenance, data archiving, data quality control using Baseline Solar Radiation Network (BSRN) standards, satellite data validation, product development, observation data preparation for model verification, solar radiation and biometeorology station installation and calibration using ISO standards, writing peer-reviewed articles, and writing Standard Operating Procedures (SOPs) for operational procedures. Mr Mabasa has an MSc in Atmospheric Physics (cum laude) and is currently registering for a PhD in Energy Studies. His research findings will aid in the advanced operation of the SAWS solar radiometric network and solar energy applications.

Mr Robert Maisha

Robert Maisha is a Lead Scientist in Data Assimilation at the South African Weather Service. He has over 14 years' experience in Numerical Weather Prediction and Modelling. He has lectured and tutored in Dynamical Meteorology, Climate Change, Applied Mathematics and Statistics. His research interest includes model development, data assimilation, climate change modelling and urban climate modelling. Mr Maisha has an MSc Degree in Meteorology, an Honours Degree Meteorology from University of Pretoria and also Applied Mathematics from University of South Africa. He is currently registered for a PhD Degree in Meteorology in urban climate modelling at the University of Pretoria. He has also worked for the University of South Africa, University of Pretoria, University of Limpopo and the Council for Scientific and Industrial Research.

Ms Mandisa Manentsa

Mandisa Manentsa is a Senior Weather Forecaster in Port Elizabeth Weather Office. She joined the organisation in 1987 as an Observer at Bisho Airport in the then Ciskei Government. She holds a national higher diploma in Meteorology which she obtained in 1993 at Pretoria Technikon.

Mr Sifiso Mbatha

Sifiso Mbatha is a Climate Service Scientist: Climate Data. He joined SAWS as an intern in 2015 and was employed in July 2016 in the same unit. He completed his BSc degree in Physics and Geography in 2013 and further obtained his Climatology Honours degree in 2014 from the University of Zululand. Sifiso is currently enrolled with the University of Venda for his Master's degree, modelling the variability of convective activity over the East Rand, South Africa.

Ms Charlotte McBride

Charlotte McBride joined the then South African Weather Bureau in 1998 as a meteorologist focusing on the development of educational publications and assisting with the communication of weather-related topics to various stakeholders. In 2010 she moved to be Manager of Climate Data in the Climate Service department, which involved quality controlling all climate data on the SAWS main climate database. This includes managing a team that is involved in data rescue activities, quality control of weather data, spatial checking of data and archiving of climate documents. Over a number of years, she has co-authored the SAWS inputs to the Bulletin of American Meteorological Society (BAMS) State of the Climate report. She is also involved with the work of the World Meteorological Organization (WMO) as a co-lead for Capacity Development and Communication under the Standing Committee on Climate Services and is part of the WMO Open Climate Data Management System Project Advisory Team. Charlotte holds an MSc in Science Education and is currently registered at the University of Pretoria for a PhD in Geography.

Mr Sandile Ngwenya

Sandile Ngwenya is a Scientist in Climate Services: Climate Data Analysis and Research. He joined the South African Weather Service in 2017. He holds a BSc degree in Geography and Hydrology and a BSc Honours degree in Climatology from University of Zululand, and an MSc degree in Environmental Sciences from University of Venda.

Mr Ayabonga Tshungwana

Ayabonga Tshungwana obtained his first BSc degree at the University of Fort Hare majoring with Physics, Maths and Applied Maths (2016). He then obtained his BSc Meteorology at the University of Pretoria through a programme called "Bridging course (2017)" and obtained his BSc Honours in Meteorology at the University of Pretoria (2018). He completed the forecasting certificate at theSouth African Weather Service in 2019.

Ms Patience Mulovhedzi

Patience Tlangelani Mulovhedzi is a scientist in Model development at the Research and Development department. She is currently enrolled for a PhD in Meteorology, researching on the cumulus convection parameterization and dynamical analysis for mesoscale convective systems within the gray zone. She has obtained a master's degree in Meteorology from the University of Pretoria in 2018. Patience has great experience in working with different Numerical Weather Prediction models and she loves programming.

Mr Jan H. Vermeulen

Jan Vermeulen has been with the SAWS for over 39 years and works as a Senior Forecaster in the National Forecasting Centre unit at head office. He is a PhD thesis student at Unisa, and his research topic is titled: Forecasting extreme very short-term rainfall in RSA for Disaster Risk Reduction purposes.

Head Office

Centurion
Eco Glades
Block 1B, Eco Park
Cnr Olievenhoutbosch and
Ribbon Grass Streets
Centurion
0157

Regional Offices

Bloemfontein
Weather Office
Maselspoort Road
Bram Fisher International Airport
Private Bag X20562
Bloemfontein
9300
Tel: 051 433 3281

Cape Town International
Weather Office
ATNS Tower
Tower Street
Cape Town International Airport
PO Box 21
Cape Town International Airport
7525
Tel: 021 934 0749/0831

King Shaka International
Weather Office
Ground Floor
ATNS Building
King Shaka International Airport
PO Box 57733
King Shaka International Airport
4407
Tel: 032 436 3820/3812

OR Tambo International
Aviation Weather Centre
Room N161
3rd Floor
OR Tambo International Airport
PO Box 1194
Kempton Park
1627
Tel: 011 390 9329/9330

Port Elizabeth
Weather Office
Roof Top
Departures Hall
Port Elizabeth Airport
Private Bag X5991
Walmer
Port Elizabeth
6065
Tel: 041 581 0403/8587

WEATHERSMART NEWS

Scientific meteorological and climatological news from the South Africa Weather Service

South African Weather Service